CHALMERS

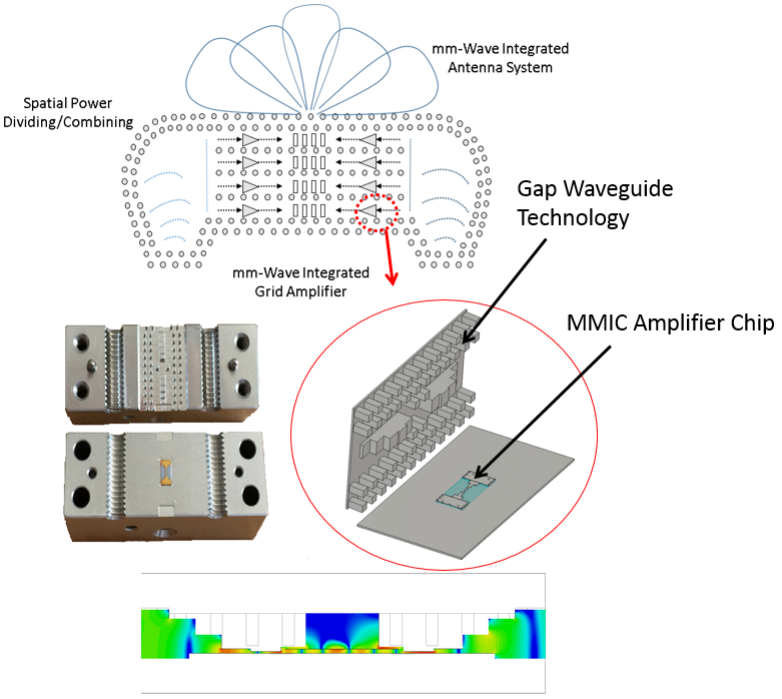

Millimeter-Wave Microstrip-to-Groove Gap Waveguide Transition for use in Gap-Waveguide-Integrated Grid Amplifiers and Antenna Arrays

Alhassan Aljarosha

Department of Signals and Systems
Chalmers University of Technology
Gothenburg, Sweden, 2016.

Millimeter-Wave Microstrip-to-Groove Gap Waveguide Transition for use in Gap-Waveguide-Integrated Grid Amplifiers and Antenna Arrays

CHALMERS
UNIVERSITY OF TECHNOLOGY

MASTER's THESIS
as part of mandatory clauses in
fulfillment of Master's Degree from the
Chalmers University of Technology, Gothenburg, Sweden

by

Alhassan Aljarosha
Department of Signals and Systems

March, 2016

Millimeter-Wave Microstrip-to-Groove Gap Waveguide Transition for use in Gap-Waveguide-Integrated Grid Amplifiers and Antenna Arrays / by
Alhassan Aljarosha. - Gothenburg : Chalmers University of Technology, 2016.

This thesis has been prepared using LaTeX

This thesis is carried out under supervision of:
Dr. Rob Maaskant
Dr. Ashraf Uz Zaman

Examiner:
Prof. Per-Simon Kildal

Keywords: gap waveguides / system integration / microstrip circuit / SIW / packaging / transition / millimeter wave.
Subject headings: gap waveguides / system integration / MMIC integration / Transition / packaging.

Technical Report No. 2016:xx
Antenna Group, Department of Signals & Systems
Chalmers University of Technology,
SE-41296, Gothenburg, Sweden.
Telephone: +46 31 772 1000

Cover design: Alhassan Aljarosha
Press: Chalmers Reproservice, Göteborg

The work presented has been performed at the Chalmers University of Technology, Sweden.

Abstract

To realize next generation mm-wave wireless systems it is vitally important to utilize cost effective manufacturing technologies and to develop low-loss waveguides and transmission lines. Furthermore, being able to interface system components through contactless transitions is another key objective. In fact, recently, optical connections between chips through fibers is being researched heavily in the photonics science field, while the quasi-optical connection as proposed in this MSc thesis between chips through waveguides presents a similar breakthrough, albeit in the mm-wave range. The proposed contactless connection between a waveguide and chip obviates the need to use RF bond wires. Furthermore, the proposed solution is also compatible with the gap waveguide technology enabling the resonance-free electromagnetic packaging of the entire RF front end.

There are numerous challenges to overcome to realize future mm-wave antenna systems. Standard waveguide components are rather low loss but are manufactured in split blocks which may lead to power leakage. Mechanical assembly of the two split blocks requires a very good electrical contact as well as precise alignment of the two blocks to achieve good electrical performance. Furthermore, the physical dimensions of the waveguide components decrease as the frequency of operation increases. This renders the manufacturing of conventional waveguide components more costly and time consuming, particularly at mm-wave frequencies.

The gap waveguide structure has the advantage of reducing the manufacturing cost and time, because the gap waveguide structure can be realized without requiring any metal contact between the upper and the lower metal surfaces of the structure. Also, the Perfect Magnetic Conductor (PMC) condition realized by the lid of nails, parallel to a PEC surface, has the ability of suppressing unwanted parallel-plate modes between the two metal blocks and allows for the resonance-free packaging of RF electronics, thereby high isolation between the RF components can be achieved.

At the same time a low-loss transition between the gap waveguide components and the active ICs, such as Monolithic Microwave/Millimeter Integrated circuits (MMIC), is neces-

sary in order to integrate active components with passive waveguide components together with antennas in a single module. It is common practice to establish a connection between a transmission line and a chip through RF bondwiring. However, the large impedance mismatch between the inductive bond wire and the MMIC requires a matching capacitor. But impedance matching can only be achieved over a certain bandwidth, depending on the Q-factor of the LC circuit. Furthermore, the matching network takes up the space, and may excite cavity modes when packaged resulting in device oscillations and cross talk effects. It is therefore the objective of this thesis to provide a novel, low-loss and broadband contactless microstrip line to groove gap waveguide transition.

An MMIC-to-waveguide transition has been designed at W-band and in such a way that it can be integrated easily in a groove gap waveguide structure, for example by using a pick-and-place technique. Both the PCB and the gap waveguide were designed and manufactured. Tolerances are allowed up to 10 microns. The simulation results of a back-to-back transition are excellent; the S_{11} is below -21 dB, while S_{21} is better than -0.35 dB over the entire W-band (75-110 GHz). Unfortunately the experimental validation of the transition is not as expected. A thorough error analysis revealed that the dimensions of the PCB were not within the tolerances as specified by the manufacturer, which is the main reason for the performance degradation. Future steps are recommended to resolve these issues.

Finally, a Swedish patent application on the transition has been filed in February 2016 (no. 1650181-9) and a conference paper to the IEEE Antennas and Propagation Symposium has been submitted.

Keywords : Gap waveguides / system integration / microstrip circuit / SIW / electromagnetic packaging / contactless connection / mm-wave

Contents

Chapter 1

Introduction

This chapter describes the context and background of this thesis. Firstly, we summarize the previous researches done in the area of waveguide integration technology and address the associated challenges. Secondly, we present the state of the art of the recent developed gap waveguide technology. Finally, we present the thesis contributions for new solutions. We conclude with the thesis outline.

1.1 Overview

The significant growth in wireless telecommunication application has motivated the increased demand for high data rates and bandwidths. This push the industry and the researchers to develop next generation wireless systems. Moving up into the millimeter-wave band region, where larger frequency bandwidths are available, these systems become smaller and more compact, enable for high level of integration.

At millimeter- and submmWave system integration, conventional integration for Rf electronics and antennas would lead to cavity resonances, cross-talk effects and the power losses in the material will be significant. Standard waveguide components are quite low loss even at millimeter-wave band. Thereby make this type of guiding structure suitable and attractive for low loss applications. However the manufacturing techniques such as diffusion bounding [1, 2] for the conventional metal waveguide at mmWave frequencies

become very complicated, in order to have a very accurate alignment between the two split blocks with good electrical contact.

The integration of active microwave components with the standard waveguide is complicated and challenging at high frequency. Highly dense MMICs are compatible with planer waveguides such as, substrate integrated waveguide (SIW), microstrip and coplanar waveguides. Transition from planar waveguide to non-planar waveguide is often challenging specially at frequencies, where precise metal contact is required to provide transformation of the EM field from one transmission line to another. Often these transitions degrade the overall system performance. The transition design from planar technology to a metal waveguide technology for the integration of active circuits such as MMICs has led to enormous works over the last decades. Some of these transitions are inline microstrip to waveguide transition based on ridge waveguide [3–5]. The advantage in such inline transition lies in the fact that both the field propagation direction in microstrip and in the waveguide are in the same direction. Transition shows good results, however these transitions are relatively narrow band as in [3] or need a precise metal contact between microstrip section and the waveguide part and matching network is also needed. Transition with E-plane probe has a broadband nature, but still need a good electric.

New waveguide technology is required to overcome the issues of conventional waveguide technology at mmWave frequencies. This new waveguide technology should takes into account the requirement on electrical connection between building blocks of the waveguide. This new gap waveguide technology was recently presented in [6] and [7].

Recently, many transitions from microstrip to gap waveguide component have been reported. A ku-band microstrip to ridge gap waveguide with 0.5 dB insertion loss has been recently presented in [8]. This structure is complicated since the field needs to be coupled between the microstrip to the ridge gap waveguide through a coupled-slot in the ground plane. Furthermore a back-short is needed, which makes the structure bulky and also influence the bandwidth performance of the structure. Other microstrip to ridge gap waveguide operates at Ka-band [9], which gives larger band width than [8]. However, accurate alignments and electrical connection between the microstrip and the ridge of the gap waveguide must be achieved. A microstrip to ridge gap waveguide transition based on capacitive coupling operating at 100 GHz is presented in [10]. This transition uses a substrate with dielectric constant ϵ_r of 9.9, which is more close to a realistic value suited for commercial MMICs. However, the transition is relatively narrow band. In [11] a

suspended-strip gap waveguide to standard rectangular waveguide transition operating at Ka-band is presented, where a rectangular coaxia line limits the bandwidth as well as a good electric contact is required between the two parts.

1.2 Problems with Conventional Metal Waveguide

Conventional waveguide shown in Fig. 1.2 has a low loss property, even at mmWave frequencies, which make this type of transmission line very attractive for a low loss applications. High level of precision, accurate alignment and very good electrical joints are the main factors and the most challenging parts to be considered. Traditional machining techniques for the conventional metal waveguides operating at mmWave frequencies are complicated and costly, specifically for mm-and submmWave system integration. Surface finish and tolerances are complex to provide in the inner surface of the hollow metal waveguide. Skin depth causes ohmic loss due to few microns of penetration of electric current into the metal walls. At mm-and submmWave frequencies, the inner surface conductivity must kept as high as possible. in some applications, the inner surface required to be plated with gold or silver.

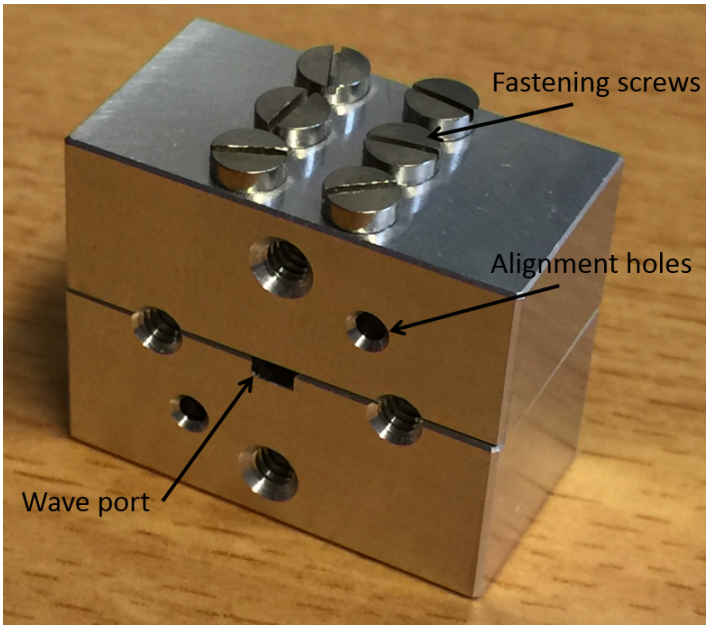

Figure 1.1: Two-block conventional rectangular waveguide

Metallized plastics injection mold techniques provide a Lightweight, high volume fabrication waveguide [12]. In spite of advantages of the plating on plastics technique, there are some possible issues, related mainly to the fabrication process, that have to be considered. Cooling step causes shrinkage of the molded plastic. Furthermore, the production of high volume hollow waveguides will increase the sensitivity to the process defects [13].

In grid power amplifiers, and planar slot array applications, where multiple waveguides are needed, the separating vertical wall between two parallel waveguides must be narrow and the electrical contact must be achieved very well, which of course is very difficult to achieve, specially at high frequencies. Spurious radiation, unwanted field coupling and leakage may become major concern which leads to substantial reduction in the over all efficiency and severe cross talk and as well as reduction in antenna gain. Thus to achieve the required electrical performance, metal milled or micromachined of rectangular waveguide components need high precision level of accuracy [14].

Regardless of several designs to innovate integrated metal waveguide forms, a convenient system with active devices and antennas completely integrated within the waveguide structure and operating at mm-and submmWave frequencies is non-existent.

1.3 Gap Waveguide Concept

In order to overcome the issues associated with conventional metal waveguide at both mm- and submmWave frequencies, recently developed high performance and low loss gap waveguide structure based on metamaterial technology will be considered.

The principle behind the gap waveguide is to create a high impedance condition forcing a cut-off of all parallel-plate modes within a certain bandwidth [15]. Ideally the high impedance surface is a perfect magnetic conductor PMC, which does not exist in nature, but it can be realized artificially within specific frequency band, and is often referred to as an artificial magnetic conductor AMC [6].
AMC can be realized in the form of textured surface such as periodic of square metallic pins [16], which is suitable for high frequency applications, or by using mushroom type EBG, for low frequency applications [17]. In gap waveguide structure, the bottom periodic textured plate creates the high impedance condition if the distance to the top metal plate

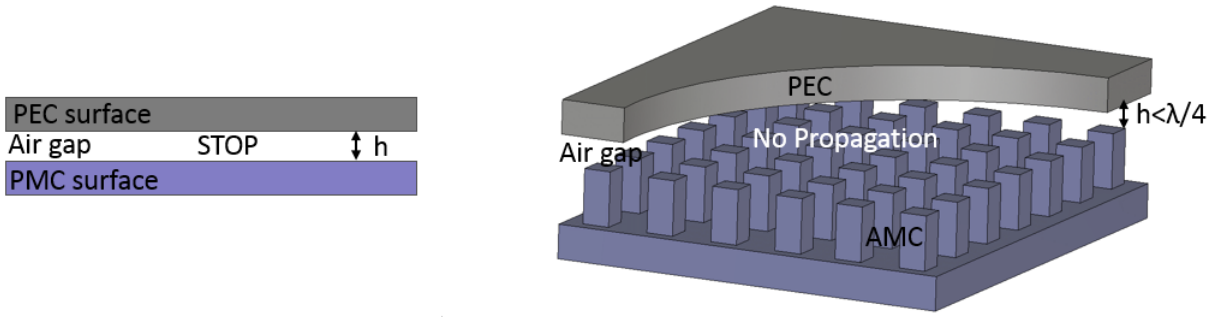

Figure 1.2: Geometry of parallel PEC-PMC to create the cutoff condition for EM fields

(Air gap height) is less than quarter wavelength. In this case all parallel plate modes are prohibited to propagate within the stopband. The desired wave is allowed to propagate along the guiding structure such as groove, metal ridge or strip, which supports either TE_{10}, or Q-TEM mode, depending on the guiding structures as shown in Fig. 1.3

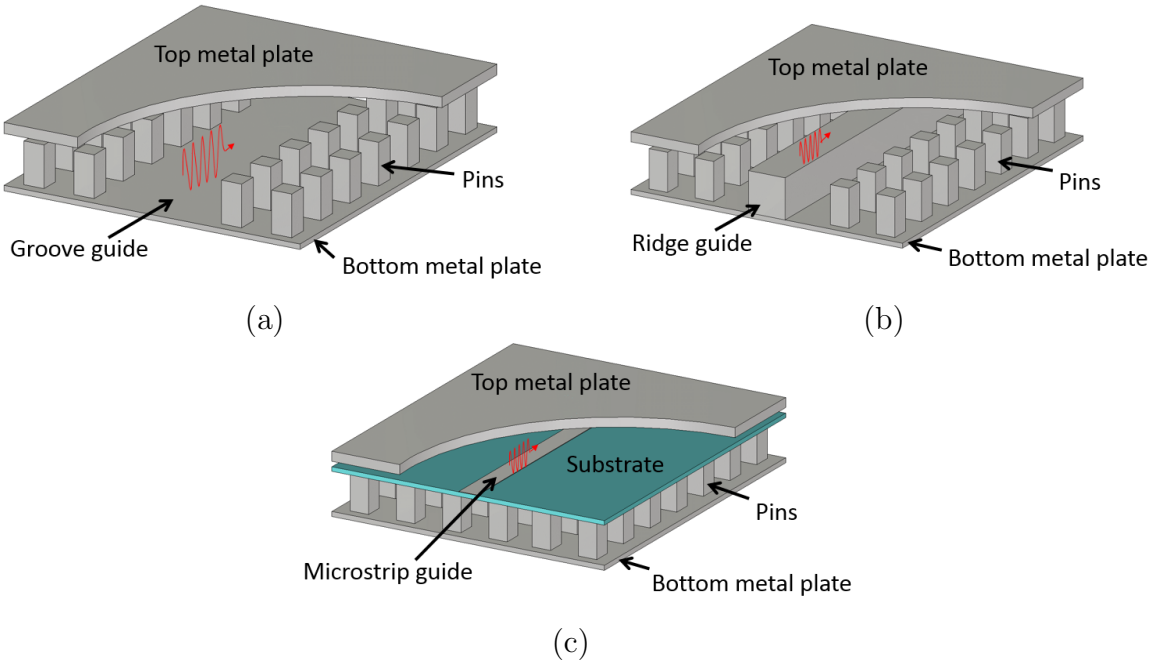

Figure 1.3: Types of gap waveguide: (a) Groove gap waveguide, (b) Ridge gap waveguide, (c) Inverted microstrip gap waveguide

In this technology, the metal waveguide structures can be realized without any metal contact between the two metal plates, which allows a very flexible and cheap manufacturing process specially at mm-and submmWave frequencies. Recently, several Ku-band,

Ka-band and V-band good performance passive components such as slot array antennas, narrow band filters have been designed in gap waveguide technology [18–20]. In addition, the gap waveguide structure has the property of cavity mode suppression, which make the gap waveguide a very appropriate solution for packaging microstrip circuits which include active components [21–23].
Gap waveguide conventional manufacturing process such as CNC milling is accurate, offering tolerances in few microns. However, when the operating frequency is above 100 GHz, CNC milling technique becomes complex and not accurate enough. Therefore, above 100 GHz micromachining process becomes suitable alternative. This process gives tolerances in microns. First micromachnined gap waveguide operating in the range 220-325 GHz is presented in [24].

1.4 Interconnects at mmWave Frequencies

For the realization of mm- and submmWave complete system, an appropriate interconnection method should be considered. Wirebonding technology is the classical method used to connect a chip with active elements attached to a package or substrate to a planner transmission line. It is an attractive method, it is low cost and robust. Bondwire provide a chip thermal conductivity, thereby, it is widely used in RF microsystem packaging.

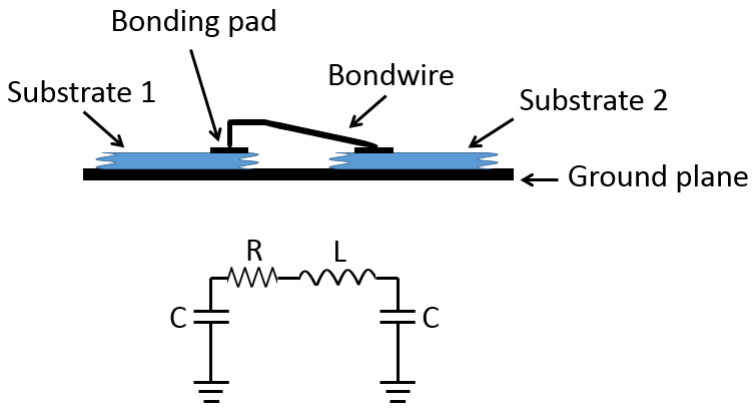

Figure 1.4: Geometry of equivalent circuit model of a bondwire at high frequency

Due to thermal expansion and tolerances in the chip size, a gap between two substrates must be kept. A wire bond transition can be modeled as a discrete lumped equivalent circuits as shown in Fig. 1.4. The components R and L represent the resistance and the

overall inductance of the bondwire respectively, while the component C represents the capacitance due to bonding pads. The nature low pass filter behaviour of the interconnect shown in Fig. 1.4, limits the operation bandwidth of the mmWave system. An extra frequency compensation network in order to increase the system operational bandwidth, thus additional space is required, which therefore a limitation for MMICs technology.

Discontinuities of the wirebond cause mode conversion which thereby results in leakage of power in terms of surface waves, parallel plate modes, or even higher order modes. The strong reflections and parasitic radiation result in cross talk and resonance effects, leading to device oscillations.

1.5 Goals and Outline of the Thesis

The design challenges for wireless communication system operating at mmWave frequencies is to realize a complete system (all-in-one), with low loss, as compact as possible and cost effective at the same time. The gap waveguide technology is the one of many prospective technologies used for integrating active components such as MMICs with the metal waveguide components due to the capabilities of suppressing cavity modes and provide resonance-free packaging. At mm- and submmWave frequencies, the dimensions of the circuits becomes shorter especially for circuits using alumina or GaAs substrate, thereby the manufacturing tolerances become critical and the emerging parasitic effects become unavoidable. There are intensive works to explore innovative alternative circuit interconnection methods, based on the electromagnetic field coupling, based on overlapping a $\lambda/4$ long transmission line section.

The aim of this work is to present a design of a low loss and broadband, contactless microstrip to groove gap waveguide transition operating at mmWave frequencies and suitable for MMICs integration. This work is the first milestone to validate an accurate and complete mm- and submmWave model for gap waveguide integrated grid amplifiers and antenna arrays based on contactless connections between chip transmission line and waveguide or/and antenna port. The novel technology of contactless connection allows assembly in a fast and an easy manner, for example using a pick-and-place technique. Simulated results and experimental validation for the designed transition are presented in this thesis. Comparison with conventional rectangular waveguide is also presented. The

proof-of-concept of the long term objective and the short term objective in presenting in Fig. 1.5.

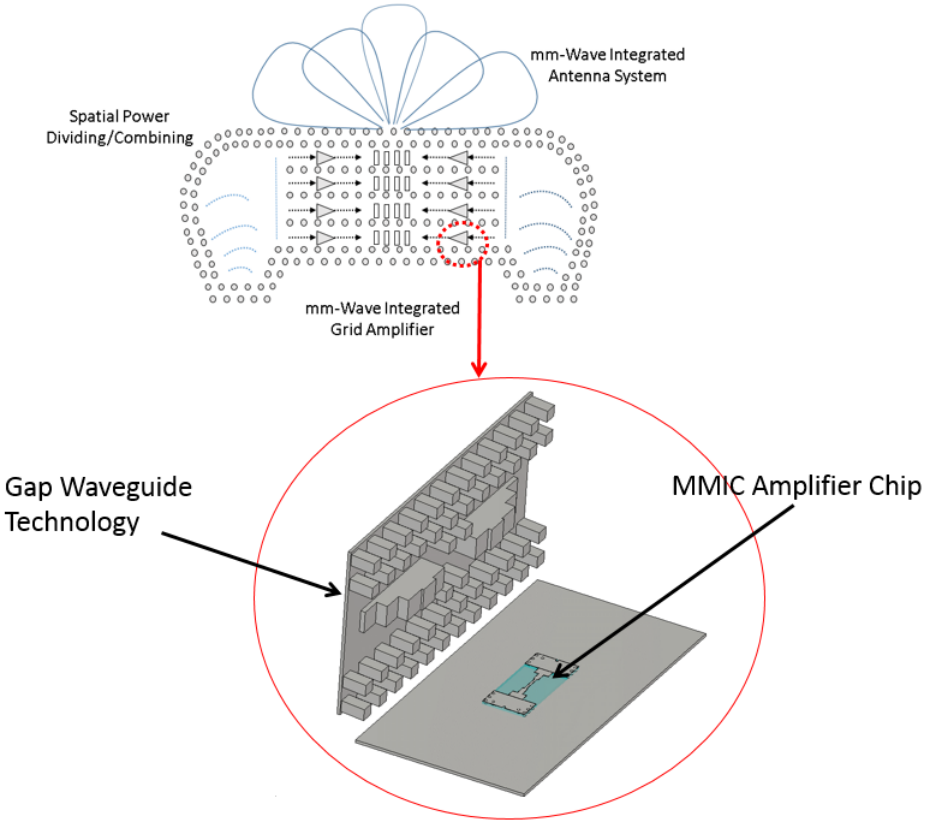

Figure 1.5: Geometry of proof-of-concept represents the aim of the thesis

The thesis is partitioned as follows: Chapter 2 starts with the design aspect of gap waveguide technology. In particular the chapter is focused mainly on the ridge gap waveguide and the groove gap waveguide. A transition design from the ridge gap to groove gap waveguide is presented in this section and the simulation result is also presented in this chapter. Chapter 3 provides the transition between SIW and ridge gap waveguide. Chapter 4 explains the integration between microstrip circuit designed for MMICs applications and the gap waveguide technology. The complete design and the simulation results of microstrip to groove gap waveguide transition using electromagnetic coupling are also included in chapter 4. Parametric study is done to demonstrate the effect of some critical parameters on the transition concept. Design modifications to satisfy the manufacturing specifications are presented. Chapter 5 represents a feasibility study for the integration of an active device such as MMIC low noise amplifier (LNA).It is a good application to prove that the concept of contactless transition works in theory. This includes demonstrating the

effect of the active element using the S-parameters model of commercial W-band LNA [25]. Finally, the conclusions of the this work and a list of recommendations are presented in chapter 6.

Chapter 2

Ridge Gap to Groove Gap Waveguide Transition Design

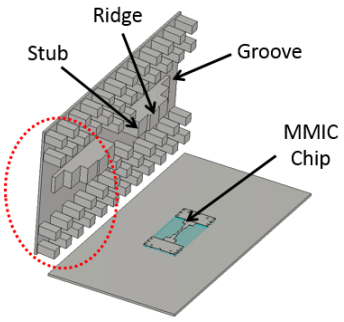

Gap waveguide comprises two parallel metal plates, where one of the two plates is replaced by a periodic metamaterial based structure (bed of nails). The absence of dielectric material property makes the gap waveguide technology attractive at mm-ans submmWave systems. This chapter represents the first part of the project; ridge-to-groove gap waveguide transition. The aim of this transition is to enable maximum power transfer between the ridge gap waveguide and the waveguide port. Stepped ridge sections of different heights are used to match the ridge height to the height of the groove gap waveguide. The chapter starts with a brief study to design the parallel plate stopband. Subsequently, we introduce the transition design followed by the simulation result.

2.1 Parallel Plate Stopband Study

The characteristics of the parallel plate stopband, such as the cut-off is the main design issue in gap waveguide technology. The stopband can be realized by creating a high impedance surface, that can forbid propagation of parallel plate modes and the surface

waves in all directions within the specific frequency band. A textured surface in the form of periodic pins, so-called bed of nails is presented in [26]. If this surface is placed closely (approximately smaller than $\lambda_g/4$ of air gap) to a horizontally metal wall, the surface will function as a high impedance surface. Often this surface is referred to artificial magnetic conductor, AMC surface.

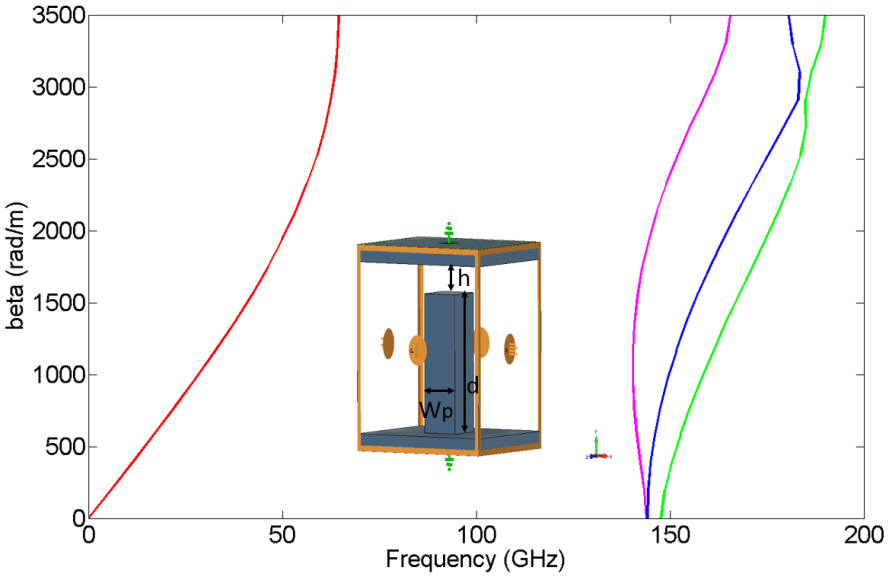

Figure 2.1: Dispersion diagram of an infinite periodic unit cell

The key parameters for designing the stopband, are the height of the pins and the height of the air gap. The height of the pins determines the lower cut-off frequency of the stopband, while the upper cut-off frequency of the stopband is determined by the pin height plus the height of the air gap [27]. The computed dispersion diagram of unit cell of infinite periodic pin is shown in Fig. 2.1. Dispersion diagram has been calculated using software CST STUDIO SUITE citeCST by using the Eigenmode-solver. The pin has a size of $d = 0.81$ mm, width of the pin is $w_p = 0.3$ mm, the period is $p = 0.9$ mm and with air gap $h = 0.19$ mm. The obtained stopband is about 69 GHz to 144.5 GHz.

In the case of groove gap waveguide shown in Fig. 1.3(a), the dispersion diagram for few rows of pins with a groove in between with width of $a = 2.54$ mm and this groove is consider to be infinitely long in z direction is shown in Fig. 2.2(a). The absolute value of vertically polarized E-field inside the groove gap waveguide is presented in Fig. 2.2(a). The propagation of TE_{10} is similar to that fundamental TE_{10} in rectangular waveguide. The ridge gap waveguide presented in Fig. 1.3(b) a ridge is used instead of a groove surrounding

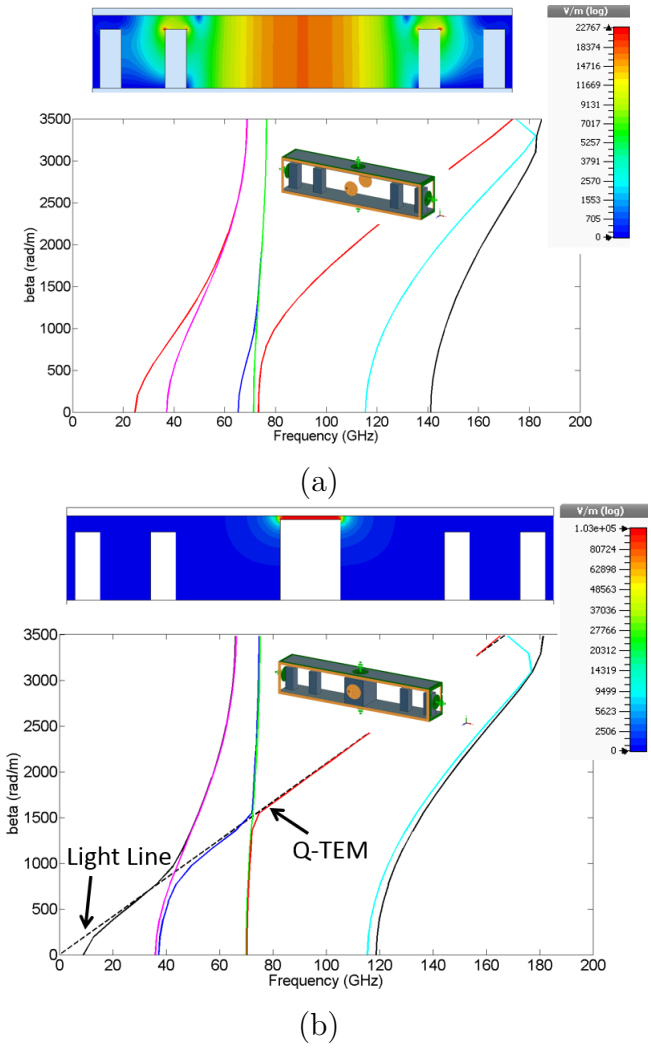

Figure 2.2: Dispersion diagram and 2-D plot of the absolute value of E-field: (a) Groove gap waveguide, (b) Ridge gap waveguide

by the periodic pin structure which stops the parallel-plate modes and allows to the desired mode to propagate within stopband. Fig. 2.2(b) shows the dispersion diagram of the ridge gap waveguide. Pin size is the same as the one used with pin unit cell and the groove one, the ridge has a height of $h_r = 0.96$ mm and a width of $w_r = 0.72$ mm.

The first design and experimental validation of a ridge gap waveguide is presented in [28] around 15 GHz. A 2-D plot of the absolute value of the E-field inside the ridge gap waveguide is shown in Fig. 2.2(b), when the groove is replaced by the ridge, a Q-TEM mode is propagating within the stopband of frequency range from 70 GHz to 115 GHz. An important issue that can be noticed from the 2-D plot is that, gap waveguides have

the property for the non-dispersive guidance of the EM field within a relatively large bandwidth. The field decays rapidly across the bed of nails. This advantageous property allows for a dense electromagnetic packaging of components in shielded cavities.

2.2 Proposed Transition Design

Groove to ridge gap waveguide transition has been designed at W-band frequency range. The geometry is shown in Fig. 2.3 the pins structure has pin size as descried in the previous section. To minimize the reflection due to impedance mismatch a 3-step tapered Chebyshev transformer based on $\lambda_g/4$ sections are used. A smooth mode transition from TE_{10} in the groove section to Q-TEM mode following the ridge in the ridge section can be obtained over the full frequency band from 75 GHz to 110 GHz. Similar transition has been designed previously at 15 GHz and is presented in [29]. Fig. 2.3 shows the complete structure with tapered steps sizes. The design parameters are the steps length of $L_1 = 0.79$ mm, $L_2 = 0.76$ mm, $L_3 = 0.87$ mm and the steps height of $H_1 = 0.92$ mm, $H_2 = 0.69$ mm, $H_3 = 0.29$ mm.

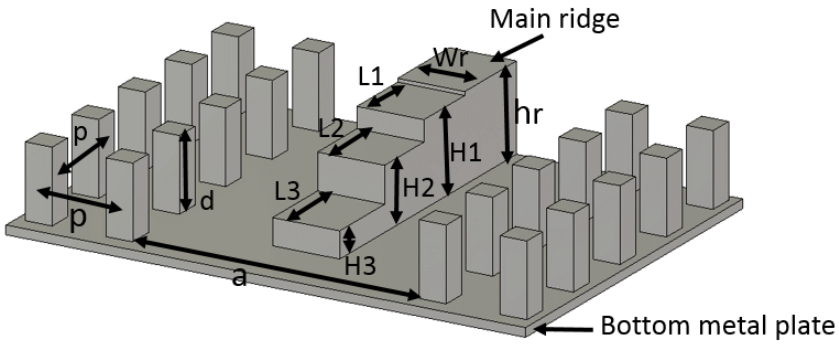

Figure 2.3: Complete structure of Groove-to-ridge gap waveguide transition (Top metal plate is hidden)

2.3 Simulation Results

The structure shown in Fig. 2.3 has been simulated and optimized by using full wave simulator CST STUDIO SUITE [30]. The simulation result shows a good performance

within the desired frequency range and is shown in Fig. 2.4. The simulated S_{11} is about -25 dB. We can conclude from the result that a good impedance matching is achieved covering the full band if interest. The very low insertion loss, ≤ 0.07 dB, is due to that all metal parts are treated as perfect electric conductor condition, PEC. But even if we consider the metal part as an aluminum; the insertion loss will not affected much, which might be ≈ 0.15 dB.

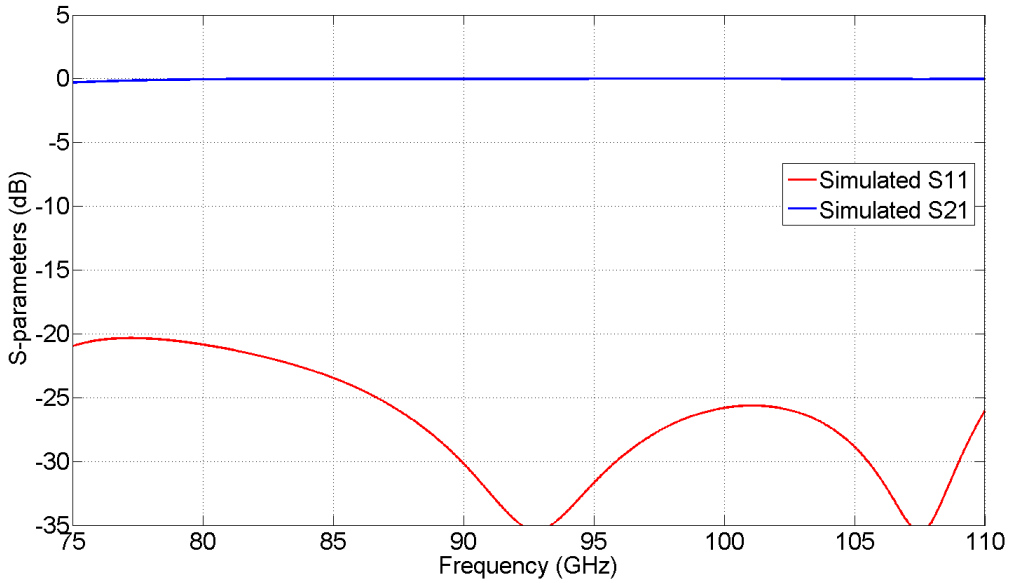

Figure 2.4: Simulated S-parameters of Groove gap to Ridge gap waveguide transition

Chapter 3

SIW to Groove Gap Waveguide Transition Design

Highly dense circuits in modern microwave and mmWave systems, such as multifunctional MMIC, which are based on microstrip line technology, need transitions in order to connect these circuits to waveguide components such as antennas and diplexer filters. Intuitive approach in designing such transition from microstrip circuit to metal waveguide is to use an SIW as a middle matching step to guide the TE_{10} waveguide mode to a TE_{10} SIW mode. This chapter provides a simple transition between an SIW and groove gap waveguide, based on the previous design described in chapter 2

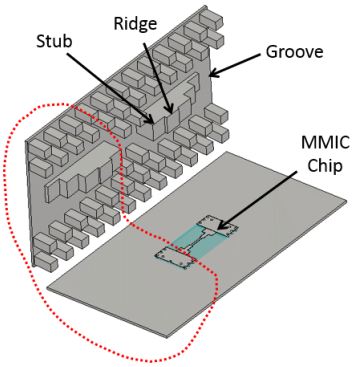

3.1 The SIW Concept

SIW (Substrate-Integrated Waveguide) can be manufactured in a planar form by using two rows of periodic plated via holes which are embedded in a dielectric substrate having a top metal layer and ground plane. The geometry of the structure and the fundamental mode TE_{10} is presented in Fig. 3.1. The key parameters for designing the SIW are, the vias diameter D, vias period P and the spacing between the two rows of via holes W_{siw}. Similar

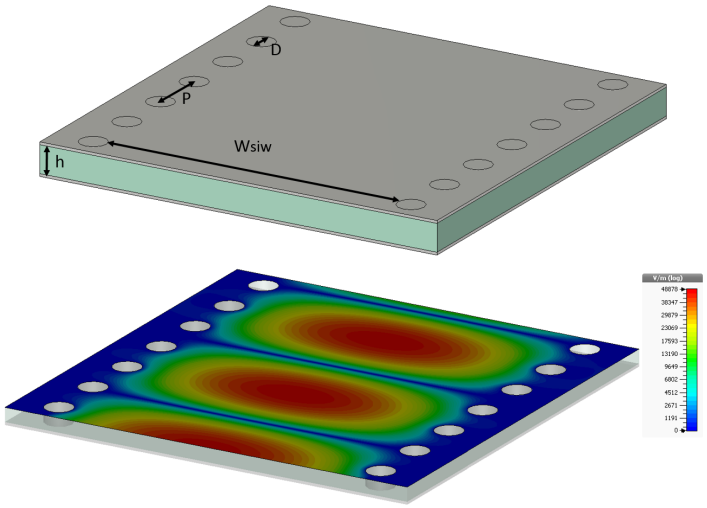

Figure 3.1: Geometry of the SIW and the fundamental mode, TE_{10} distribution inside the SIW

to a rectangular waveguide, the SIW has the same cut-off frequency for the dominant mode TE_{10} based on the formulas as given by [31]:

$$f_{c(\mathrm{TE}_{10})} = \frac{c}{2W_{\mathrm{eff}} \cdot \sqrt{\epsilon_r}} \tag{3.1}$$

$$W_{\mathrm{eff}} = W_{\mathrm{siw}} - \frac{D^2}{0.95P} \tag{3.2}$$

Where ϵ_r is the relative permittivity of the dielectric material and W_{eff} is the width of the integrated waveguide.

The SIW possesses many advantages over other type of transmission line, as it allows a complete circuits integration on substrate, specially the design of high dense mmWave circuits which provides low losses and high Q-factor [32]. At mm- and submmWave system, the microstrip line is not preferable; it support lossy dispersive hybrid modes [33]. Moreover, the dimensions are smaller resulting in complex manufacturing process and thereby tolerances become very tight.

In this section, we present a transition form SIW to ridge gap waveguide and then the ridge gap section can be matched to a groove gap waveguide using the transition explained in the previous chapter 2.

3.2 Proposed Transition Design

The structure of the proposed transition operating at W-band is depicted in Fig. 3.2. The novel structure consists of two parts. The first part is the ridge to groove transition part. This part has been designed recently and presented in 2.2. While the second part, is the SIW which is directly mounted to the top metal plate of the gap waveguide part. This design will significantly reduces the electrical and mechanical complexity of the transition. The SIW is designed on a 0.1 mm substrate substrate of high dielectric constant (alumina substrate of ϵ_r of 9.9). Alumina offers good compatibility with commercial InP or GaAs based MMICs at mmWave frequencies. The two parts are separated by an air gap t_g of 0.03 mm as shown in Fig. 3.3(a).

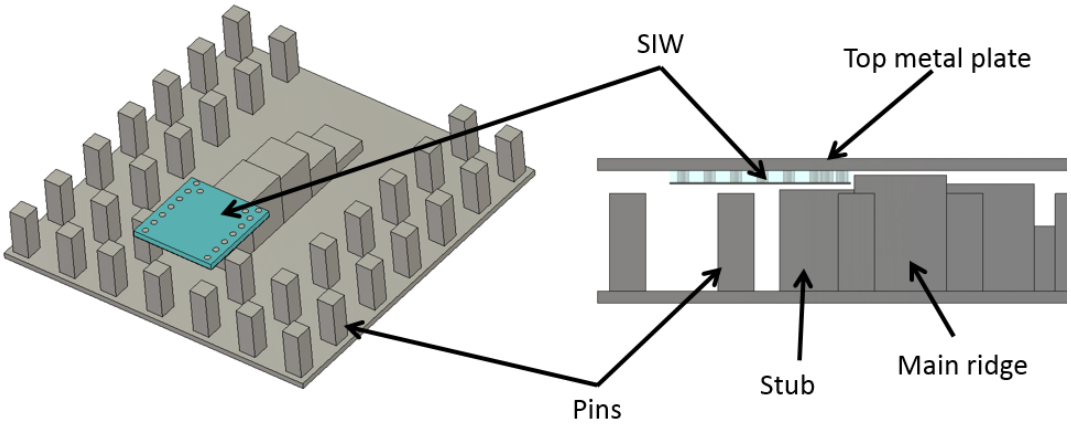

Figure 3.2: Proposed structure of the SIW to ridge transition, Perspective view (Top metal plate is hidden) (left), Side view (right)

The transition is based on the transformation of the E-field in the dielectric of SIW part to ridge of the gap waveguide using electromagnetic coupling, based on a stub (an extended ridge part) of $\lambda/4$ long, as shown in Fig. 3.3, has an air gap of t_v of 0.05 mm below SIW part. Open ended stub exhibits capacitive effect. In order to maximize power transfer between the two transition parts, two plated vias are added to form an inductive iris at end of the SIW. Fig. 3.3(b) demonstrate the matching concept. In this transition no soldering or electrical contact is required, may be conductive glue to fasten the SIW circuit, which makes the transition more appropriate for high frequency applications and to get more flexibility for replacing or changing the mmWave circuits such as MMIC in a bigger system module.

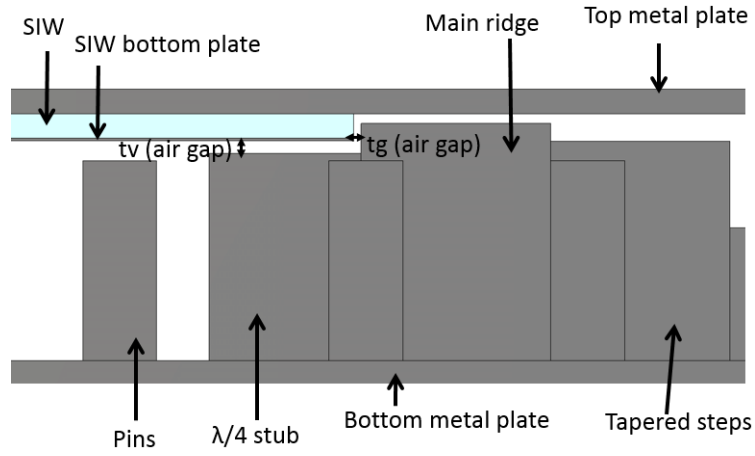

(a)

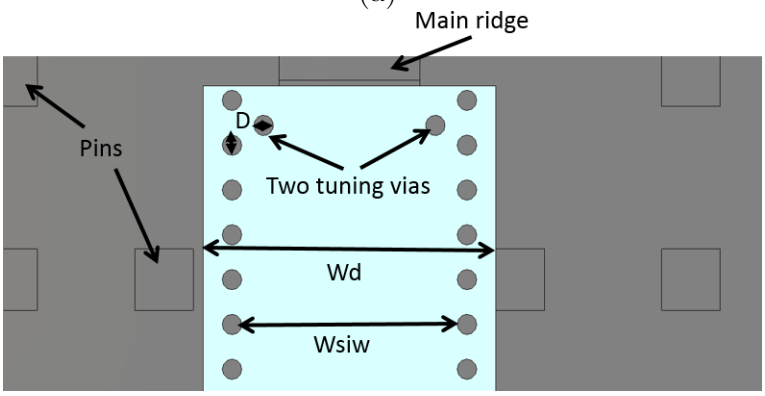

(b)

Figure 3.3: Zoomed: (a)Air gap separations in both horizontal and vertical directions, (b) (Top view) Two added plated vias

The single-mode transmission line network mode for the proposed transition is shown in Fig. 3.4, where reference number 1 represents ridge gap waveguide, reference numbers 2 and 3 represent SIW, reference number 4 represents the open-ended $\lambda_g/4$ stub, grounded to reference number 2 and the reference number 5 represent an open circuit (air gap between the ridge 1 and the SIW 2). The EM-field propagates in the ridge gap waveguide, a part of the field will direct go inside the SIW, while the other part of the field will propagate between the stub and the SIW's ground plane, reflect back and joins the field that could propagate directly inside the SIW.

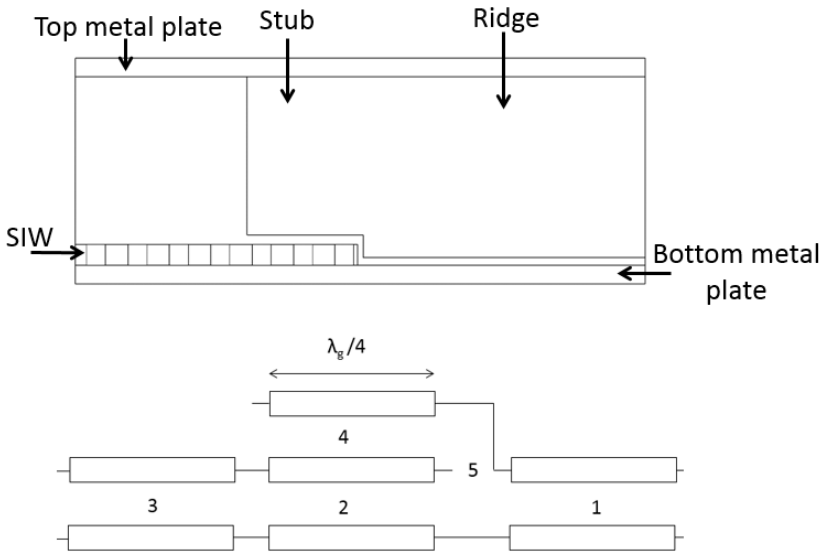

Figure 3.4: Simplified single-mode transmission line model of the (up-side down) ridge gap waveguide to SIW transition

3.3 Simulation Results

The transition is designed to cover the full W-band. The parameters of the gap waveguide part presented in 2.2 are kept the same in this transition design. The SIW has a shorted metal holes profile with holes diameter of D of 0.1 mm and period P of 0.22 mm. The CST

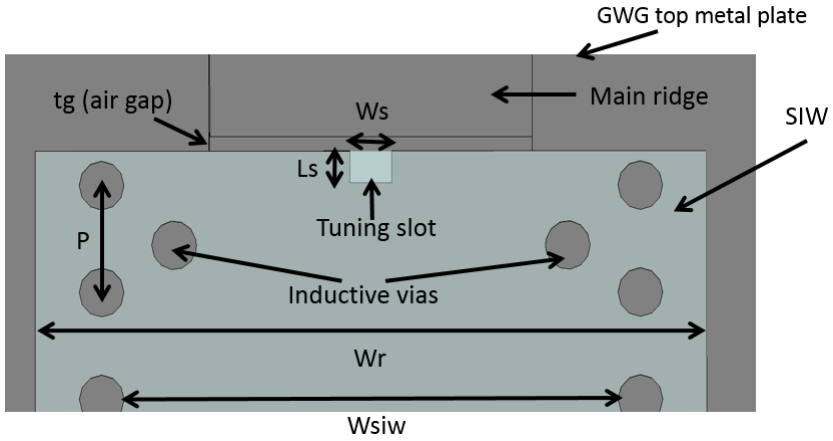

Figure 3.5: U-Shape tuning slot in the SIW metal plate (zoomed)

microwave studio is used to carry out the design and the simulation of the structure. The

width W_{siw} is 1.1 mm, while the width W_d of the dielectric substrate is chosen to be 1.5 mm, which is compatible and represents width of most commercial MMIC operates at mmWave frequencies.The SIW bottom metal plate consists a U-shaped non-metalized slot, which is a parameter used to tune the transition of TE_{10} inside the dielectric material to quasi-TEM of the ridge gap waveguide mode as shown in Fig. 3.5. Simulated S-parameters of the single transition design are shown in Fig. 3.6(a). Good transition performance covering the full W-band was obtained with very low insertion loss lower than 0.29 dB. Therefore, the scheme is very well suited for direct integration of passive waveguide components with MMIC.

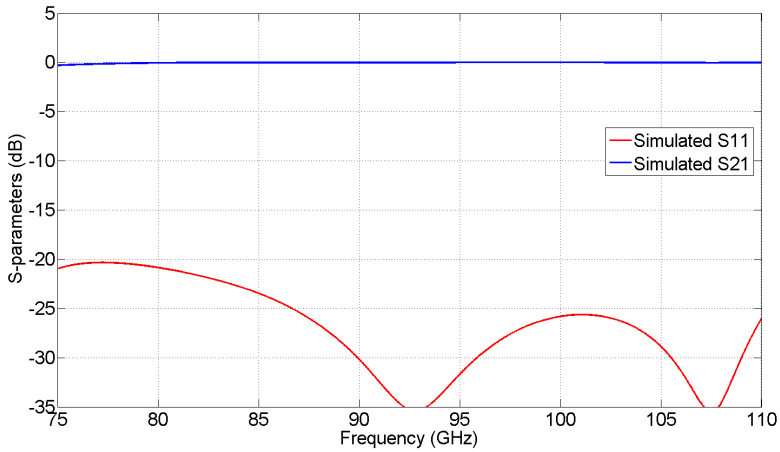

(a)

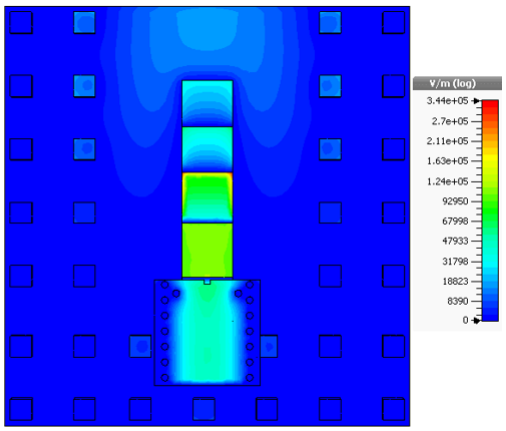

(b)

Figure 3.6: (a) Simulated S parameters of the proposed transition operating at W-band, (b) (Top view) Absolute value of coupled E-field between the SIW and the ridge gap waveguide

Fig. 3.6(b) shows the absolute value the electric field at the center frequency. The plot shows a smooth transition between the SIW and the ridge gap waveguide. The simulated S_{11} is below -21 dB over the entire band, while the insertion loss is better than 0.3 dB.

Chapter 4

Microstrip to Groove Gap Waveguide Transition

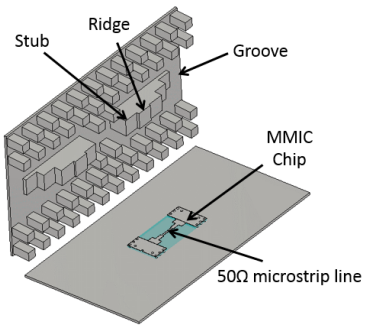

In the previous chapters, transitions between different parts of passive components (Ridge to Groove Gap Waveguide as in chapter 2 and SIW to Ridge Gap Waveguide as in chapter 3) have been designed. Simulation results showed good performances for both transitions at mmWave frequencies. Active elements such as amplifiers are fabricated using MMIC technology which is based on using planar technology such as microstrip line or coplanar waveguide. Transition between planar circuits such MMIC and non-planar circuits such gap waveguide is an important process in the integration of such active circuits. This chapter presents a full back-to-back transition from microstrip to groove gap waveguide based on the previous transitions presented in chapters 2 and 3.

4.1 Preliminary Transition Design

The main idea of this transition is based on electromagnetic coupling of the E-field or H-field from a 50 Ω microstrip line to a groove gap waveguide using intermediate transition step such as SIW to ridge gap waveguide in order to maximize the transformation of the

electromagnetic field.

The first part of the transition is the PCB part, which include the transition from a 50 Ω microstrip to SIW that will be directly attached upside down to the top meta plate of the gap waveguide. while the other part of the transition, is the ridge to groove gap waveguide that is completely presented in chapter 2. For the PCB part, both SIW and Microstrip PCB have the same dielectric material, 99.5 % alumina substrate material with dielectric constant of $\epsilon_r = 9.9$, the thickness of the substrate $h = 0.1$ mm and the width of $W_{\mathrm{d}} = 1.5$ mm, which is comparable to the width of most commercial MMIC circuits operating at mmWave frequencies. Fig. 4.1 presents the PCB part of the this transition, indicating the main design parameters.

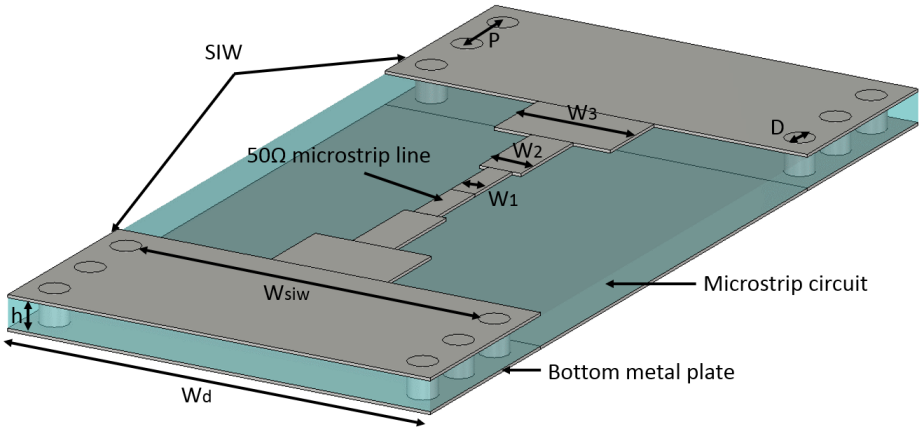

Figure 4.1: Bach-to-back Microstrip to SIW transition

SIW design for this transition is presented in chapter 3. The key parameters of the SIW design are the spacing between metalized holes P and the width W_{siw}. These parameters should be designed carefully to minimize radiation loss and the return loss. Since the propagation constant of the fundamental mode TE_{10} is directly related to the width of the waveguide, therefore the thickness of the SIW is kept at the thickness of h = 0.1 mm, which is the thickness of most of the MMIC chips operating at W-band. The microstrip portion consists of $\lambda_{\mathrm{g}}/4$ step-tapered microstrip sections which used to connect a 50 Ω line to the SIW. The step-tapered transformer transforms a standard 50 Ω microstrip line impedance to the SIW impedance, so that the Q-TEM microstrip line mode can be transformed smoothly into TE_{10} SIW mode. The electromagnetic field coupling between the SIW and ridge part of the gap waveguide will be done by the aid of an extra $\lambda_{\mathrm{g}}/4$ stub positioned below the air gap between the SIW part and the main ridge part, which

is presented in Fig. 3.3.

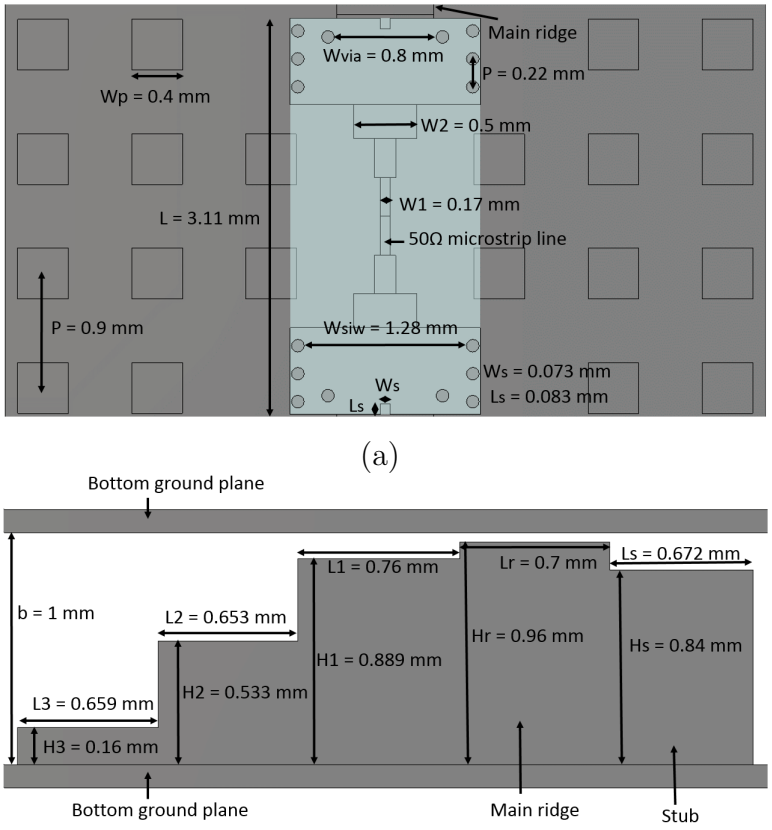

Figure 4.2: Microstrip to groove gap waveguide design parameters: a) (Top view) Microstrip circuit's design parameters (zoomed), b) (side view) Ridge gap waveguide design parameters

4.2 Simulation Results

The proposed transition (back-to-back) has been simulated. The width of the 50 Ω microstrip line W_{50} is 0.08 mm at center frequency f_o of 92.5 GHz for 9.9 dielectric constant. The key parameters that needs to be optimized are the the Chebyshev ridge transformer of the gap waveguide and the step-tapered microstrip line sections. The position of the tuning inductive vias and the U-shaped tuning slot in the ground plane of the SIW can influence

the performance of the transition. Both the slot size and the position of the tuning vias are optimized as well. Fig. 4.2 shows the design parameters of the back-to-back microstrip line to groove gap waveguide.

The simulated S-parameters of the back-to-back microstrip line to groove gap waveguide are presented in Fig. 4.3.

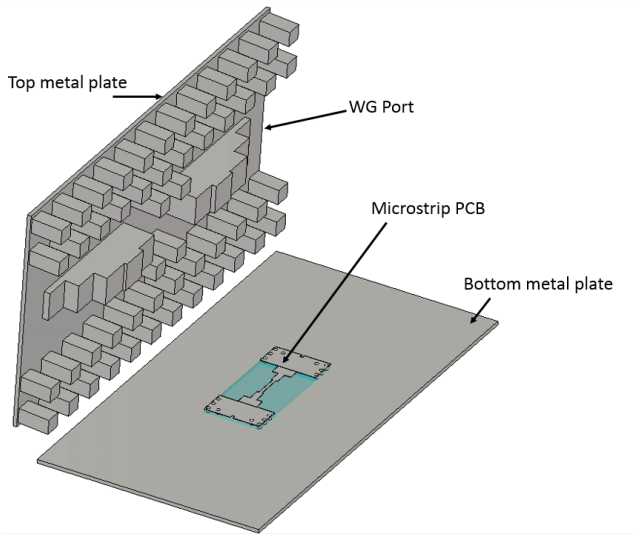

(a)

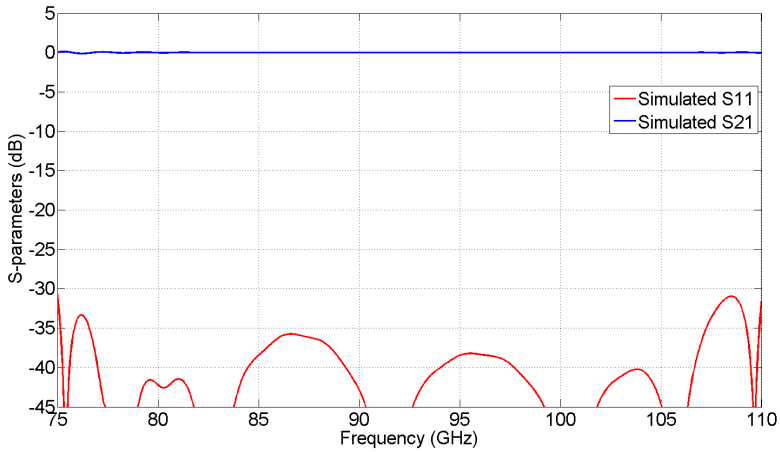

(b)

Figure 4.3: (a) Geometry of back-to-back Microstrip to Groove gap waveguide, (b) Simulated S-Parameters of back-to-back Microstrip line to Groove gap waveguide

As shown in the plot, the return loss is better than -30 dB achieved over the entire W-band, while the insertion loss values are less than 0.14 dB along the entire W-band, this

is due to the fact that the metal parts of the structure are considered as a perfect electric conductor condition and the dielectric material loss was ignored in the simulation. This design enhances the compatibility of integration of active components such as MMIC to the gap waveguide structure in a fast and an easy manner.

4.3 Parametric Study

Since the transition is achieved based on the electromagnetic field coupling through the air gap between the SIW and the ridge gap, parametric study in terms of S-parameters is presented. This study is done by sweeping the air gaps in both directions, horizontal t_g and vertical t_v as shown in Fig. 4.4. For the case of air gap between the SIW and ridge gap (t_g), the results are not exactly the same. The differences at lower frequencies are smaller compared to the differences at higher frequencies.

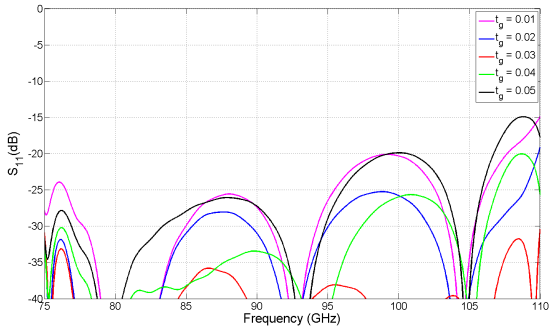

(a)

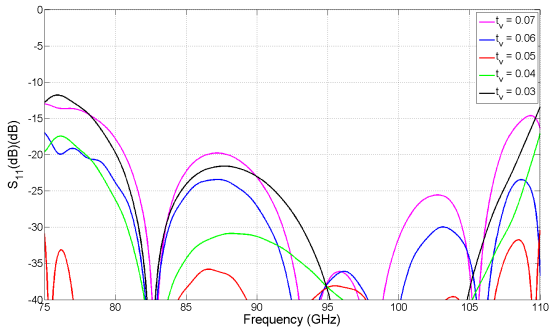

(b)

Figure 4.4: Parametric effects on the transition performance, (a) the effect of the air gap t_g ,(b) the effect of the air gap t_v

As a conclusion of this parameter effect, we observed that the using the air gap (t_g) (air gap in horizontal direction with respect to the SIW) within ± 20 μm, the S_{11} still good enough, and the values are below -20 dB for most of the W-band. This shown in Fig. 4.4(a). For the case of air gap between the SIW and the stub (t_v) (air gap in vertical direction with respect to the SIW), the results are quit different for both lower and higher frequencies for different values of t_v. The values of S_{11} are blow -15 dB for air gap t_v within ± 10 μm.

4.4 Modification in the Preliminary Transition Design

In order to manufacture the structure, typical metal milling is needed. Mechanical tools and mechanical tolerances at mmWave frequencies are critical and they will influence the design. The design needs to be robust enough to meet the mechanical requirements and the measurement process. Modifications will include both the gap waveguide part as well as the microstrip PCB part.

Bed of nails profile must has a spacing of 0.6 mm between two adjacent pins, where the milling tools can go through during milling process. In order to adjust this and keep the period of pins $p = 0.9$ mm, smaller pin width $w_p = 0.3$ mm will be used instead. This is better than changing the period, since we designed dispersion diagram of pin structure based on periodicity of $p = 0.9$ mm and this is presented in section 2.1. The four extra pins at the middle of the structure will be replaced by two pins, in order to follow the manufacturing specifications. Moreover attaching the PCB part in the exact position is critical and difficult. To reduce the misalignment between the PCB and the ridge part of the gap waveguide section, a groove with the same dimensions as the PCB size in the top metal plate is designed. Note that the groove must have a depth equivalent to the thickness of the glue or soldering layer that will be used to attach and hold the PCB to bottom metal plate, which is approximated as $h_g = 0.018$ mm. These modifications are presented in Fig. 4.5. As seen in Fig. 4.5b, four Mickey-Mouse ears are add at the corners of the alignment groove where the milling tool can continue a bit more in the corner and return. Furthermore, the RF components dimensions at mmWave frequencies shrink and they become critical and are difficult to manufacture. Therefore, the PCB part should be

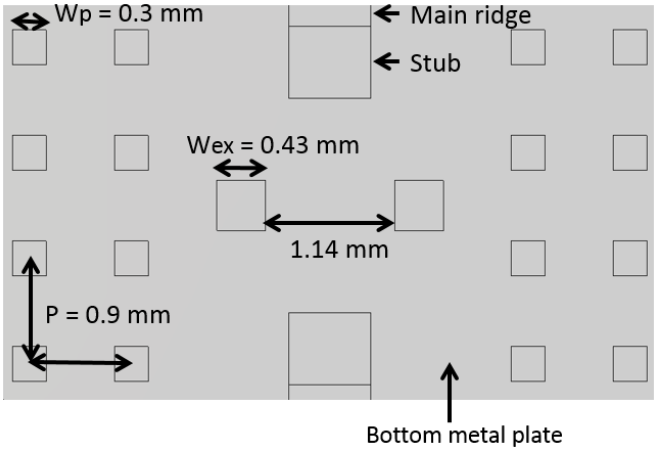

(a)

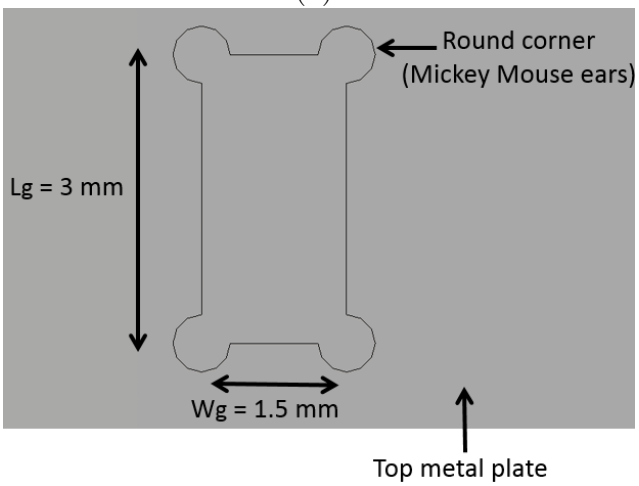

(b)

Figure 4.5: (a) (Bottom view) Changes in the pins sizes and the two extra pins used instead of four pins, b) (Top view) Top metal plate with the groove for PCB alignment

redesign in order to meet the manufacturing requirements.

As presented in Fig. 4.6, dielectric substrate thickness of $h = 0.1016$ mm should be used instead. Another specification we need to follow is the metallization part. A metallization of width $w_m = 0.0254$ mm from the edges should have a thickness of $t_m = 0.001$ mm, due to specification on the dicing of the PCB in order to minimize the burrs during dicing process. Note that all other metallization parts used for the PCB have a thickness of $t = 0.01$ mm. Fig. 4.7, shows the manufactured PCB, where the modification at the edge is appeared. Tolerance at the edge decreased, and this due to dicing tools, but it is accepted. To employ the measurement setup, an additional matching step is

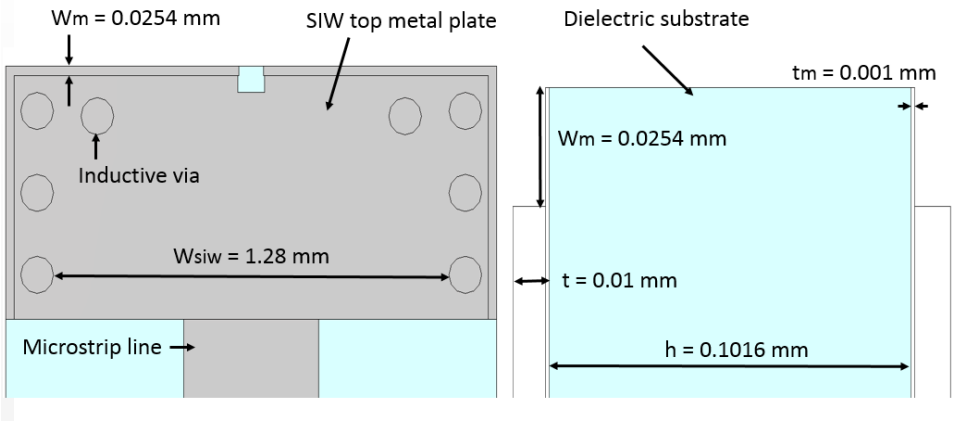

Figure 4.6: (Left) is the front view of the PCB layout (zoomed), (Right) is the side view presenting the thickness of the metal layer (zoomed)

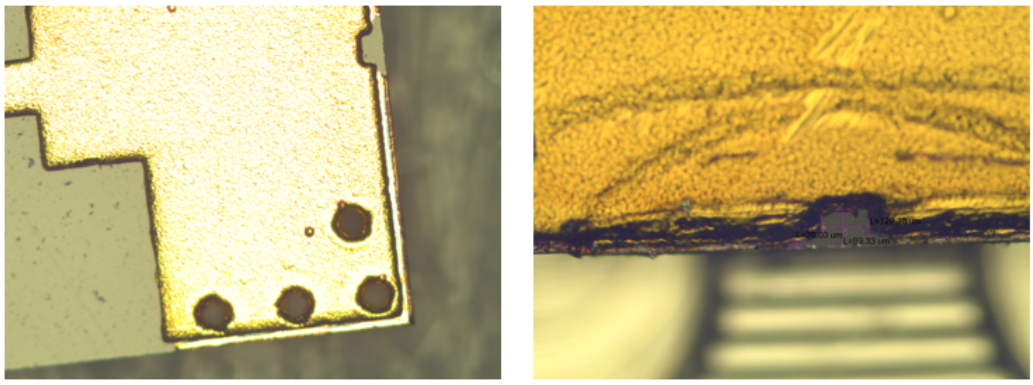

Figure 4.7: PCB manufacturing tolerances: (Right) shows the tolerances for metalized vias and the metal thickness at the edges, (Left) (zoomed) shows the manufacturing tolerances for the tuning slot

considered in order to connect the structure with a standard flange of WR_{10}. Matching step is a grooves in the top and bottom plate of the gap waveguide, which makes the height of groove gap waveguide same as that of standard WR_{10} waveguide. Moreover two small ridges needed to be designed at the middle of the matching grooves in order to minimize losses due to reflections at the ports. One more step should be consider to connect the standard flange WR_{10}, the last row of pins which is closer to the port should be replaced closer, where the separation between the two columns are equal to the standard WR_{10} opening of $b = 1.27$ mm. These changes are presented in Fig. 4.8.

The redesigned structure has been simulated. Changes in order to follow the manufac-

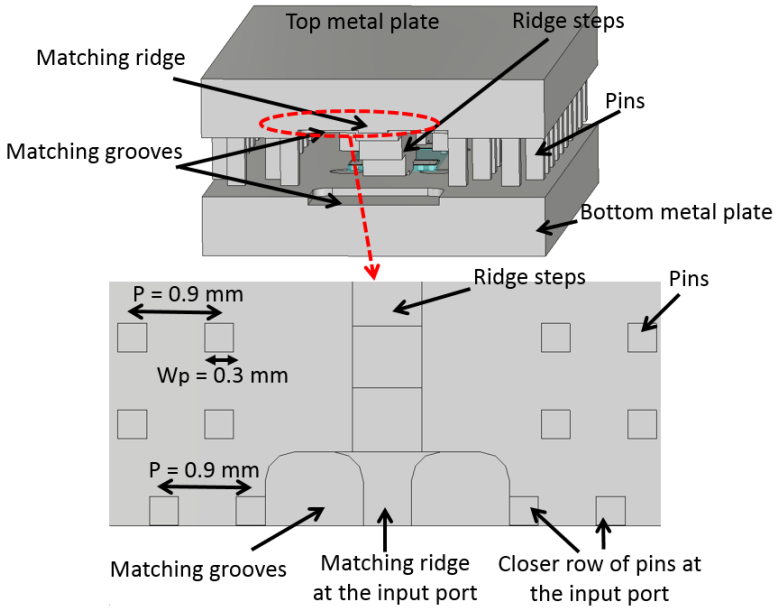

Figure 4.8: (Top), Matching grooves and the matching ridge at the port of the gap waveguide (zoomed), (Bottom), Changes in the pins profile at the port to match WR_{10} standard flange(zoomed)

turers specifications affect the overall transition performance. Most of the design parameters are optimized again. Fig. 4.9 presents the simulated S-parameters of the back-to-back structure. The PCB part has a width of $W_d = 1.5$ mm and length of $L_d = 3$ mm, which is suited for most commercial MMIC. As we can see, S_{21} did not affect by the changes, while S_{11} has values below -20 dB over the entire band. The degradation is due to the additional steps at the waveguide port, which may cause extra reflections.

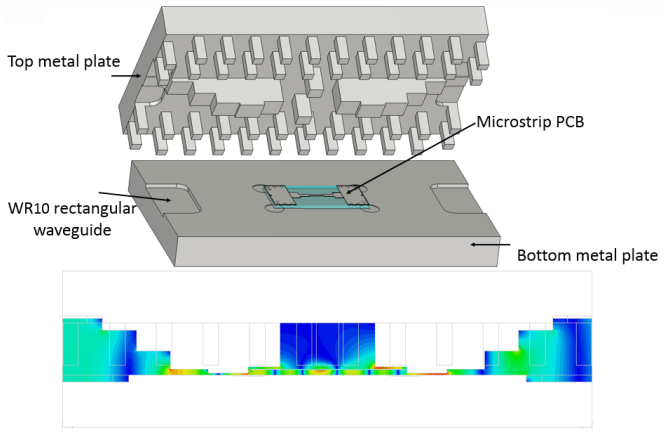

(a)

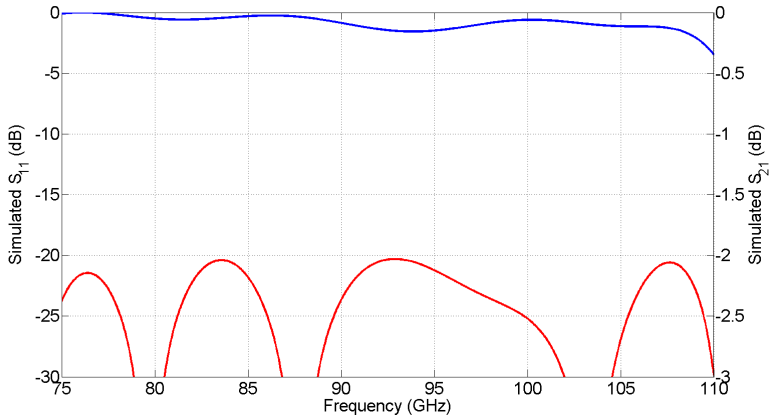

(b)

Figure 4.9: (a) Modified geometry of back-to-back Microstrip to Groove gap waveguide and the field distribution inside the structure, (b) Simulated S-Parameters of back-to-back Microstrip to Groove gap waveguide

Chapter 5

Manufacturing and Measurement

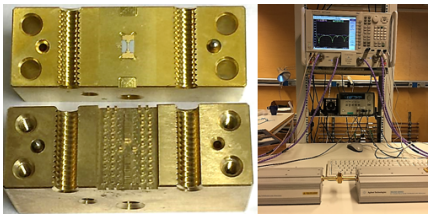

In chapter 4,the back-to-back transitions between microstrip line to groove gap waveguide using electromagnetic coupling, has been proposed. In order to validate the transition design, this chapter include the process of fabrication and the measurement steps using high performance VNA. The measured results will be compared with the simulation results. A part of this chapter will focus on the challenges that we faced to get the match between simulated and measured results and the way how we could to investigate and solve the degradation in the performance

5.1 Prototype and Assembly

The gap waveguide prototype shown in Fig. 5.1(a) has been manufactured by using aluminium material, using CNC milling machine, with machining tolerances were small in the micron level. Two extra alignment pins were added, in order to aligned the two parallel metal plates of the structure. Moreover, in order to provide a good alignment when we connect the flanges during measurement, two alignment holes were added on both ends of the structure.

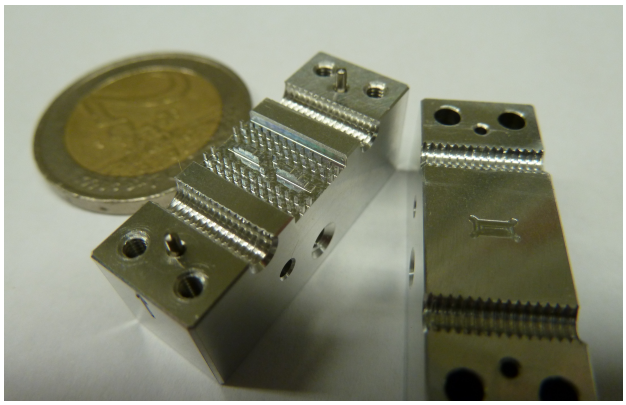

(a)

(b)

Figure 5.1: (a) Prototype of the back-to-back gap waveguide structure used in the transition, (b) Prototype of the microstrip PCB used in the transition

Fig. 5.1(b) shows the manufactured PCB using Thin-Film Technologies. A polished Alumina substrate of 99.6 % purity with permittivity of $\epsilon_r = 9.8$ and loss tangent of $\tan\delta = 0.0002$ measured at 10 GHz. Alumina is a ceramic material, which provides good chemical and mechanical capabilities and it supports both, laser and dicing tools. According to the manufacturer, in the dicing process, there will be some burrs will appear in the metallization layer closer to the edges, they may be up to 25.4 μm pullback at the edge that is void of metal, so they do not dice through metal, since the dicing accuracy is not good enough to maintain < 25.4 μm. In order to keep metallization extends to the edge, a 0.76 μm layer of copper will be sputtered at the edge, for that thickness, burrs will be minimal. In Fig 5.2, we can see the effect of dicing at the edges.

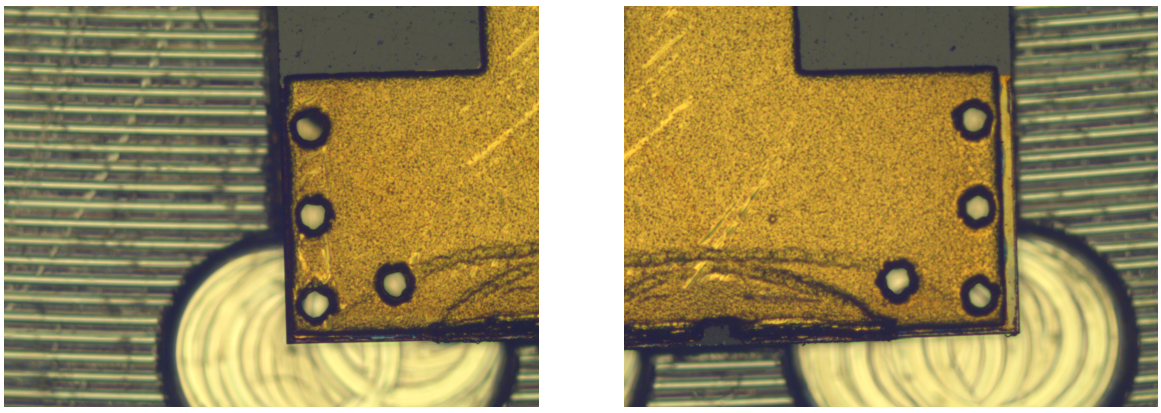

Figure 5.2: The effect of dicing process at the edge and the metallization copper layer to minimize the effect of dicing

The measured tuning slot size as, L_s is around 0.099 mm, while the width W_s is around 0.129 mm. The tuning slot does not affect the whole transition performance, it has a minor effect, but it used to improve the operating bandwidth of the transition. The measured plated via holes dimensions are within the designed dimensions range $\approx$ 0.11 mm, which were done by using laser beam to drill the holes, and then plated by using gold material.

The two structures, the gap waveguide and the PCB, were put together using a conductive epoxy resin. Fig. 5.3 shows the complete structure with attached PCB inside the guiding groove in the top metal plate of the gap waveguide. The depth of the groove was designed to be match to the thickness of the conductive epoxy resin layer. Manual assembly is considered an extremely critical process at mmWave, where the tolerances in the range of 20-50 μm, which is challenging to control and it is not an optimal method to assembly RF circuits at mmWave frequencies.

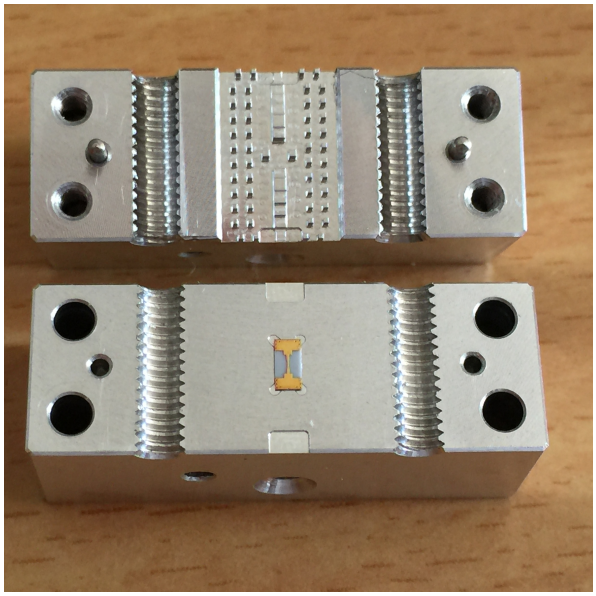

Figure 5.3: The complete structure, Microstrip line to groove gap waveguide before the assembly and the measurement

5.2 Measurement Results

The prototype has been measured using PNA-X, Agilent performance network analyzers connected to the two OML extension Modules designed for WR-10 flanges (75-110 GHz)

as shown in Fig. 5.4(a) . A TRL (Thru-Reflect-Line) standard calibration process at the W-band was applied. The purpose of the calibration is to remove the effects of the cables and connectors which used during the measurement and to start the measurement at the end standard flange, WR_{10}. Fig. 5.4(a) shows the measurement setup, while Fig. 5.4(b) shows the measured S_{11} and S_{21}. In Fig. 5.5, we plot the simulated and the measured results together, it is clear to see the mismatch between the simulated and measured S-parameters of the transition. There are different possibilities behind this mismatch and the degradation in system performance needs to be investigated.

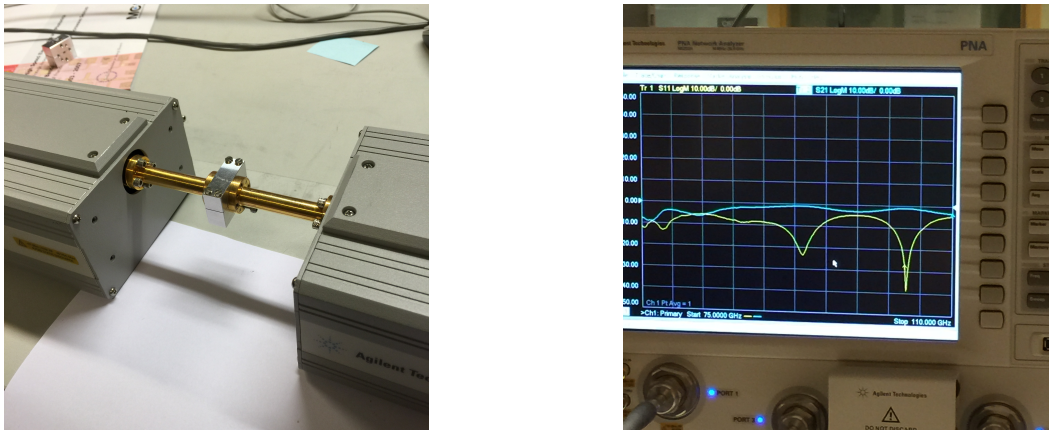

(a) (b)

Figure 5.4: (a) Measurement setup, (b) The measured S_{11} and S_{21}

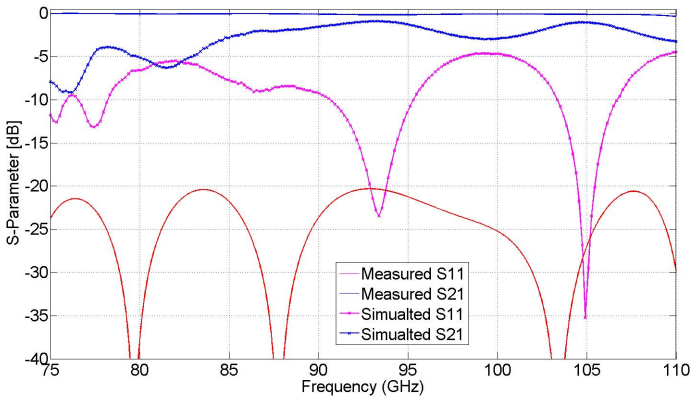

Figure 5.5: Simulated and measured S-parameters of back-to-back Microstrip line to groove gap waveguide transition

We had some doubts regarding the electrical contact between the PCB ground plane and the aluminium plate, since a typical aluminium oxide layer acts as an isolation layer.

The used conductive epoxy resin in the assembly process was permanent, and it might be possible this layer of epoxy could not provide a good electric contact between the PCB ground plane and the aluminium plate. The direction was to manufacture a new prototype, a copy of the aluminium one, by using the brass material instead of the aluminium. The manufactured prototype is shown in Fig. 5.6. The PCB was mounted using a high conductive glue, which could be easily to replace the PCB, in the case if we have assembly failure. A comparison between the simulated and measurement results is presented in Fig. 5.6. An enormous value of loss was observed and the matching between simulated and measured S_{11} was not good. This means that, the actual problem was not regards to the electric contact between the two ground planes. Different parameters have been studied in order

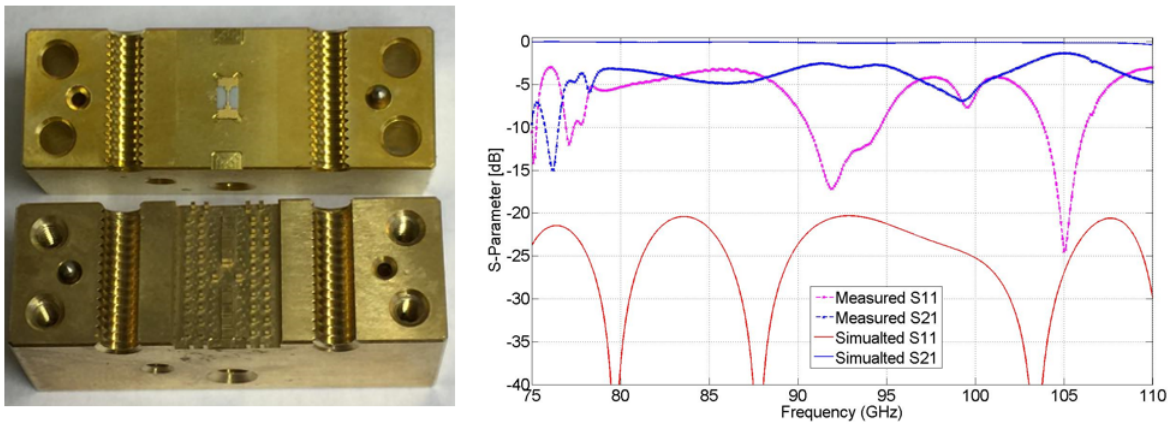

Figure 5.6: Brass prototype of microstrip to groove gap waveguide transition and the simulated and measured S-parameters

to figure out what was happened. The degradation in the transition performance needs to be investigated through the input ports. Briefly, port misalignment must be studied, the term, port misalignment, particularly done by swept the port in both vertical and horizontal directions in the ranges of $\pm$ 25 μm. The swept results are shown in Fig. 5.7, the mismatch at the port interface has a larger effect at the higher frequencies, since discontinuities have larger effects on shorter wavelengths. After port tolerances investigation, shortly, we conclude that the degradation in the transition performance and the excess reflection characteristics have not limited by the mismatch and misalignment at the port interface. A small separation gaps in the range of 15 μm between the waveguide ports and the structure inputs leads to $\leq$ 2 dB leakage loss and a almost negligible reflection loss, where $S_{11} \leq$ -15 dB over most the entire band. The demonstration plot is shown in Fig. 5.8 represents the effect of gap separation due to mechanical tolerances during the

measurement.

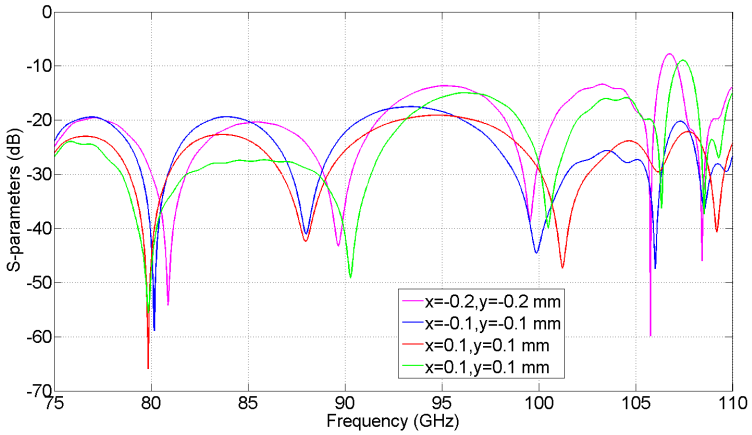

Figure 5.7: Brass prototype of microstrip to groove gap waveguide transition and the simulated and measured S-parameters

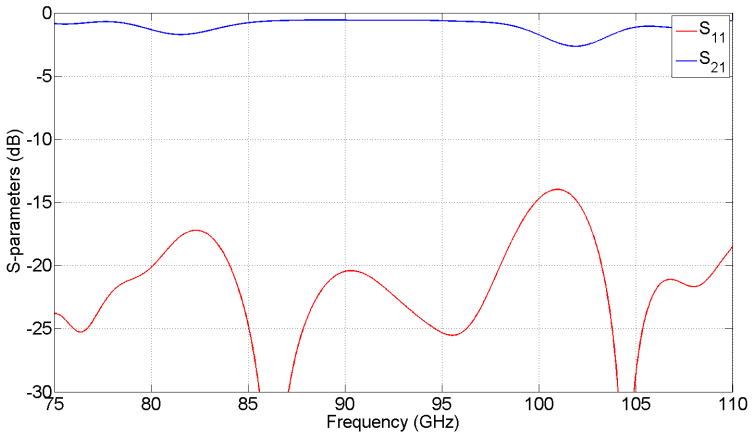

Figure 5.8: S-parameters simulation for 15 μm air-gap separation between the waveguide port and the the input of the structure

From the plot we can conclude that, a small gap between the structure and the standard flanges will lead a part of the power to leak outside the structure and thereby, degrade the system performance. To overcome misalignment problems, a most recent contactless pin flanges [34, 35] will be used in order to eliminate the leakage. The pin waveguide flange operating at W-band is shown in Fig. 5.9. The contactless pin flange has the property of being easy to include in the measurement equipment setup, moreover, the fastening screws can be avoided during the measurement, but just keeping the prototype

and the pin flanges cramped together. The measurement arrangement and the measured S-parameters are shown in Fig. 5.10

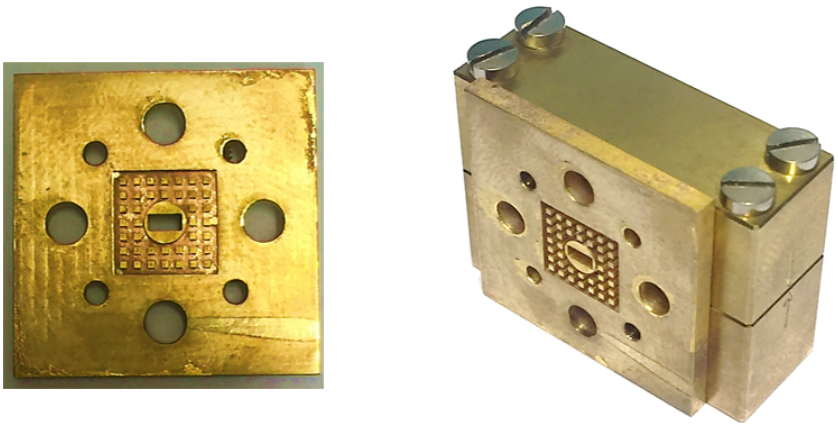

Figure 5.9: Contactless pin waveguide flange operating at W-band and the arrangement of the pin flange with the prototype to be measured

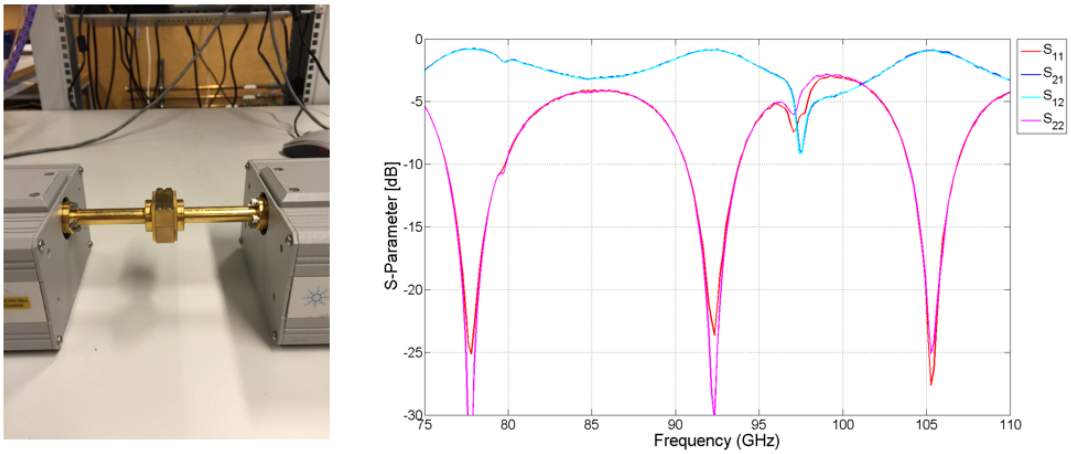

Figure 5.10: The prototype under test and the S-parameters simulation for 15 μm air-gap separation between the waveguide port and the the input of the structure

Better performance in terms of leakage and matching was observed, specially at the lower frequencies < 80 GHz.In order to complete the comparison between the simulation and the measurement results, one can have a look at the phases characteristics of the two results. Fig. 5.11 shows the results for both of transmission coefficients S_{21} phases and of reflection coefficients S_{11} as a function of frequency. The results show a very small phase difference between the simulated and measured transmission coefficients. However,

the phase difference in the case of simulated and measured reflection coefficients is large. Many designed factors will contribute in degradation of the system phase performance and these factors need to be investigated.

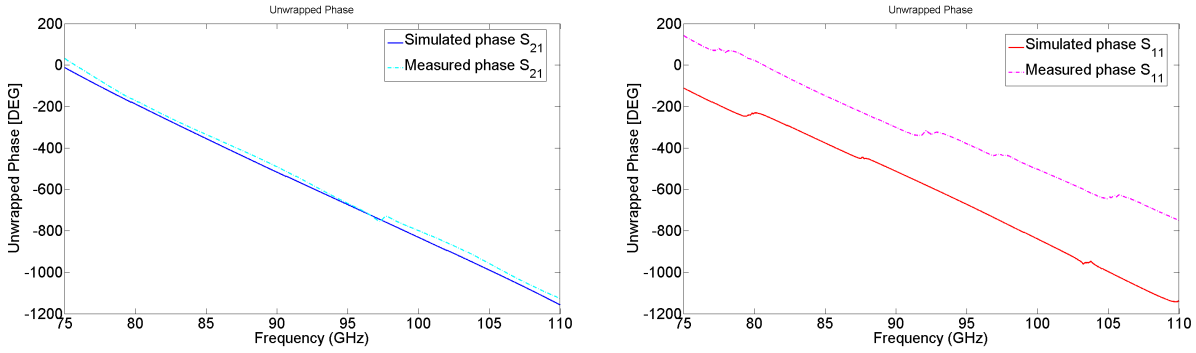

(a) (b)

Figure 5.11: (a) Unwrapped phases for both simulated and measured transmission coefficients S_{21} , (b) Unwrapped phases for both simulated and measured reflection coefficients S_{11}

Another parametric study was done to investigate the effect of dielectric constant of the substrate on the transition performance. The relative permittivity of the alumina was swept in the range between ϵ_r =7-11. The simulation result is shown in Fig. 5.12. It is clear from the simulation that the performance will be changed if the dielectric constant of the substrate is altered. This simulation result motivated the study to be focused on the PCB part.

A useful test we could try is to remove the PCB from the structure and simulate the magnitude and phase of the return loss, then, these simulation results will be compared with the measured results of the same case, no PCB inside the structure. This step will give us a better explanation about the behaviour of the structure without any dielectric material inside. The return loss will be theoretically almost 0 dB, since the field will reflect back from open-circuited stub, a few power will travel through the structure, but this amount of power can be negligible. Fig. 5.13 shows a good match between the simulation and measurement in terms of S-parameters.

Unwrapped phase in Fig. 5.14 illustrates the phases match between simulated and measured results of S_{11} and S_{21} in case of no PCB was attached in the structure. A very small phase difference between the simulation the the measurement, this is due to

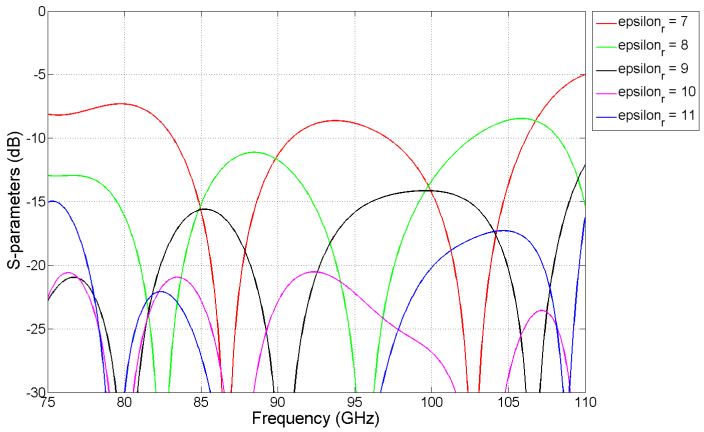

Figure 5.12: S-parameters simulation for different values of dielectric constant of the alumina substrate

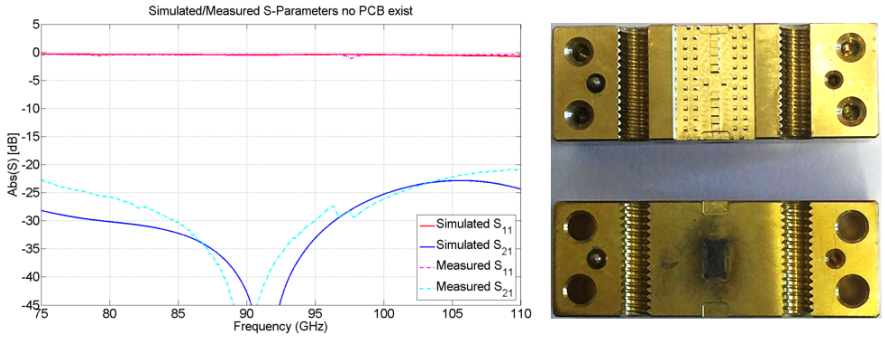

Figure 5.13: Comparison between simulated and measured S-parameters of back-to-back transition, in the case of no PCB is attached inside the structure

system calibration and the measurement setup. From those results we can say that, the degradation in the system performance is mainly due to the PCB, which may be have different permittivity as well as different loss tangent, or it might has different dimensions.

5.3 Comparison with Rectangular Waveguide

In order to check if there is a difference in the transition performance, we compare the transition using gap waveguide technology and the same transition using conventional rectangular waveguide, having the same dimension. The rectangular waveguide was man-

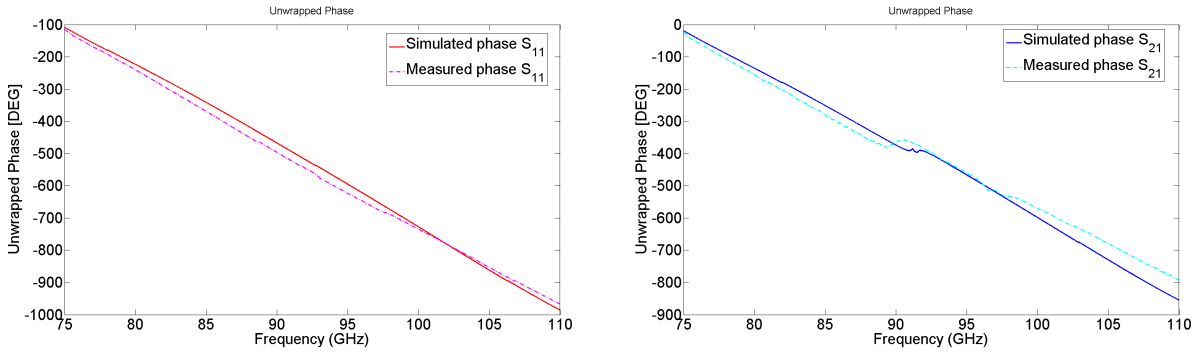

(a) (b)

Figure 5.14: (a) Unwrapped phase for simulated and measured S_{11} in case of no PCB is attached inside the structure, (b) Unwrapped phase for simulated and measured S_{21} in case of no PCB is attached inside the structure

ufactured in the same process as the gap waveguide one, we had used. All dimensions are kept the same to compare between the two devices correctly. Fig. 5.15 shows the manufactured prototype.

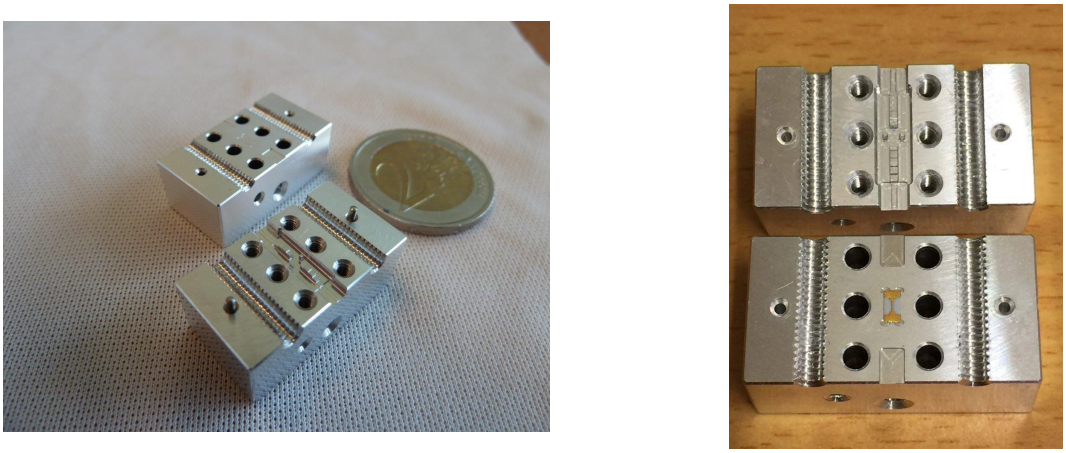

(a) (b)

Figure 5.15: (a) The rectangular waveguide prototype, (b) Microstrip line to waveguide back-to-back transition

The measured result gives a different performance in term of losses and the result can be seen in Fig. 5.16. The insertion loss is in the average around 1.5 dB over the entire W-band, except the at upper frequency 110 GHz, where the insertion loss is about 2.2 dB. The S_{11} is almost as the same as the S_{11} of the same transition using the gap waveguide. The S_{11} has values $<$ -10 dB at frequencies below $<$ 95.7 GHz.

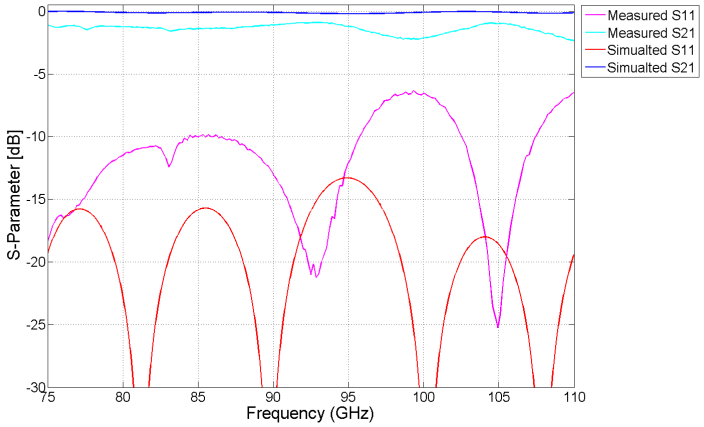

Figure 5.16: Simulated and Measured S-parameters of the back-to-back Microstrip line to rectangular waveguide using waveguide pin flanges

Chapter 6

PCB Characterization

In previous chapter 5 we investigated issues in defining the problem regarding the mismatch between the simulation and the measurement results and we concluded that the PCB is the main cause behind the degradation in the transition performance. However, in the present chapter we will define and compare various study parameters of the PCB and their contribution to the system performance. PCB comprises of a 50 Ω microstrip line to SIW transition with step tapered microstrip line. Practically this PCB suffer from three main types of losses, which are, conductor loss in the metallization part of the PCB, dielectric loss in the alumina substrate and the radiation loss which could be ignored in this design. The first two types will be considered in this study.

6.1 Impacts of PCB Metallization

To have a better problem formulation and more accurate assumptions, we try to build a circuit representing transmission line mode. The simplified model is represented as parallel plate separated by an air of constant thickness all over the specified length. The model is represent the section of PCB metal layer and the open-ended stub as shown in Fig. 6.1. The discrete lumped-element circuits represent the transmission line parameters.

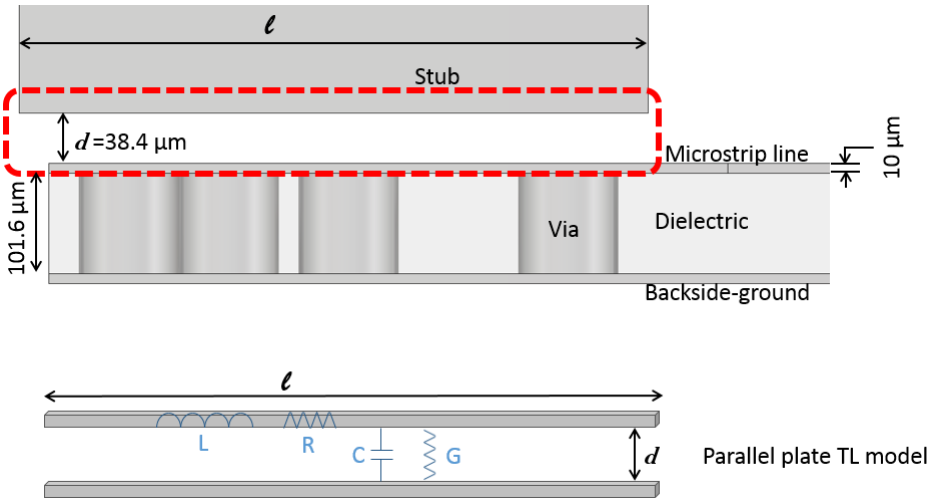

Figure 6.1: the designed air gap between the open-ended stub and the PCB, which is represent as parallel-plate transmission line model of length l and the air separation thickness is d, with the equivalent lumped elements

The impedance Z_o of the line can described as a function of the line parameters as

$$Z_o = \sqrt{\frac{R + j\omega L}{G + j\omega C}} \tag{6.1}$$

As presented in [36], these line distributed parameters can be expressed in terms of the line length l and the separation thickness d as

$$R = \frac{2R_s}{l} \tag{6.2a}$$

$$L = \frac{\mu d}{l} \tag{6.2b}$$

$$G = \frac{\omega \epsilon'' l}{d} \tag{6.2c}$$

$$C = \frac{\epsilon' l}{d} \tag{6.2d}$$

The air-filled space between the two conductor plates has $\epsilon^{"} = 0$, $\epsilon^{'}$ =1 and $\mu = 1$, thereby the main factors that affect the line impedance are the length of the line, the separation between the two conductors and the operating frequency as illustrated in equations 6.2[a-d].

In the transition design l represents the length of the stub, which ideally, it should has l=$\lambda/4$, in order to create an infinite load impedance (open-ended transmission line).

Afterwards the stub length is tuned in order to get a better match and a wider bandwidth. The metallization thickness was designed to has a value of t=10μm as shown in Fig. 6.1. Fig. 6.2 shows the measured metallization thickness of the manufactured PCB under the microscope. It shows that the measured metallization thickness is about

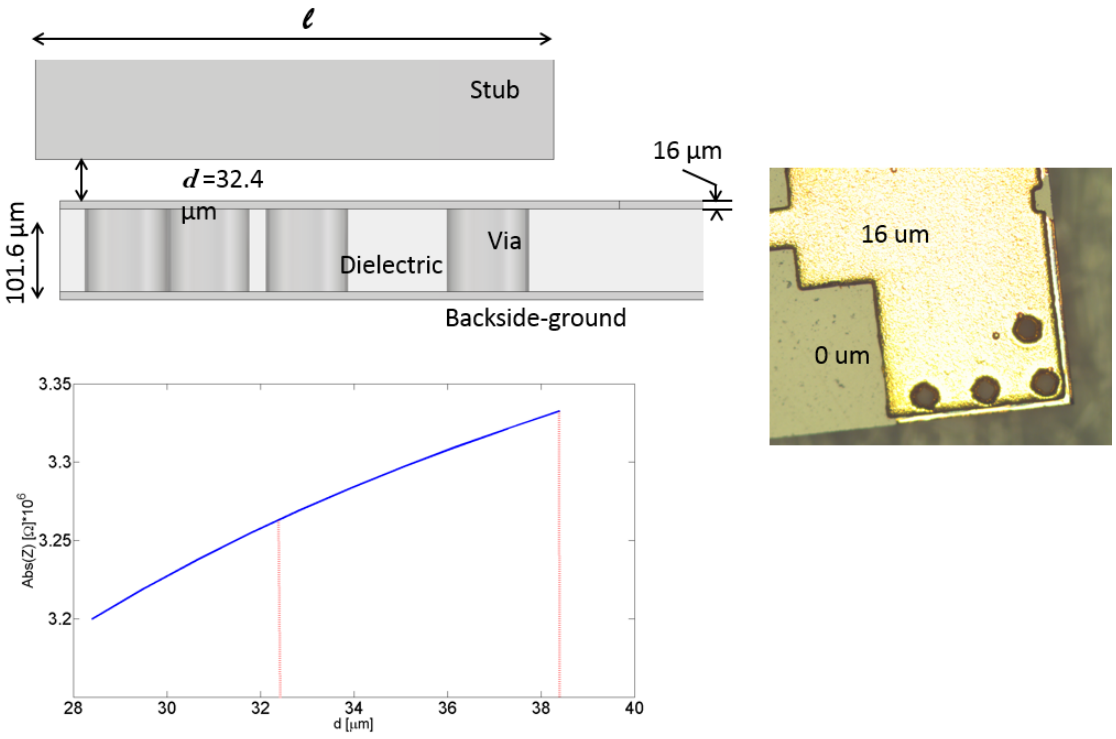

Figure 6.2: Zoomed CST model showing the air gap underneath the open-ended stub and the microscopic image representing the measured metallization thickness and the plot shows the line impedance variations

t =16 μm, thereby we have about 6 μm reduction in the separation between the conductors (air gap between the the stub and metal layer of the PCB. This of course will affect the line impedance 6.1,therefore, the impedance decreases as the air gap between the stub and PCB decreases, and impedance mismatch at the designed frequency (92.5 GHz) will result in a poor return loss, where the simulated S_{11} has a value of -13 dB. In 50 ohm microstrip circuit, thicker metallization (if we consider the signal line only), cause differences in frequency specially at the higher frequencies above 100 GHz as illustrated in Fig. 6.3. The last two dips in S_{11} at 103.5 GHz and at 110 GHz have shifted down to 99 GHz and to 109 GHz respectively.

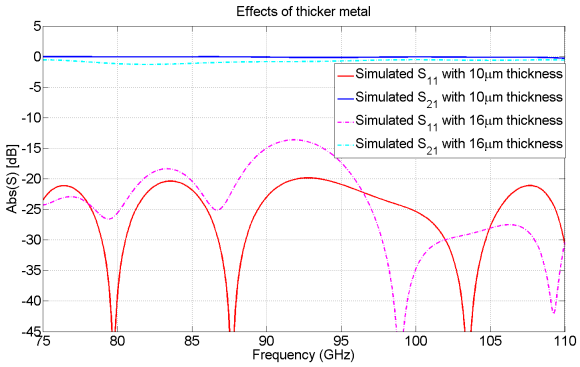

Figure 6.3: S-Parameters for the designed transition and for the case of 16μm PCB metallization thickness

Another factor to take into account at mmWave, is the surface roughness, which increases the surafce impedance and thereby more extra loss will be added to the performance. In order to examine the surface roughness, a microscopic images were taken and they are illustrated in Fig. 6.4. As we can see the surface was not well finished and at some points the metal thicknesses are extremely thin almost zero, which will have adverse effect on the system performance.

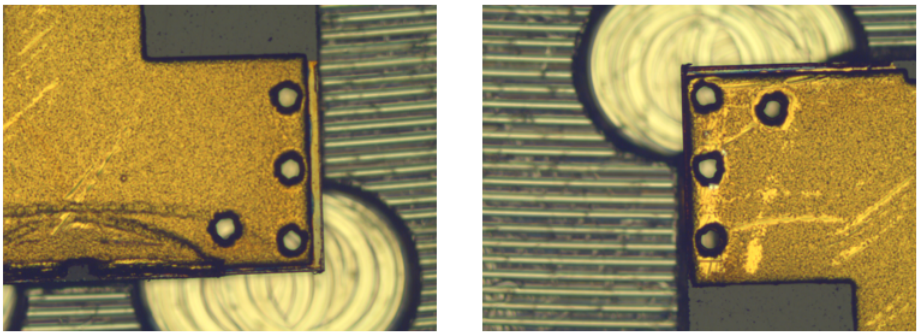

Figure 6.4: Microscopic images of two different parts of the PCB top metal surface

6.2 Impacts of PCB Dielectric Material

We can analyze the effects of substrate parameters on the system performance in two different ways, the first way is to study effect of changing the substrate dimensions and

the second way is to study the effect of changing the substrate permittivity.

The transition has been designed by using the substrate thickness of 101.6 μm and the manufacturer agreed to fabricate the PCB with this thickness. However the microscopic measurements showed that the manufactured PCB has a dielectric thickness lies in the range between 123-125 μm. These changing in the thickness will affect the thickness of air gap between the open-ended stub and the PCB, therefore affecting the impedance as described in the previous section. Inserting the average value 124 μm in CST and compare the S-parameters at this value with the designed value. Fig. 6.5 shows the effect of increasing the dielectric substrate thickness on the system performance. As we can see,

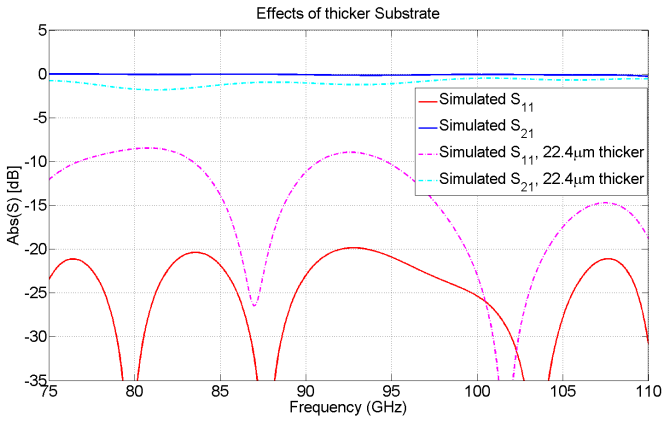

Figure 6.5: Simulated S-parameters, showing the effect of changing dielectric thickness on the transition performance

S_{11} went up to -9 dB and S_{21} went down to has a value of -1.9 dB at frequency of 80.7 GHz. The frequency shift is about 1.8 GHz toward lower frequencies.

The second alternative that has an impact on the system performance is the dielectric substrate relative permittivity and the loss tangent. The values of these two important parameters are not constant value, but they are frequency dependent. However, the available data for the alumina material from manufacturer is only at 10 GHz. According to the study done in [37], the permittivity and the loss tangent of the alumina substrate permittivity will be reduced by increasing the operating frequency, as well as the loss tangent will be increased. It shows that the dielectric constant reduces down to ϵ_r =9 and the loss tangent increases up to tanδ =0.05. The difference in the permittivity of the alumina at different frequencies (75-110 GHz) will result in different propagation performance and thereby, the transition performance will be affected as shown in Fig. 6.6. Now we will examine the

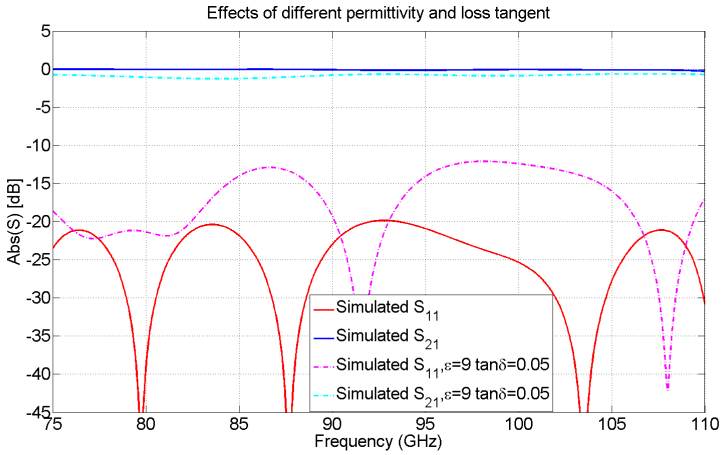

Figure 6.6: Simulated S-parameters, showing the effect of changing dielectric permittivity and loss tangent on the transition performance

phase parameter that gives more efficient explanation about changing the dielectric permittivity and loss tangent. This parameters will be directly effected by the permittivity of the dielectric. Fig. 6.7 shows the simulated phases of S-parameters.

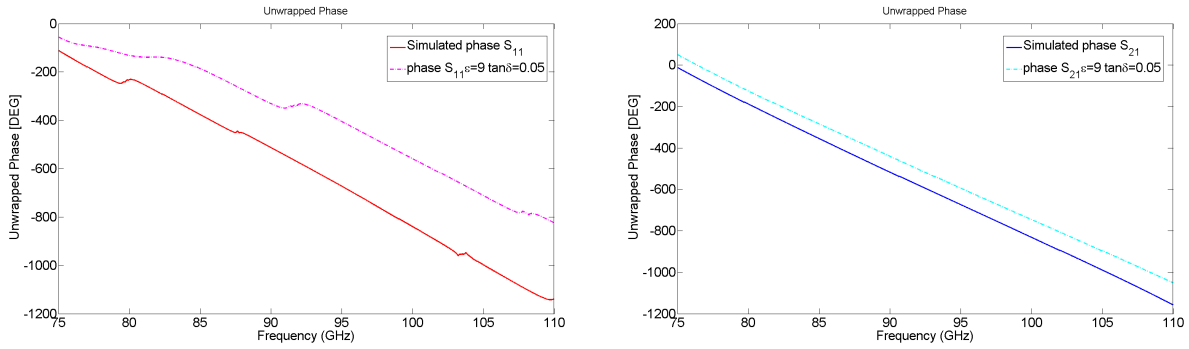

(a) (b)

Figure 6.7: (a) Simulated S_{11} phases, (b) Simulated S_{21} phases

As we can see the phase is directly proportional the permittivity of the substrate, and is described as

$$\phi = \beta l \tag{6.3a}$$

$$\phi = \frac{2\pi f_o}{c}\sqrt{\epsilon} l \tag{6.3b}$$

Combining both changes, the dielectric material properties and the physical measured dimensions of the PCB in the simulation, the result is illustrated in Fig. 6.8.

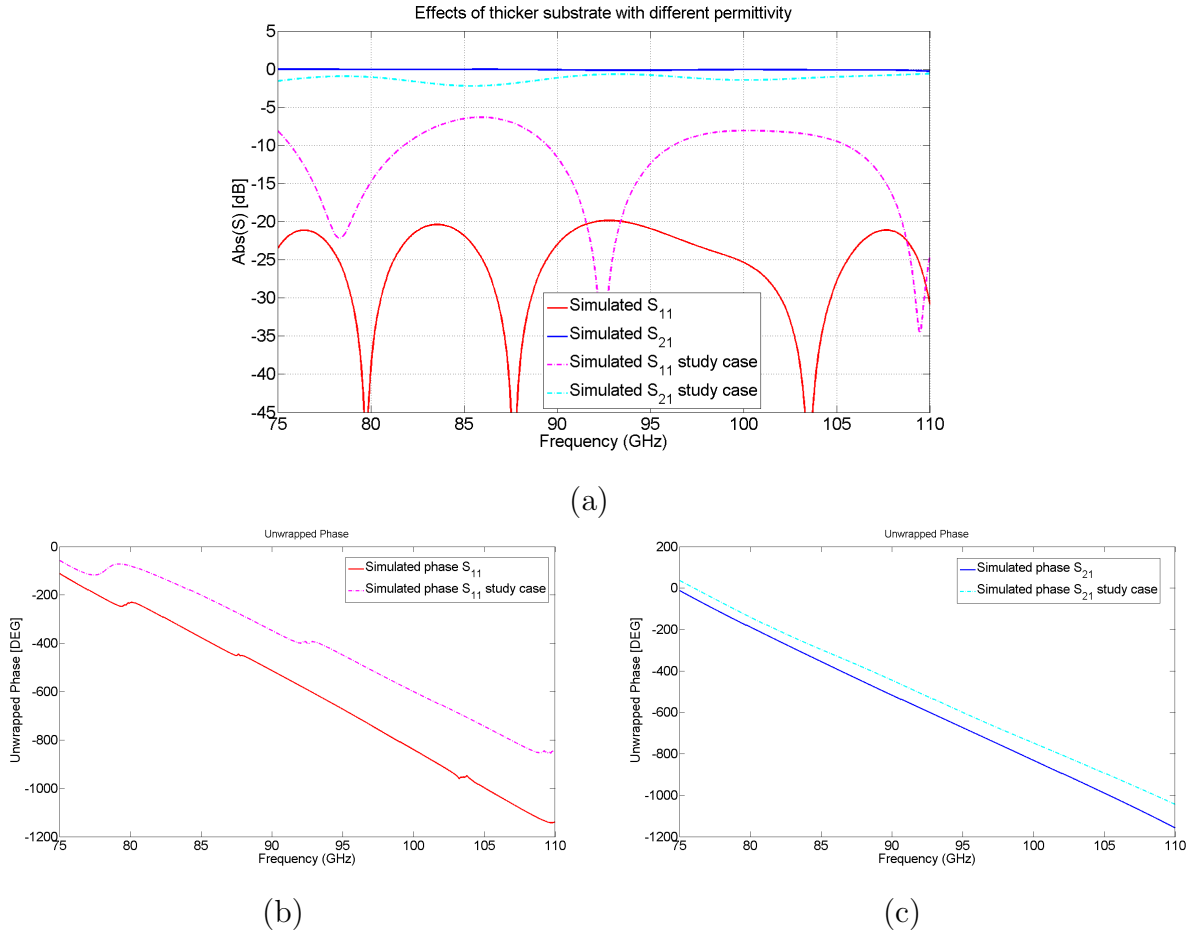

Figure 6.8: (a) Simulated S-parameters for the both designed transition and the study case, (b) Simulated S_{11} phases, (c) Simulated S_{21} phases

Finally we will combine all those effects and build a model that could match the measured prototype and simulate this model. Fig. 6.9 shows the simulated model and the measured prototype S-parameters. As you can see the simulated model shows a good match between the measured prototype and simulating S-parameters including the changes, ϵ_r =9, tanδ =0.05 and the alumina with thickness 0.124 mm. We have 4 GHz frequency shift toward the higher frequencies and this is due to some other tolerances which are not included in this study. these tolerances might be due to the assembly or due to gap waveguide milling tolerances.

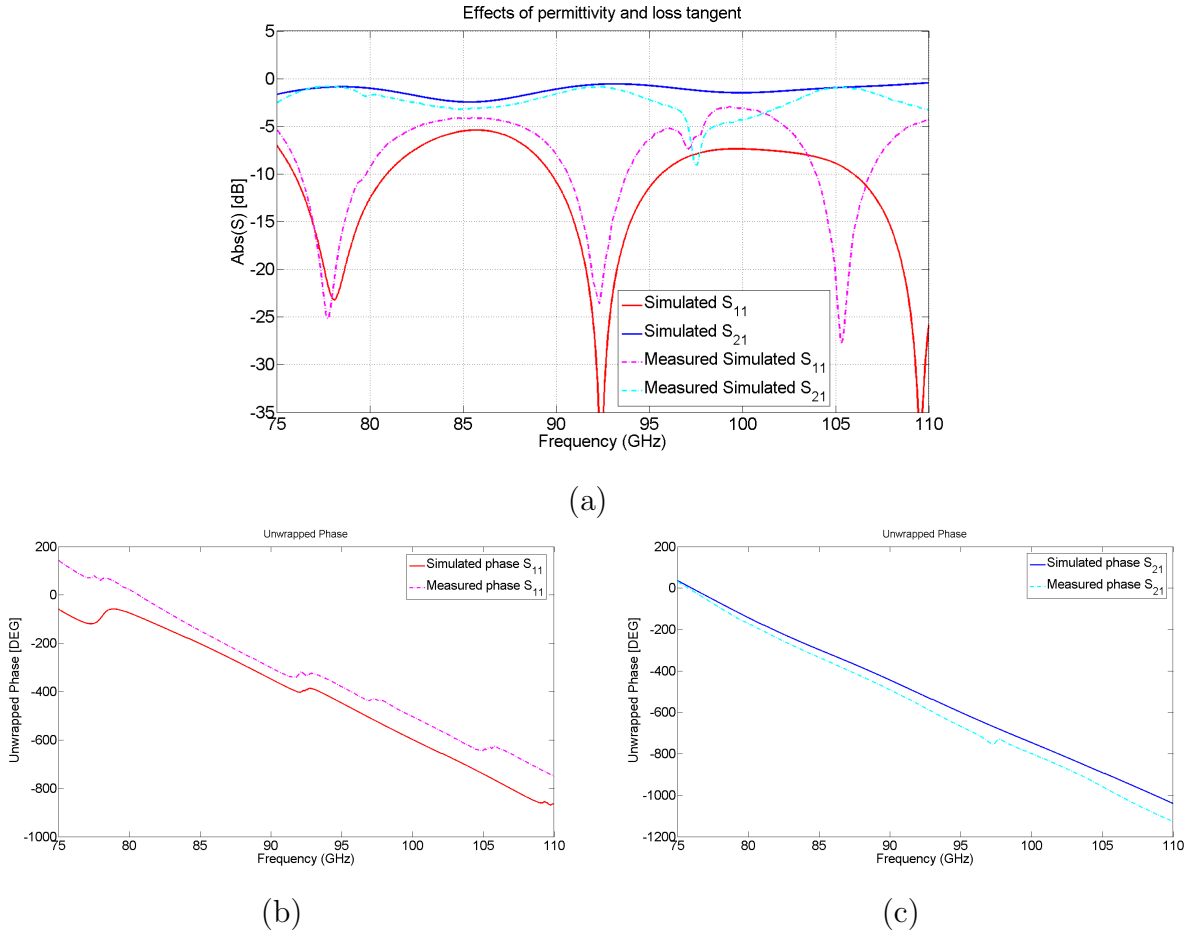

Figure 6.9: (a) Model simulated S parameters and the measured S parameters of back-to-back transition, (b) Simulated and measured S_{11} phases, (c) Simulated and measured S_{21} phases

Chapter 7

Feasibility Study of Integration of MMIC LNA

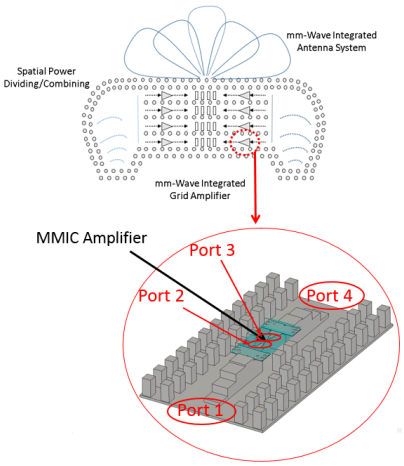

The aim of this chapter is to build a practical model in order to examine the proposed transition concept, when an active device is present. This chapter is considered as an initial study of a unit cell in a complete mmWave system comprises grid of amplifiers integrated with an array antenna. DC biasing access network to the MMIC amplifier will be designed and simulated. We wish to investigate the effect of DC network and the DC wirebonding in the the whole system performance, but such investigation needs more time to cover all effects,thereby, this study will be in the future work. Finally, we incorporate the LNA S-parameters model inside the 4-port system. The LNA model will be analyzed using CAESAR system simulation software.

7.1 Introduction

The proposed model shown in Fig. 7.1, represents a preliminary test for incorporating an active device such as MMIC low noise amplifier (LNA) in the groove gap waveguide. A

simulation result for the passive 4-port structure is presented in Fig. 7.2. The pusrpose of this quick simulation is to check how much power gain we can use for the LNA amplifier before it start oscillation. The oscillation will happened if there is a positive feedback between the output and the input ports of the amplifier, thereby, a part of energy will coupled from the output to the input of the device. The amplifier will be connected between the two ports, reference numerals 2 and 3 as indicate in Fig. 7.1. The amplifier power gain must not exceed specified maximum level to avoid the oscillation, this maximum level correspond to the level of return loss between port 2 and port 3, S_{23}. the maximum level can be read from Fig. 7.2. Briefly, the amplifier power gain < 35 dB.

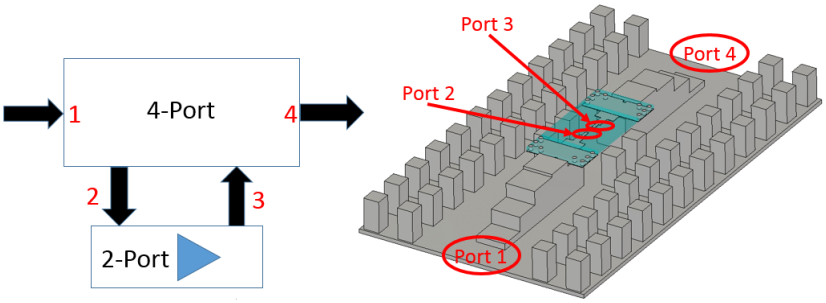

Figure 7.1: Preliminary structure of incorporating active device in back-to-back Microstrip-to-Groove gap waveguide

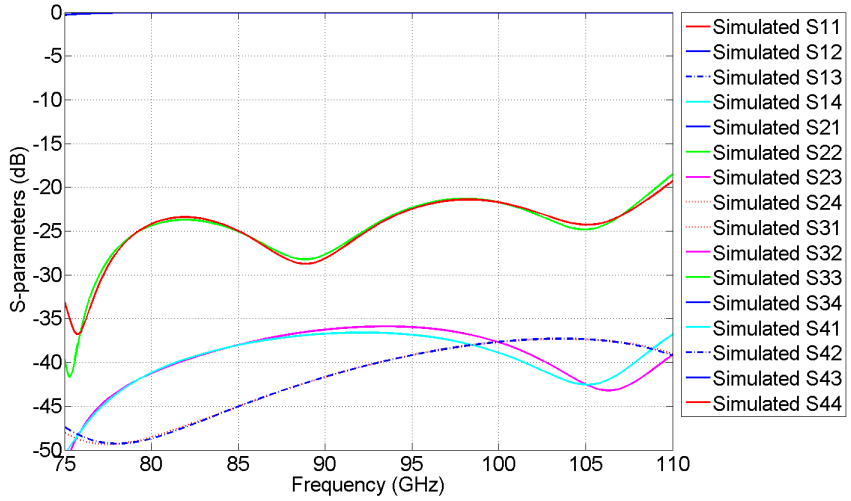

Figure 7.2: The simulated S parameters of 4-port back-to-back Microstrip line-to-groove gap waveguide structure

To simplify the design, and give a fast proof-of-concept, an existing commercial W-

band MMIC LNA [25], is used in order to test design performance.

Practically, two alternatives we can follow to incorporate the amplifier within our design. One way we can save time and get a good model is to extend our model, both the alumina PCB and the gap waveguide, by the size of the given chip, which has a length of 2.9 mm and width of 1.1 mm as given in [25]. A drawing shows the the process of amplifier integration is presented in Fig. 7.3. The LNA chip on a carrier substrate, would

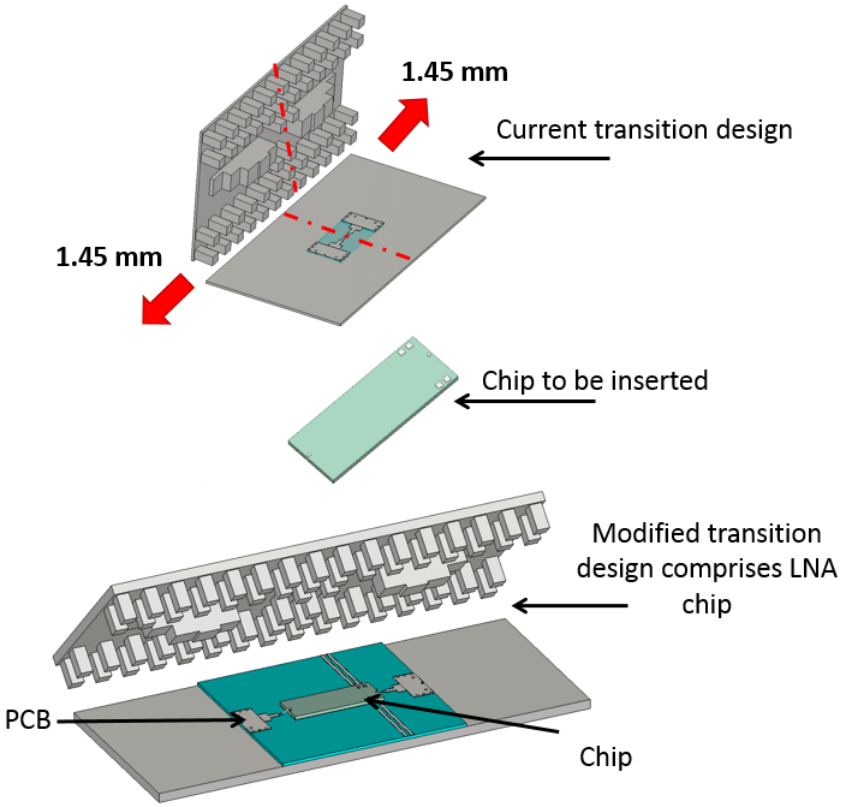

Figure 7.3: Structural Modification for LNA chip integration inside the gap waveguide

be attached to top side of the PCB and through RF wirebonding they will be connected. In this case, a very good repeatability for the bondingwire can be achieved. DC biasing for the amplifier, will pass through the bottom metal plate extended outside the structure. The LNA chip will be packed within the gap waveguide, that is, no extra packaging issue is needed.

The second way that we could use to integrate the amplifier, is to modify the PCB itself; both the dielectric material and the dimensions will be changed to be compatible to

the LNA circuit, thereby, the LNA circuit and the PCB will be one circuit and both have the same dielectric material, as shown in Fig. 7.4. This methodology will be more practical and more attractive, the mainstream RF bondwiring is completely been avoided.

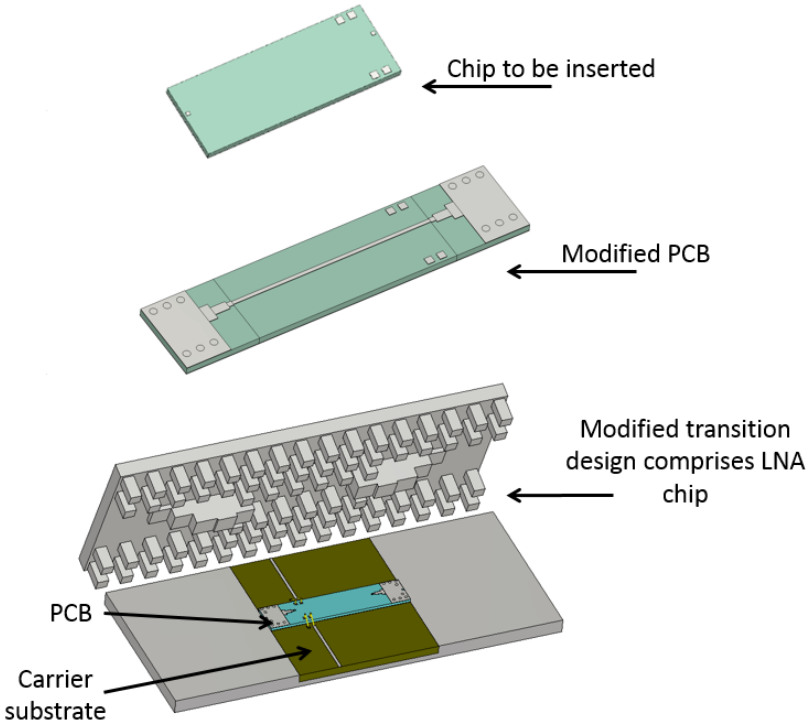

Figure 7.4: Geometry for LNA integration

7.2 DC-Biasing Access Design

In order to integrate a LNA within a gap waveguide, an appropriate DC biasing access is required. The suggested DC access network for the LNA is presented in [25]. The typical layout for the suggested biasing circuit and the final geometry for integrating the DC biasing circuit within the gap waveguide is shown in Fig. 7.5 according to the suggested arrangement provided in [25]. The carrier substrate comprises the DC biasing network build on Rogers-Ultralam 2000 dielectric material has a dielectric constant ϵ_r =2.5. The first bypass capacitors should be closer to the amplifier typically at distances $\leq$ 0.762 mm from the amplifier. Typical passive DC biasing network, for both gate and drain, comprises of 2 shunt capacitors each has a value of 100 pF, two series resistors each has a value of

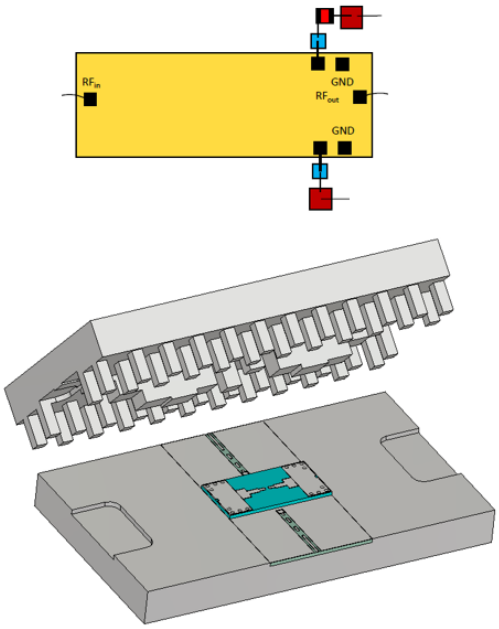

Figure 7.5: DC access network implementation

10 Ω and two extra shunt capacitors with larger values approximately of 0.1 μF for each capacitor.
The main aim of those capacitors is to short circuited the RF signal that could leak into the DC biasing network. The appropriate Dc biasing point has a typical value of Vd =2 V and Vg -0.4 V. The gate and drain DC can be accessed from both sides of the gap waveguide, which is considered a simple and flexible design.

The isolation between the two paths can be studied by adding two extra DC pads on the chip surface at the both sides of the RF signal path. DC wirebonding connected the DC pads by the DC lines on the carrier substrate. Fig. 7.2(a) illustrates the simulated schematic in order to examine the coupling between RF and DC signals, where two extra discrete ports assigned at the inputs of the two DC lines. As illustrated, Ports 1 and 4 represent the wave guide ports, while ports 2 and 3 represent the active component ports and Ports 5 and 6 represent the DC inputs. As we can see from the simulation result in Fig. 7.2(b), the isolation between DC and RF paths is better than 40 dB over the entire band.

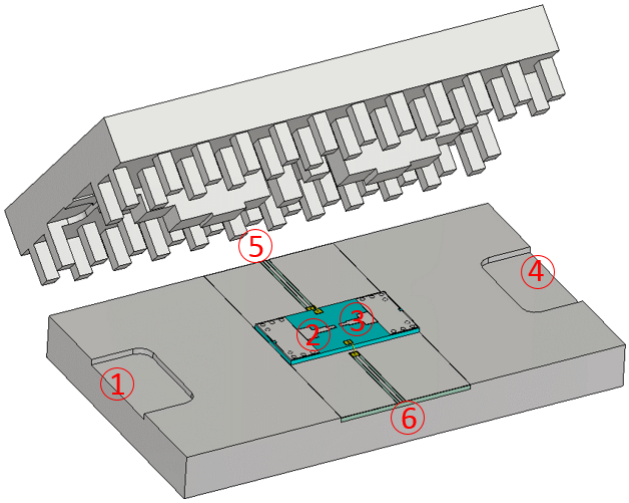

(a)

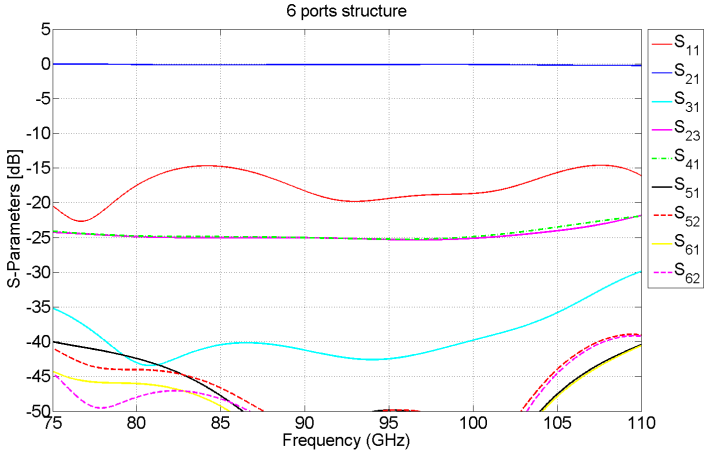

(b)

7.3 Incorporating MMIC LNA S-Parameters Model

In order to test the performance for integrate an LNA model inside the gap waveguide, the S2P file was created from the S-parameters of the LNA [25]. The CST schematic layout for which the S-parameters of the LNA are used to create 2-port block is shown in Fig. 7.6. The LNA has a linear gain of 17 dB in the frequency range between 80 to 100 GHz. The measured noise figure is about 4.2 dB within the frequency range. The integration of the LNA amplifier within the gap waveguide has been modeled and simulated using system software simulation CAESAR. Fig. 7.7 shows the output result of the S-parameters. The simulated S_{11} and S_{22} shows a stable device within the operating bandwidth $\leq$-2 dB, while

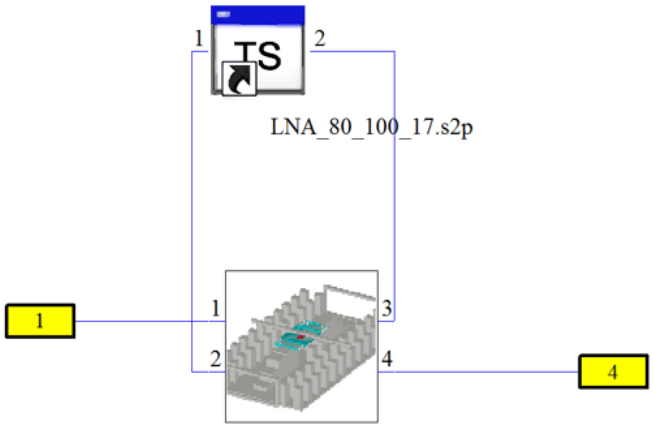

Figure 7.6: Schematic view contains a 3D CST transition model and the S-parameters model

the gain lies in the range between 14 to 22 dB.

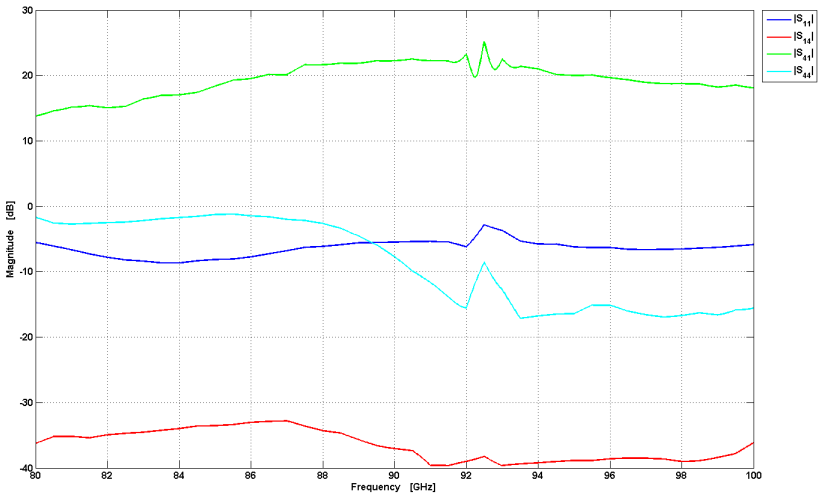

Figure 7.7: Simulated S-parameters using CAESAR system software

Chapter 8

Conclusions and Recommendations

8.1 Conclusion

Shifting toward mm- and SubmmWave frequencies in order to increase the data rate and the bandwidth add enormous unexpected challenges to the system designers. For example radiation loss due to leakage and interconnections such as the bondingwires, which normally has an inductance effect, limits the operational frequency band. Discontinuities also limits the generation of high power at mmWave frequencies as well as limits the flexibility for the integration of active components with passive waveguide components. Furthermore, practically in the designing of microwave and mmWave components, the packaging issue is to be considered in a separate process, therefore add more complexity to the circuits.

In this thesis, a transition from PCB microstrip line to groove gap waveguide has been proposed and tested. This new transition allows easy integration of RF electronics to the waveguide components. The first three chapters of this thesis deal with the basic aspects of the gap waveguide technology. The classical transitions between the different types of the gap waveguide such as ridge gap waveguide and groove gap waveguide are also presented in chapter (2). The last two chapters of this thesis are focused on the investigation of the transition between PCB microstrip line and the groove gap waveguide, which is considered as an initial step toward the integration of an active circuit such MMIC low noise amplifier in order to generate power at mm- and SubmmWave frequencies. This design can be considered as all-in-one system integration concept, which thereby enables a flexible design

and high degree of repeatability for the chip using pick-and place technique.

We have simulated and studied the back-to-back microstrip line to groove gap waveguide transition by using the electromagnetic coupling between the SIW and the ridge gap waveguide. The simulated port reflection is $< 1\%$ and the power transmission coefficient is $> 99\%$ over the entire W-band.Milling accuracies are in the range of few microns, while the tolerances is around 20 microns. It is foreseen that this technology is going to lead to a breakthrough in the mm- and SubmmWave frequency bands. At SubmmWave frequencies it is envisioned that the entire technology can be integrated in a cost-effective manner onto a physically small (but electrically large) chip through a micromachining process. Such technologies will enable low-loss mmWave systems, high SNR receiving antenna systems, and ultra fast communication links. The mismatch between the simulated and measured prototype is mainly due to the manufactured PCB; which has a dimension larger than the design dimension. Moreover, the dielectric material behaviour changed at mmWave frequencies, the relative permittivity became smaller and the tangent delta became larger.

8.2 Recommendations

The proposed design is unique and regarded as a cornerstone in the direction toward a novel contactless integration concept and will overcome interconnection and packaging problems of integrated circuits and antennas at mmWave frequencies. Still, the experimental validation of the transition shows a different performance result than what was expected. A thorough error analysis revealed that the dimensions of the PCB were not within the tolerances as specified by the manufacturer, which is the main reason for the performance degradation. Therefore a problem formulation and an accurate analysis depending on what we have done in chapter 8 will be the next step. The purpose is to resolve the assembly and manufacturing tolerances issues in order to have a measured prototype which match to the required design goal. However, this thesis presents a starting step toward the design of a complete structure in terms of integration of active and passive components and antennas with self-packed module (All-in-one) solution within the gap waveguide, where the losses are minimum. This may open the door to use grid amplifiers to generate power at mm- and SubmmWave frequency bands by involving the concept of spatial power combining/dividing. The concept of perfect magnetic conductor (PMC) is employed in order to isolate the amplifiers electrically from each other, thereby, enabling reduction in feedback

and therefore, provides a higher stability condition for one amplifier cell. This concept is presented in Fig. 8.1. A preliminary study of the RF isolation for two parallel transition placed side by side is presented in Fig. 8.2. The integration of active components with gap waveguide and antenna with one module, still has many challenges need to be solved during this research activity, such as, the accurate design for the carrier substrate comprising the DC power biasing and appropriate RF decoupling circuit. Moreover the thermal instability may cause thermodynamics problems and the active device may suffer from imbalance and starts to oscillate and the noise will be increased, thereby, thermal modeling needs to be studied, in order to ensure a thermal stability environment.

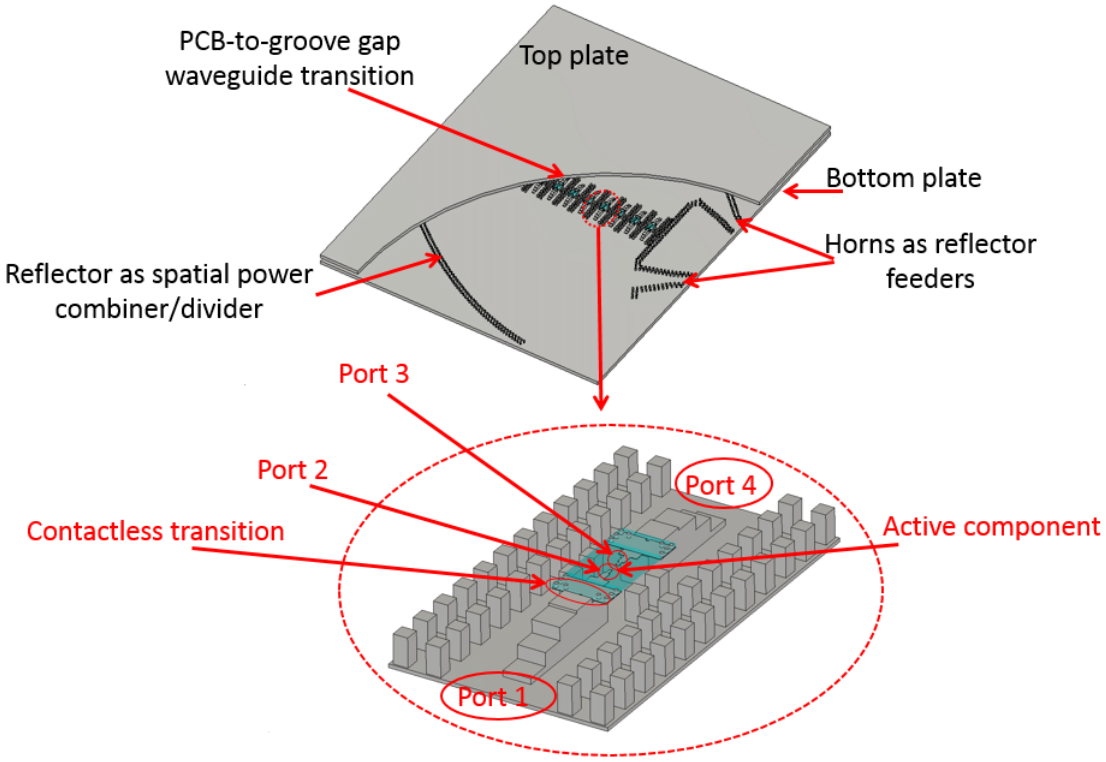

Figure 8.1: (Top) Preliminary structure of incorporating an array active devices in back-to-back Microstrip-to-Groove gap waveguides using spatial power combiner/divider, (Bottom) The unit cell of 4-port back-to-back Microstrip Line-to-Groove gap waveguide structure

Another research activity, is to modify the contactless transition in a proper way, so that, the PCB and the unpackaged active component are build on one single substrate, that could has high relative permittivity and to test the transition in different high frequency ranges. This will enable us examine and test an unpackaged active element with the gap waveguide technology. Extending a one single on chip integrated amplifier to several paral-

lel chains of active elements, such as, on chip grid amplifiers in order to increase the output power, will be challenging and intractable. But such a system will be a groundbreaking research in generating power at mm- and SubmmWave frequencies, including the demonstration of full packaging system comprises high enhanced antenna array performance and grid amplifiers in gap waveguide technology.

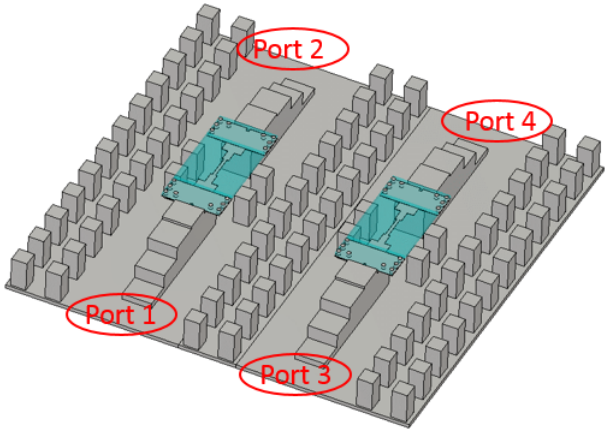

(a)

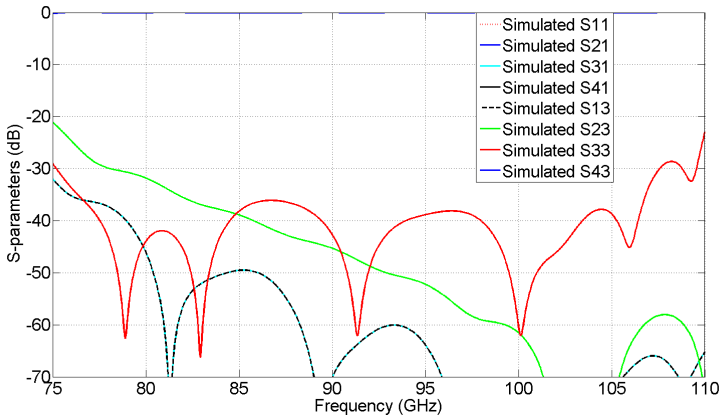

(b)

Figure 8.2: (a) (Perspective view) Two parallel cells of back-to-back Microstrip line-to-Groove gap waveguide (Top metal plate is hidden), (b) The simulated S parameters of two cells back-to-back Microstrip line-to-Groove gap waveguide structure

Appendix A

mm-Wave Contactless Connection for MMIC Integration in Gap Waveguides

Alhassan Aljarosha
Department of Signals and Systems
Chalmers University of Technology
Gothenburg, Sweden
alhalj@student.chalmers.se

Rob Maaskant, Ashraf Uz Zaman and Per-Simon Kildal
Department of Signals and Systems
Chalmers University of Technology
Gothenburg, Sweden
rob.maaskant@chalmers.se, zaman@chalmers.se, per-simon.kildal@chalmers.se

***Abstract*—A contactless, broadband and low-loss microstrip-to-groove gap waveguide transition operating at W-band is presented. The principle of operation is based on transforming EM fields from the SIW to the ridge gap waveguide mode via electromagnetic coupling. This is advantageous, since the proposed solution avoids the use of metal contact between the SIW and one of the waveguide parts. Furthermore, metamaterial-based gap waveguide technology provides a resonance-free packaging solution.**

I. Introduction

There is a strong desire to increase the bandwidth and thereby the data rate of wireless communication systems. This has led the researchers and engineers to shift toward the millimeter-wave band or higher. Integrating active components such as an MMIC in a waveguide at millimeter-wave frequencies is often critical in terms of packaging as well as the transition between the chip's transmission lines and the waveguide. Transitions from microstrip lines to waveguides have gained a lot of interest. In the last decades, several papers have been presented in this direction. Some of these transitions are based on microstrip line to conventional ridge waveguides [1], [2]. These transitions perform well, however, such transitions need metal contacts between the microstrip line and the waveguide. Moreover, partially dielectric-filled waveguide cause manufacturing problems at higher frequencies. A microstrip to conventional waveguide transition at high frequencies is typically very complex because it requires an accurate alignment and good electrical joints when manufacturing and assembling split block sections of conventional waveguides. By introducing the gap waveguide technology [3], [4], critical electric contact and cavity-mode resonance can be avoided [5]. Recently, many transitions from microstrip line to gap waveguide components have been developed. A Ku-band microstrip line to ridge gap waveguide with 0.5 dB insertion loss has been designed [6]. This structure is complicated since the field needs to be coupled between the microstrip line to ridge gap waveguide through a slot. Furthermore, a back-short is needed which makes the structure bulky and also reduces the bandwidth. Another microstrip line to ridge gap waveguide transition operating at Ka-band is presented in [7]. This transition gives larger bandwidth than [6]. However, accurate alignment and electrical connection between the microstrip line and the ridge gap waveguide must be achieved. A contactless microstrip to ridge gap waveguide transition operating at 100 GHz is presented in [8].However, an accurate alignment between the microstrip patch and the ridge section. Furthermore, the transition exhibits a relatively narrow bandwidth.

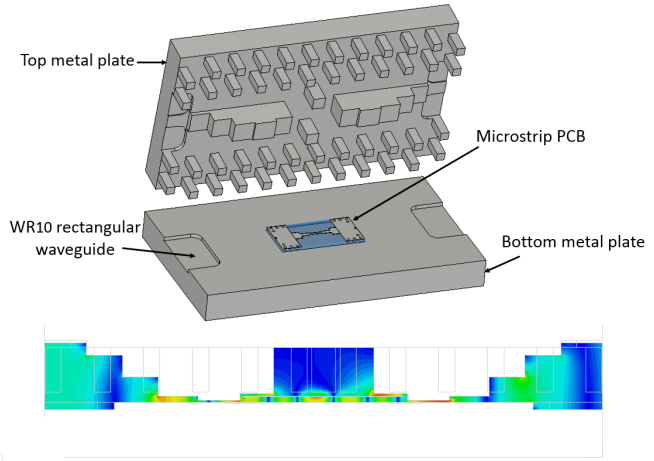

Fig. 1. The configuration of the proposed microstrip-to-groove gap waveguide transition and side view of the field guided through the structure

It is therefore the objective of this paper to provide a new compact and broadband contactless microstrip line to groove gap waveguide transition which is less susceptible to alignment problems and which particularly allows assembly in a fast and an easy manner, for example using a pick-and-place technique, as depicted in Fig. 1.

II. Design of the Proposed Transition

The proposed back-to-back microstrip line to groove gap waveguide transition comprises a PCB of high permittivity substrate, attached to the bottom metal plate. The PCB comprises a transition of microstrip line to SIW and the gap waveguide structure comprises a transition of ridge gap to groove gap waveguide as shown in Fig. 2.

Both the SIW and microstrip PCB employ the same alumina substrate with dielectric constant of $\epsilon_r = 9.9$, which is comparable to most of the MMICs used at millimeter-wave frequencies.

Electromagnetic coupling of the EM field between the SIW and the ridge gap waveguide is achieved by using a $\lambda_g/4$ stub positioned at a slight distance above the PCB and also at a slight distance from the SIW edge, such that there is

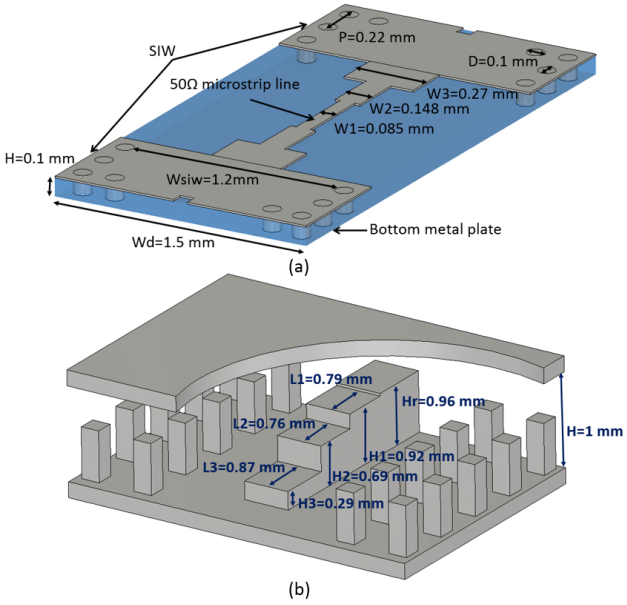

Fig. 2. (a) Back-to-back Microstrip to SIW transition, (b) Ridge gap to groove gap waveguide transition

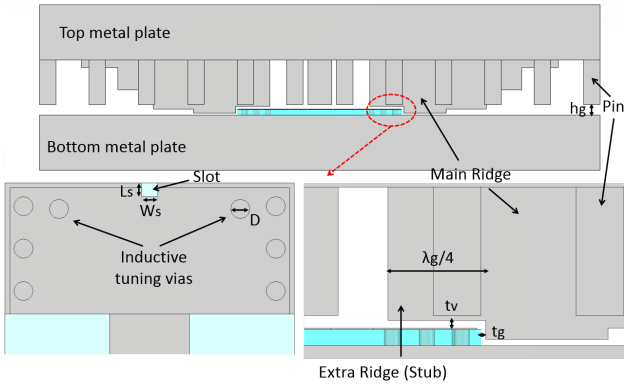

Fig. 3. Back-to-back transition, (zoomed) Slot size in the SIW ground plane, $W_s = 0.083$ mm, $L_s = 0.071$ mm, (zoomed) the air gaps in vertical, $t_v = 0.048$ mm and in horizontal, $t_g = 0.03$ mm and $h_g = 0.19$ mm

an air gap between the $\lambda_g/4$ open-ended stub and the SIW, effectively providing a short-circuit connection. Two inductive tuning vias and a U-shaped slot, as seen in Fig. 3, are used to compensate for the capacitance of the stub, thereby increasing the operational bandwidth. The commercial full-wave software CST Microwave Studio was used to design and simulate the transition. The simulation results of the back-to-back transition are shown in Fig. 4. The insertion loss and the return loss values are below 0.35 dB and larger than 21 dB over the entire W-band, respectively (PEC materials).

III. Conclusions

A novel concept to realize a contactless microstrip line to groove gap waveguide transition through near-field electromagnetic coupling has been designed and simulated. The Quasi-TEM microstrip line mode is well-matched to the TE_{10} mode of the SIW waveguide, which in turn is coupled to the ridge gap waveguide mode via a tuning stub partially

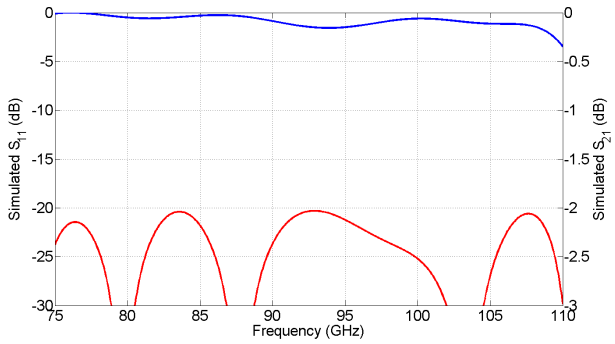

Fig. 4. Simulation result of proposed back-to-back transition

overlapping the PCB. Simulation results have shown an excellent performance; the simulated port reflection is smaller than 1% and the power transmission coefficient is larger than 99% over the entire W-band. The PCB part is directly packaged within the gap waveguide structure, so that there is no need for an additional packaging step. This is of significant importance when integrating MMICs operating at millimeter-wave frequencies.

Acknowledgment

The work has been funded by a VR Young Researcher grant, the European Research Council (ERC) under the 7th framework programme ERC Grant Number 321125 and the Swedish Governmental Agency for Innovation Systems (VINNOVA) within the VINN Excellence Center Chase at Chalmers.

References

[1] Y. Zhang, J. Ruiz-Cruz, K. Zaki, and A. Piloto, "A waveguide to microstrip inline transition with very simple modular assembly," *IEEE Microw. Wireless Compon. Lett.*, vol. 20, no. 9, pp. 480–482, Sep. 2010.

[2] A. Rebollo, B. Larumbe-Gonzalo, R. Gonzalo, and I. Ederra, "Full w-band microstrip-to-waveguide inline transition," in *The $8^{rt}h$ European Conference on Antennas and Propagation (EuCAP 2014)*, pp. 2591–2593.

[3] P.-S. Kildal, E. Alfonso, A. Valero-Nogueira, and E. Rajo-Iglesias, "Local metamaterial-based waveguides in gaps between parallel metal plates," *IEEE Antennas Wireless Propag. Lett.*, vol. 8, pp. 84–87, 2009.

[4] P.-S. Kildal, "Three metamaterial-based gap waveguides between parallel metal plates for mm/submm waves," in *Proceedings of the 3^{rd} European Conference on Antennas and Propagation (EuCAP 2009)*, pp. 28–32.

[5] E. Rajo-Iglesias, A. Zaman, and P.-S. Kildal, "Parallel plate cavity mode suppression in microstrip circuit packages using a lid of nails," *IEEE Microw. Wireless Compon. Lett.*, vol. 20, no. 1, pp. 31–33, Jan. 2010.

[6] B. Molaei and A. Khaleghi, "A novel wideband microstrip line to ridge gap waveguide transition using defected ground slot," *IEEE Microw. Wireless Compon. Lett.*, vol. 25, no. 2, pp. 91–93, Feb. 2015.

[7] A. Zaman, T. Vukusic, M. Alexanderson, and P.-S. Kildal, "Design of a simple transition from microstrip to ridge gap waveguide suited for mmic and antenna integration," *IEEE Antennas Wireless Propag. Lett.*, vol. 12, pp. 1558–1561, Dec. 2013.

[8] A. A. Brazlez, A. Zaman, and P.-S. Kildal, "Investigation of a microstrip-to-ridge gap waveguide transition by electromagnetic coupling," in *AP-S International Symposium, IEEE Antennas and Propagation Society*, Jul. 2012, pp. 1–2.

Appendix B

M1 P1SE00 AB/ab 2016-02-12

Title:

A TRANSITION ARRANGEMENT COMPRISING A CONTACTLESS TRANSITION OR CONNECTION BETWEEN AN SIW AND A WAVEGUIDE OR AN ANTENNA

TECHNICAL FIELD

The present invention relates to a transition arrangement comprising a transition between an SIW, associated with, or of, a circuit arrangement, e.g. an active or a passive circuit arrangement, and a waveguide or an antenna or antenna interface, having the features of the first part of claim 1.

The invention also relates to a method for providing transition arrangement having the features of the first part of claim 23.

BACKGROUND

Transitions, or connections, between a circuit and e.g. a waveguide or an antenna are needed for many different applications, e.g. within microwave or millimetre wave technologies etc. Particularly due to the increasing demand for high-speed wireless links, e.g. for ultra-fast mobile Internet, high resolution automotive radar links, Gbit/s data and video links, accurate imaging devices for medical and security applications etc. it is attractive to be able to use the millimetre, or the sub-millimetre, wave frequency region, since in these frequency regions, larger frequency bandwidths are available. Thus, the use of high frequencies is steadily gaining more interest.

For example, electronically steered antennas in an antenna array system based on e.g. mm-wave technology have an enormous potential, being capable of multiple instantaneous beams, each of which corresponding to a relatively large antenna aperture area

providing high receiving sensitivity or a large antenna gain. However, such systems are complex and high costs are involved with complex antenna array systems employing many antenna elements. At millimetre-wave frequencies it becomes possible to combine antennas with integrated circuits in a single process since the size of the antennas is reduced to a fraction of a millimetre, allowing them to be placed on a carrier together with an integrated circuit (IC). This reduces the fabrication costs and time, and the antennas are smaller than dielectric-free antennas.

Several problems are associated with transitions between e.g. a package comprising a high-frequency circuit and a waveguide port or an antenna.
A waveguide transition generally converts its dominant waveguide mode to a microstrip or coplanar transmission line mode.

Direct ridge-to-transmission line connections have been proposed, but suffer from drawbacks, particularly from a manufacturing point of view, since the circuit may easily break.

For a connection between a transmission line and a chip (circuit) a bond-wire or a flip-chip connection has been used. Such a connection contributes with a substantial reactance at high frequencies, causing extra losses and reduction in the achievable bandwidth. Another disadvantage in using bond-wire connections at high frequencies is that bond-wires may lead to impedance mismatch, are inductive and hence limit the bandwidth and the bond-pad contact area of the circuit becomes very small at high frequencies and bonding often destroys the high-frequency pad, thus affecting the yield. Bond-wires may further produce spurious radiation and may excite cavity modes when packaged. Moreover, e.g. for antennas,

the substrate on which the antennas are located will be lossy at millimeter-wave frequencies, which means that e.g. the antenna radiation efficiency is reduced. A low radiation efficiency, however, is not acceptable for systems requiring high power efficiency, or systems handling high powers. For example, in communication systems high SNR (Signal-to-Noise Ratio) is of utmost importance to allow the use of higher-level modulation schemes maximizing the data rate. Thus, such known solutions concerning antenna/waveguide-circuit transitions involve the drawbacks of the performance being degraded due to the use of RF-bond wires, as a result of which packaging problems arise, and e.g. resonances occur, and antennas and transmission lines suffer from high losses.

Flip-chip connections also suffer from several disadvantages. Due to the lack of a carrier, they cannot be easily replaced and they are not suitable for manual installation. Still further they require very flat mounting surfaces, which often is difficult to arrange, and sometimes difficult to maintain as the boards are heated and cooled. Further, the short connections are very stiff, so the thermal expansion of the chip has to be matched to the supporting board or the connection may crack. The underfill material acts as an intermediate between the difference in Coefficient of thermal Expansion of the chip and the board.

Connections between a circuit and a transmission line based on flip-chip connections also involve large alignment problems, and misalignment may lead to the integration being ruined.

WO 2014/154232 discloses a transition between an SIW (Substrate Integrated Waveguide) and a waveguide interface. However, contact

is needed between the metal waveguide and the SIW structure on two sides, requiring soldering or similar. Moreover the structure requires a 90° non-planar setup, which is disadvantageous for several reasons.

US 2014/0091884 shows a transition between an SIW and an air-filled waveguide, which also requires contact between the metal waveguide and the SIW structure on two sides. In addition, a tapering substrate is required which is disadvantageous for fabrication reasons.

In all known devices, replacement of the entire transition is needed if the circuit is damaged.

Thus, several problems are associated with the provisioning of a transition between a circuit, passive as well as active, and a waveguide or an antenna, and, so far, no satisfactory solutions have been suggested.

SUMMARY

It is therefore an object of the present invention to provide a transition arrangement comprising a transition between a circuit arrangement, e.g. an active or a passive circuit arrangement, particularly an SIW, and a waveguide or an antenna or antenna interface, as initially referred to, through which one or more of the above-mentioned problems are overcome. The circuit arrangement may comprise one or more active and/or passive circuits in general, e.g. one or more RF circuits, particularly one or more millimetre wave circuits or sub-millimetre wave circuits or one or more active MMICs (Monolithic Microwave Integrated Circuit) and multiple

circuit-to-waveguide transitions for one and the same circuit arrangement, or MMIC.

It is also a particular object to provide a transition, or connection, having a high, optimized, yield which is not affected by bonding onto small bond-pad areas and through which losses due to the presence of bond-wires and galvanic contact can be reduced or avoided.

It is also a particular object to provide a high frequency transition arrangement which is less susceptible to alignment problems, and which particularly allows easy circuit alignment.

It is also a particular object to provide a transition arrangement which is easy and cheap to fabricate, and which allows assembly in a fast and easy manner, for example using a pick-and-place machine.

It is a particular object to provide a transition arrangement which can be used for a large variety of different frequencies, from very low frequencies up to very high frequencies.

A most particular object is to provide a transition arrangement which can be used for different circuit arrangements, passive as well as active, one or more MMICs of arbitrary size, i.e. also large MMICs, and even more generally, circuits of many different kinds including hybrid circuits, RF circuits, operating at millimetre or sub-millimetre wave frequencies.

Another object is to provide a transition arrangement allowing high radiation efficiency.

A further object is to provide a transition arrangement which has a good matching capability.

It is also an object to provide a transition arrangement which is reliable and precise in operation.

Particularly it is an object of the invention to provide a transition arrangement through which the need to use RF bond-wire connections can be avoided or reduced.

Still further a particular object is to provide a transition arrangement between a circuit arrangement and one or more antennas and/or one or more waveguides.

Therefore a transition arrangement as initially referred to is provided which has the characterizing features of claim 1.

Still further it is an object to provide a method for fabricating a transition arrangement having the features of the first part of claim 23 through which one or more of the above mentioned problems are overcome.

Therefore a method as initially referred to is provided which has the characterizing features of claim 23.

Advantageous embodiments are given by the respective appended dependent claims.

It is one particular advantage of the invention that, in implementations comprising a transition between a circuit arrangement and an antenna, with the novel integration concept,

interconnection and packaging problems of antennas and ICs are overcome. Furthermore it is an advantage that bond wiring of high-speed signal lines is not needed and e.g. antennas can be made ultra-low-loss (metal-only).

Particularly a transition according to the invention works from very low frequencies up to very high frequencies. If the circuit is provided on an application board, then it may comprise an SIW-transition from the application board to the waveguide. The SIW or the SIWs form part of the circuit arrangement, which can be either on a chip, or off-chip, i.e. on an application board.

BRIEF DESCRIPTION OF THE DRAWINGS

The invention will in the following be further described in a non-limiting manner, and with reference to the accompanying drawings, in which:

Fig. 1 is a view in perspective of a transition arrangement according to a first embodiment of the present invention,

Fig. 2 is a cross-sectional side view of the transition arrangement of Fig.1,

Fig. 2A is a schematic section model of the transition arrangement shown in Fig.1,

Fig. 2B is simplified schematic single-mode transmission line network model of the section model of Fig.2A,

Fig. 2C is a cross-sectional side view of an alternative embodiment of a transition arrangement according to the invention,

Fig. 3 is a very schematic, simplified planar view from below of the transition arrangement shown in Fig.1,

Fig. 4 is a view in perspective showing another embodiment of a transition arrangement according to the invention,

Fig. 5 is a view in perspective showing still another embodiment of a transition arrangement according to the invention,

Fig. 6 is a view in perspective showing still another embodiment of a transition arrangement according to the invention,

Fig. 7 is a view in perspective showing another embodiment of a transition arrangement according to the invention,

Fig. 8A is a schematic illustration of a transition arrangement comprising a transition between an antenna and a circuit arrangement according to the invention,

Fig. 8B is a schematic illustration of the transition arrangement in Fig.8A in a position for assembly, and

Fig. 9 is a schematic illustration of another transition arrangement between an antenna and a circuit arrangement according to the invention.

DETAILED DESCRIPTION

Fig. 1 schematically illustrates a transition arrangement 100 according to a first embodiment of the invention comprising an SIW (Substrate Integrated Waveguide) ridge-waveguide transition or connection. The transition arrangement 100 comprises a rectangular waveguide 10 which comprises a first conducting, e.g. metal, plate 1 (here a bottom metal plate), a second conducting, e.g. metal, plate 2 (here a top metal plate) and longitudinal conducting, e.g. metal, side walls 3,3 connected to the second (top) conducting metal plate 2. In the following the plates and the walls are referred to as conducting plates or metal plates for reasons of simplicity.

The rectangular waveguide 10 further comprises a ridge 4 which here extends between, and in parallel to, the metal walls 3,3 in a section of the second metal plate 2 of the rectangular ridge waveguide 10. An SIW 20 is attached to the first metal plate 1, here at an end section thereof, opposite to the side or section of the second metal plate 2 where the ridge 4 is located such that, when the first and second metal plates 1,2 are assembled, here interconnected or mounted, e.g. by means of screws or any other appropriate connecting elements (not shown), an inner end section of the SIW 20 will be located such as to face a stub 5 forming an extension of the ridge 4, but here being of a smaller height. The SIW 20 is so located that a slight distance, e.g. corresponding to an air gap, is provided between the SIW 20 upper surface facing the stub 5 and the stub 5 and so that it ends adjacent, at a slight distance, e.g. corresponding to an air gap, from, the edge formed at the outer end of the ridge 4, where hence a step is provided between the stub 5 and the ridge 4, for forming the transition. The air gap is an impedance tuning parameter that can be modified,

tuned. In one particular embodiment the air gap between the SIW edge and the edge of the ridge 4, i.e. the air gap in a horizontal plane with respect to the plane of the PCB or similar may be in the range of 0.003λ-0015λ, and the air gap between the SIW 20 and the stub 5 (the air gap in the normal plane with respect to the plane of the PCB or similar) may be in the range of 0.01λ-0.021λ. It should however be clear that the figures of these dimensions are merely given for exemplifying reasons and by no means limiting purposes for a particular embodiment and can be larger as well as smaller, and can be modified, tuned, for different structures. The length of the stub 5 corresponds to $\lambda_g/4$, λ_g being the guide wavelength of the waveguide section formed by the stub 5 and the metallization (an SIW first ground plane) 9. Typically λ_g is associated with a frequency in the centre of the operational bandwidth.

The SIW 20, forming part of, or comprised by, a circuit arrangement (not illustrated, and as such not forming part of the invention) comprises a dielectric substrate 6 with a plurality of metal vias 7 and two, a first and a second, SIW ground planes 9,9’ which are connected through the vias 7, wherein the second, in the shown embodiments, bottom, SIW ground plane 9’ is connected to the first conducting plate 1. The dielectric substrate typically has a thickness of e.g. 10-100 µm, and, if the circuit is provided on a chip, preferably has a high permittivity, e.g. 10-13, although these figures by no means are given for limitative purposes; they may be higher as well as lower. If, on the other hand, the circuit arrangement is disposed on an application board, the substrate may have a low permittivity, e.g. down to 2-3. However, the inventive concept is not limited to any specific permittivity of the dielectric substrate of the SIW. The SIW is a part of a circuit

arrangement, which can be provided either on the chip, or off-chip, i.e. on an application board (not shown).

Also additional matching vias may optionally be provided, not shown in Fig.1 but shown e.g. in Fig.4, which however are not necessary for the functioning of the inventive concept, but advantageous in so far that they contribute to impedance tuning and improvement of the performance over the bandwidth.

SIW 20, which comprises an SIW waveguide which here is provided on a chip or similar comprising any a circuit arrangement (not shown in Fig.1), and serves the purposes of acting as a waveguide of the circuit arrangement and of the stub 5. The SIW 20 is e.g. used to feed the circuit. Hence, there is also a transition or an interface between the chip or the circuit and the SIW, commonly a microstrip, or e.g. a co-planar waveguide, but this will not be further described with reference to Fig.1, since such transitions are known in the art and do not form part of the basic inventive concept, which is concerned with the transition between, here, the waveguide 10 and the SIW 20.

In alternative embodiments, not shown, the chip may be provided on an application board, which is a conventional PCB hosting the chip or naked die. Thus, according to the invention the SIW structure can be arranged on a chip or a naked die itself (high frequency applications), or on a carrier PCB (low frequency applications). When the chip is arranged on the chip, there is no need for any RF-bonding, whereas if it is arranged on a low permittivity application board, e.g. a carrier substrate, RF-bonding is needed for bonding it to the high permittivity chip but not from the SIW on the application board to the waveguide.

Through the additional stub 5, arranged as an extension of, or forming part of, the ridge 4, the open-ended stub impedance is converted into an equivalent short-circuit at the ridge where ridge 4 and stub 5 join, providing a coupling of the electromagnetic field between the SIW 20 waveguide and the ridge (part) 4 of the rectangular waveguide 10. A waveguide input port 25 is schematically indicated. The stub 5 can also be said to comprise two conductors, the stub 5 and the first SIW ground plane 9, i.e. the stub 5 supports an EM field mode in-between two conductors, namely the ridge 5 and the SIW ground plane 9.

According to the invention at least a quasi-planar, contactless transition or connection is provided between the SIW 20 and the ridge 4 of the second conducting plate 2, the second ground plane 9’ of the SIW 20 being connected to the first conducting plate 1. The transition is at least quasi-planar in so far that the width is larger than the height, and it is not a 90° setup. The two parts, the first metal plate 1 comprising the SIW 20 and all electronics, and the second metal plate 2 comprising the ridge 4 and the stub 5 are to be placed on top of, facing, each other such that the transition between the SIW 20 and the ridge 4 of the rectangular waveguide 10 is formed as discussed above.

Fig.2 is a cross-sectional side view of the transition 100 shown in Fig.1 taken along a line indicated A-A in Fig.1, but for the transition arrangement in an assembled, here mounted, state wherein the first and second metal plates are connected by means of fastening means, e.g. screws or similar. In the shown embodiment the SIW 20 (second ground plane 9’) is attached to the first (bottom) metal plate of the rectangular waveguide 10. The waveguide ridge 4 is associated with the second, top, metal plate 2 and ends

at a slight distance from an inner edge of the SIW 20 in an assembled, here mounted, state of the waveguide, i.e. such that there is an air gap between the ridge 4 and the SIW 20. The ridge 4 extended by means of the $\lambda_g/4$ stub 5 protrudes such as to cover part of the SIW 20, at a slight distance therefrom, i.e. providing an air gap as discussed above, such that the contactless transition is provided.

The first SIW ground plane 9 serves as a common ground plane for the SIW 20 and the stub 5, and the second SIW ground plane 9' serves as a common ground plane for the SIW and a waveguide or an antenna. In Fig. 2 are also shown the vias 7 of the SIW 20, the SIW first ground plane 9.

As also mentioned above, according to the invention the stub 5 can also be said to comprise two conductors, namely stub 5 itself and the first SIW ground plane 9 acting as its ground plane.

It should also be clear that, alternatively, the SIW 20 may be attached to the second or top metal plate 2 instead, in which case the ridge 4 and the stub 5 have to be on the first, opposite, conducting plate 1. It should further be clear that the metal walls 3,3 can be associated with any one of the first or second metal plates 1,2. Moreover it should be clear that, in alternative embodiments, there may be more than one ridge, e.g. several ridges, e.g. arranged to be located in different directions, with each a quarter wave-length stub to provide two-or multiport devices.

Generally, the contactless transition from the ridge 4 of the waveguide 10 to the SIW structure 20 inside the wave-guiding structure provided by means of stub 5 (and SIW ground plane 9;

which actually is part of the SIW) matching can be implemented in many different manners, and generally it can be applied N times to feed a chip with a circuit, thus comprising N SIW-to-waveguide transitions of the type discussed above leading to an N-port device. The ridges then go out in various different directions from the chip.

Fig.2A is view similar to Fig.2, but wherein the different elements are represented as sections also schematically illustrated in the simplified single-mode transmission line network model of Fig.2B for explanatory reasons.

Thus, in Figs.2A and 2B, reference numeral 101 represents a ridge rectangular waveguide, reference numeral 201 is taken to represent the SIW 202 and stub ground plane for a section representing the quarter wavelength open-ended stub section 400. One of the conductors of the ridge rectangular waveguide 101 becomes connected to the bottom conductor of the SIW 201, while the upper conductor of SIW 201 forms the bottom ground plane of the open-ended stub section 400 which transforms the reference numeral 500 effectively from an open circuit to a short circuit, so that an electrical connection between 101 and 201 is effectuated.

Referring to Fig.2, this can be expressed as there being two paths for the EM-field; namely a first path directly inside the dielectric substrate, SIW 20, which then passes on to the path in-between ridge 4 and the first conducting plate 1, as well as a second path in-between stub 5 and the first SIW ground plane 9. The second path is open, completely mismatched at its end, so that the field is reflected, and joins the field having taken the first path, i.e. adds on to the field of the first, straight going, path, and then proceeds onto the waveguide in-between ridge 4 and the

first conducting plate 1. The field can be said to jump from (or into) the SIW or the chip without being reflected. The electromagnetic waves thus are guided from the waveguide into the substrate (SIW) without any galvanic contact between the first SIW ground plane 9 and the ridge 4 and the stub 5.

Fig.2C shows an alternative embodiment of a transition between an SIW 20 and a ridge waveguide. The SIW 20 is placed and connected inside a groove 101 provided in the first conducting plate 1_1, or e.g. the bottom ground plane, and is located at a slight distance, comprising an airgap, from a groove edge 102, , which edge 102 here is substantially perpendicular to a longitudinal extension of the first conducting plate or block 1_1. It should however be clear that the edge 102 may also form an angle with the planar extension of the first plate 1, or e.g. taper linearly or exponentially. Many alternatives are possible. The EM field needs to propagate from a port 25 to the SIW 20 or vice versa without being obstructed, since obstructions may lead to impedance mismatch effects causing a reduced bandwidth, the airgap hence facilitating the transition, the SIW substrate not being blocked.
The electromagnetic field in the ridge waveguide will couple to the SIW 20 by means of $\lambda g/4$ stub 5_1, which converts the open-ended impedance to an equivalent short-circuited impedance. In other respects the functioning is similar to that described above with reference to Figs.1-2B and will therefore not be further described here. Similar elements bear the same reference numerals.

Fig.3 is a schematic bottom view of the transition arrangement 100 of Fig. 1 with the first, bottom, metal plate 1 removed for illustrative purposes. It can be seen how the ridge 4 ends adjacent the SIW structure 20 and how the $\lambda g/4$ stub 5 (dashed line) extends

across part of the SIW structure 20, hence providing the planar contactless transition or contactless connection interface between ridge 4 and the SIW 20. The other elements have already been discussed above with reference to Figs.1 and 2, and will therefore not be further discussed here.

Figs.1-3 show a single port transition package; it should also be clear that it could be symmetrical, with a stub arranged also at the other end of the ridge, with a common SIW or also e.g. one or more further SIWs, for example forming a two-port or a multi-port device.

Fig.4 shows an embodiment of a transition arrangement 100A comprising, here, two contactless back-to-back microstrip line-to-waveguide transitions, each comprising a contactless transition between a ridge 4A of a ridge waveguide 10A and a SIW structure 20A comprised in a circuit arrangement 11A provided on a chip (or application board). The transition arrangement 100A comprises a first metal plate 1A to which a chip with a microstrip integrated circuit 11A comprising two SIWs 20A,20A is attached.
Each SIW 20A comprises a dielectric substrate 6A with a first SIW ground plane 9A and a second SIW ground plane 9A' on either sides thereof and through which a plurality of vias 7 run as also discussed above with reference to Fig.1. The chip or circuit arrangement 11A comprising the SIWs 20A,20A is illustrated with two SIW-to microstrip transitions 12A,12A between a respective SIW 20A and the circuit arrangement 11A, wherein the microstrip lines are interconnected by means of a circuit 13 comprising two on-chip interface ports and active components, which however will not be further discussed herein, since the inventive concept is concerned mainly with the transitions between the respective SIW

20A and the respective ridge 4A of the ridge waveguides 10A,10A as discussed above.

The transition arrangement 100A also comprises a second metal plate or waveguide block portion 2A comprising a ridge waveguide arrangement with two ridge waveguides 10A,10A disposed between two longitudinal wall sections 3A,3A disposed in parallel, the ridge 4A of each ridge waveguide 10A ending at a location adjacent the outer end of a respective SIW structure 20A in an assembled or mounted state of the two metal plates or waveguide block portions 1A,2A. Each ridge 4A,4A is extended by means of a quarter wavelength stub 5A,5A as discussed with reference to Figs.1-3 above. It should be clear that even if only stubs with a rectangular shape are explicitly shown, the inventive concept also covers stubs with a triangular shape, a sector shape or any other appropriate shape. The stubs 5A,5A here have a height which is somewhat lower than that of the respective ridges 4A,4A. Here short-circuited pins 16A,16A (optional) are provided adjacent the $\lambda g/4$ stubs 5A,5A, at the outer free ends thereof pointing away from the respective ridges 4A,4A of the ridge waveguides 10A,10A, and transversally displaced with respect to one another to prevent EM-field leakage so that the fields from the waveguide will be coupled to the chip, i.e. no field will propagate underneath the chip and create a cavity. The short circuit pins 16A may further prevents the fields from passing through directly in a back-to-back configuration, which is not desired since the fields must follow the paths from ridge 4A to SIW 20 and back again. Passing through directly increases the feedback and thus decreases the input to output isolation in e.g. amplifier circuits, thus causing oscillations. Thus, pins 16A may also avoid the circuit arrangement and the transition to excite spurious, undesired, modes close to

the circuit which, when inside a cavity, create cavity resonances. Generally, in all embodiments the short circuit pins are optional, but if they are included, they are arranged so as to connect the first and second conducting plates.

Optionally, additional vias 17 as discussed with reference to Fig.1 above may be provided. A waveguide input port 25, referring to the whole aperture opening, is schematically indicated.

As in the embodiment described with reference to Figs.1-3, the metal plates or waveguide block portions 1A,2A are to be assembled, here mounted, and releasably secured to each other in any appropriate manner. Through the arrangement of the present invention, the circuit arrangement 11A comprising the SIWs, e.g. a PCB, may easily be replaced, e.g. in the case of malfunctioning or if it is ruined, or simply if it should be exchanged through another chip or circuit arrangement with different properties. The inventive concept is as also indicated above applicable to any kind of circuit arrangement, e.g. a high (RF) frequency package comprising a circuit arrangement, such as an MMIC (Monolithic Micro/Millimetre-wave Integrated Circuit) or any other circuit arrangement, e.g. wherein one or several MMICs or hybrid circuits are connected, or mounted on a carrier and interconnected, or in general one or more circuits, active or passive, is in the following also simply denoted “circuit”, and to chips disposed on an application board, i.e. the SIW may be disposed on a chip or a naked die itself, or disposed on a carrier substrate. Thus, the circuit arrangement may comprise an application board with a naked die holding an active semiconductor circuit, active components, schematically indicated 13 in the figures, where there are two on-chip interface ports, or it may represent a high permittivity naked

die as a whole including the SIWs 20A, microstrip-to-SIW transitions 12A and doped semiconductors at 13 (not shown).

Fig.5 shows an embodiment of a transition arrangement 100B comprising, here, two back-to-back microstrip line to waveguide transitions, each comprising a contactless transition between a ridge waveguide structure 14B,14B of a rectangular waveguide 10B,10B and an SIW structure 20B comprised in a circuit arrangement 11B of a chip or application board comprising SIW-to-microstrip transitions 12B,12B in-between SIWs 20B,20B and the microstrip line connecting the circuit components. The transition arrangement 100B comprises a first metal plate or waveguide block portion 1B to which a chip (or an application board holding the chip) with a microstrip integrated circuit 11B comprising SIWs 20B,20B is attached. The attachment of the circuit arrangement 11B comprising the SIWs 20B,20B to either one of the conducting, metal plates or waveguide blocks 1B,2B, of the SIW-to-waveguide transitions based on λg/4 stubs 5B,5B to the respective opposite conducting, metal plate, as well as other elements relevant for the functioning of the inventive concept have already been described with reference to Fig.1, Fig.3 and Fig.4.

The circuit arrangement 11B comprising the SIWs 20B,20B and the SIW-to-microstrip transitions 12B,12B between the respective SIW 20B,20B and the circuit 11B are not further discussed herein, since the inventive concept is concerned mainly with the transition between the respective SIWs 20B,20B and the waveguides 10B,10B of the, here, rectangular waveguide arrangement, and since the SIW-to-microstrip transitions have been discussed above with reference to Fig.4, similar elements bearing the same reference numerals but with an index “B”.

The second metal plate or waveguide block portion 2B of the transition arrangement 100B comprises two impedance transformers comprising stair sections 14B,14B, each comprising a number of steps (here three-step Chebyshev transformers) connecting the respective waveguide ridges 4B,4B to the respective rectangular waveguide arrangement 10B ending with a respective waveguide port 25 of which one is very schematically illustrated in Fig.5, i.e. at a location adjacent a respective outer end of the respective SIW structure 20B,20B in an assembled, here mounted, state of the two metal plates or waveguide block portions 1B,2B. To provide for the contactless transitions, each ridge 4B,4B comprising or connecting to a transformer section 14B,14B is extended by means of a quarter wavelength stub λg/4 5B,5B located adjacent the ridge 4B,4B similar to the transition arrangements described with reference to the preceding embodiments, with the difference that the λg/4 stubs 5B,5B are located adjacent, or as extensions of, the ridges 4B,4B of the respective transformer sections 14B,14B. Said stubs 5B,5B have a height which is somewhat smaller than that of the ridges 4B,4B.

The first and second waveguide blocks 1B,2B may comprise standard-flange waveguide matching steps (not shown). Short-circuited pins 16B,16B are provided adjacent to the stubs 5B,5B, at the outer free ends pointing away from the respective waveguide ridges 4B,4B of or connecting to the respective transformer section 14B,14B, and transversally displaced with respect to one another to prevent EM-field leakage as already discussed above with reference to Fig.4.

Also as in the embodiments described with reference to Figs.1-3 and 4, the waveguide blocks or metal plates 1B,2B are to be

assembled, mounted, and releasably secured to each other in any appropriate manner. The chip or the circuit arrangement 11B comprising the SIWs 20B,20B may easily be replaced e.g. in the case of malfunctioning or if it is ruined, or if it should be exchanged through another chip or circuit arrangement with different properties or serving another purpose.

In other respects the functioning is similar to that described above with reference to the embodiment of Fig.4, and other preceding embodiments, and will therefore not be further discussed herein, similar elements bearing the same reference numerals, but being provided with an index “B”.

Fig.6 shows an embodiment according to the invention comprising a microstrip integrated circuit to ridge gap waveguide back-to-back transition arrangement 100C. The EM-field from microstrip lines of the circuit arrangement 11C, e.g. a PCB, is electromagnetically coupled to, here, two symmetric ridge gap waveguides 10C,10C using the intermediate steps comprising the inventive transition between the waveguide of the SIWs 20C,20C and the ridge gap waveguides 10C,10 maximizing the EM-field transmission.

The transition, as also referred to above, can be said to be divided into a first and a second part, wherein the first part comprises the circuit part, the circuit arrangement, 11C, e.g. a PCB, and comprises the microstrip-to-SIW transitions 12C,12C, the circuit arrangement 11C comprising the SIWs 20C,20C and being attached to the first, here bottom, metal plate 1C of the ridge gap waveguides 10C,10C. This first part of the, or each, transition is straightforward and e.g. comprises step-tapered microstrip line sections connecting a 50 Ω microstrip line to the SIWs used to transform the Quasi-TEM microstrip line to the TE10 mode in the

SIWs 20C,20C. However, as already discussed above, the invention is not limited to any particular transition between the circuit arrangement 11C and the SIWs 20C,20C.

The second part of the, or each, transition, to which the invention is specifically directed, comprises the transitions between the SIWs 20C,20C and the ridges 4C,4C of the ridge gap waveguides 10C,10C. The additional λg/4 stubs 5C,5C serve the purpose of providing an electromagnetic coupling of the EM-field between the SIW 20C,20C waveguides and the ridges 4C,4C of the ridge gap waveguides 10C,10C by inverting the impedance and creating short circuits, hence providing contactless transitions.

In the embodiment shown in Fig.6, the waveguides 10C,10C comprise so called gap waveguides comprising a periodic or quasi-periodic structure 18C e.g. formed by a plurality of metallic pins 118 extending substantially perpendicularly to, here, the second metal plate or the second waveguide block 2C, and arranged to face the circuit arrangement 11C comprising the SIWs 20C,20C. The pin structure 18C comprising a pin bed replaces the metal waveguide walls 3,3A,3B in the preceding embodiments, and in such gap waveguide structures the first and second metal plates 1C,2C are disconnected, i.e. not joint, and there is no need for any screws or other connecting means. Thus, in such gap structures, e.g. Figs. 6,7,8A,8B, the first and second conducting plates, blocks or similar are assembled, without requiring being properly mounted or interconnected e.g. by means of appropriate fastening means, as e.g. the arrangements shown in Figs. 1-5. Further, gap structures are advantageous when mechanical tolerances are an issue, or when connections between waveguide split blocks need to be established, and may also prevent leakage, and thus to stop undesired

propagation of waves when packaging circuits. By means of the periodic or quasi-periodic pin structure 18C, waveguide modes are blocked from leaking into the circuit arrangement 11C comprising the SIWs 20C,20C from the ridge gap waveguides 10C,10C. Thus no power in a form of waveguide higher order modes can propagate between the waveguides and the circuit arrangement, and leakage in the transitions will be reduced or prevented.

The plurality of metallic pins 118 are disposed in parallel and each pin may have a circular, rectangular or a square-shaped cross-section and protrude perpendicularly with respect to a planar surface of the second metal plate or waveguide block portion 2C.

In advantageous embodiments, to which the invention is not limited, the width, the cross-sectional dimension, of square shaped pins may be about 0.1λ-0.2λ, λ being the wavelength of the centre frequency of the relevant frequency band, and the height of the pins is about λ/4, e.g. between 0.15λ and 0.3λ.
Particularly the period is between approximately 0.25λ and 0.4λ.

The distance between the top of the pin surface, and the ground plane of the circuit arrangement (here the SIW first ground plane 9C) should in advantageous embodiments be less than λ/4, although it may be larger as well as smaller.

Since the periodic structure, also denoted texture, is so designed that it stops propagation of waves over a specific frequency band for which it is designed, the shape and dimensions and the arrangement of e.g. pins, are selected correspondingly.

The non-propagating or non-leaking characteristics between two surfaces of which one is provided with a periodic texture (structure), is e.g. known from P.-S. Kildal, E. Alfonso, A. Valero-Nogueira, E. Rajo-Iglesias, "Local metamaterial-based waveguides in gaps between parallel metal plates", IEEE Antennas and Wireless Propagation letters (AWPL), Volume 8, pp. 84-87, 2009. The non-propagating characteristic appears within a specific frequency band, referred to as a stopband. It is also known that such stopbands can be provided by other types of periodic structures, as described in E. Rajo-Iglesias, P.-S. Kildal, "Numerical studies of bandwidth of parallel plate cut-off realized by bed of nails, corrugations and mushroom-type EBG for use in gap waveguides", IET Microwaves, Antennas & Propagation, Vol. 5, No 3, pp. 282-289, March 2011. These stopband characteristics are also used to form so-called gap waveguides as described in WO/2010/003808.

The described periodic or quasi-periodic textures may be used in particular embodiments of a transition arrangement according to the present invention.

In other respects the transition arrangement 100C and its functioning is similar to the transition arrangement described with reference to Fig.4, and other preceding Figures 1-3,5 and will therefore not be further described herein, and similar elements bear similar reference numerals but are provided with an index "C". The short-circuited pins 16C are optional as also referred to above; they may simply also comprise gap pins 18C.

Fig. 7 shows another embodiment of a transition arrangement 100D comprising a gap waveguide arrangement, more specifically a

microstrip IC to groove gap waveguide back-to-back transition arrangement. The E-field from e.g. a microstrip line of the circuit arrangement 11D, e.g. PCB, is electromagnetically coupled to the groove gap waveguides 10D,10D using the intermediate steps comprising the waveguides of the SIWs 20D,20D and the groove gap waveguides 10D,10D to maximize the EM-field transmission. The first parts of the transitions comprising the transitions 12D,12D from microstrip line to SIWs 20D,20D of the circuit arrangement 11D which is attached to the first, here bottom, plate 1D of the gap waveguide arrangement are, as also mentioned above, straightforward and may e.g. comprise step-tapered microstrip line sections connecting a 50 Ω microstrip line to the SIW waveguides used to transform Q-TEM microstrip line mode to the TE10 mode in the respective SIWs 20D,20D and the invention is not limited to any particular first part transition between the circuit arrangement 11D and the SIWs 20D,20D.

The second part of each transition comprises the transitions between the SIWs 20D,20D and the groove gap waveguides 10D,10D.

The transition arrangement 100D (cf. the embodiment described with reference to Fig.4), in addition to a first metal plate or waveguide block portion 1D, to which the circuit arrangement 11D comprising the SIWs 20D,20D, is attached, further comprises a second metal plate or waveguide block portion 2D comprising a groove in which impedance transformer sections 14D,14D are arranged (cf. Fig.5), each comprising a number of steps (here a three-step Chebyshev transformer) forming a stair connecting ridges 4D,4D of the groove gap waveguides 10D,10D to the groove of the gap waveguide arrangement, ending by a respective waveguide port 25.

To provide the contactless transitions according to the invention, an electromagnetic coupling of the EM-field between the SIWs 20D,20D to the ridges 4D,4D of the gap waveguides 10D,10D respective λg/4-stubs 5D,5D are connected to ridges 4D,4D of the gap waveguides 10D,10D to invert the impedance and create a respective short circuit.

Each ridge 4D,4D is thus extended by means of a quarter wavelength stub 5D,5D as also discussed with reference to Figs.1-3 above, and in particular with reference to Fig.5, each stub 5D,5D having a height which is somewhat smaller, lower, than that of the respective ridge 4D,4D such that an air gap is created between the respective λg/4-stub 5D,5D and the SIW 20D,20D.

The first and second waveguide blocks 1D,2D may comprise standard-flange waveguide matching steps (not shown). Short-circuited pins 16D,16D may be provided adjacent the stubs 5D,5D as in the preceding embodiments at the outer free ends pointing away from the respective ridges 4D,4D, and transversally displaced with respect to one another to prevent leakage as also discussed earlier in the application. The top (here) metal plate comprises a pin structure 18D comprising a plurality of pins, e.g. a pin bed, 118 or similar as also described with reference to Fig.6 which will therefore not be further discussed here, and, as described with reference to Fig.6, the first and second waveguide blocks 1D,2D remain disconnected, not joined, also when assembled.

Figs. 4-7 in principle all illustrate two-port devices, e.g. for amplifiers, but can be extended to comprise any circuit having various number and types of ports. Examples are frequency converters (mixers), power amplifiers, LNAs (Low Noise

Amplifiers), signal sources, frequency multipliers and different combinations of such components etc.

The waveguide structures may comprises metal plates or waveguide split block assemblies comprising a first waveguide block portion or a first conducting, metal plate, forming the respective half of one or more waveguides, and a second waveguide block portion or second metal plate forming the respective other half of said one or more waveguides.

In Figs.1,4-7 the waveguide assemblies are illustrated in an open, non-assembled (gap structures) or unmounted state.

When the waveguide blocks, or the first and second conducting plates, are connected (mounted or assembled), e.g. one or more waveguides are formed, the split may be along the broad dimension of a rectangular cross-section of the waveguide.

Although in the illustrated embodiments the first conducting, metal, plates or block portions are taken to form a bottom portion, it should be clear that, in alternative embodiments, the metal plate or block portion disposition may be different, e.g. reverted, or the metal plates or waveguide blocks or antenna parts may comprise two metal plates or blocks disposed and formed in any other appropriate way, on condition that the SIW(s) is/are provided on a block or conducting portion opposite to the block or conducting plate comprising e.g. the ridge waveguide(s) extended with the stub(s).

The first and second conducting plates or blocks, e.g. waveguide blocks or antenna parts may, as referred to above be connected by

screws or other fastening means, unless being gap arrangements as e.g. described with reference to Figs.6,7,8A,8B, in which case they are merely assembled and truly disjoint, and guiding pins (not shown) may in some embodiments be provided for assuring an accurate positioning of SIWs and stubs enabling the provisioning of the SIW-waveguide transitions according to the invention.

The invention is, as also referred to above, not limited to any specific circuitry, and supporting electronics is not shown for reasons of clarity and since it does not form part of the main inventive concept.

The first conducting plate is adapted to host said circuit arrangement comprising the SIW or the SIWs, and may e.g. comprise one or more receiving cavities. In alternative embodiments the circuit arrangement comprising the SIW or the SIWs is, preferably releasably, mounted onto the first (or second) block portion or conducting plate in any other appropriate way, e.g. by welding, gluing or similar.

In general, the two-port back-to-back structures can be used in many different ways. For example, when a circuit is hosted on a PCB/chip, one waveguide port can be used as an input, and if the chip hosts an amplifier, the other waveguide port can be left open to radiate the field as an open-ended waveguide. Hence, it represents an antenna with integrated electronics. As another example, the back-to-back structure may in principle represent any other type of non-radiating active or passive two-port device.

In particular embodiments of the present invention the transition arrangement comprises a transition between a circuit arrangement

of any kind as discussed above and an antenna, some examples of which are given in Figs.8A,8B and 9 below. Except for the/a waveguide being substituted by an antenna, the functioning and the involved elements are similar and can be of different kinds as discussed with reference to the waveguide embodiments shown in Figs.1-7, and will therefore not be described in further detail herein.

Particularly it may be an antenna structure based on the ridge concept as disclosed in Fig.4 or an antenna structure based on a rectangular concept as disclosed in Fig.5, and it may also be a an antenna structure comprising a gap waveguide as described e.g. in Figs. 6 and 7 above. Features and elements having been discussed and shown already with reference to preceding embodiments are hence not further discussed with reference to the antenna implementations of Figs.8A,8B and 9, and are indicated through the same reference numerals, but bearing an additional index “E” and “F” respectively.

Fig.8A shows a transition arrangement 100E according to the invention comprising a microstrip integrated circuit to ridge slot antenna transition. The transition is based on electromagnetic coupling of the EM-field from e.g. a microstrip line 12C of the circuit arrangement 11E, e.g. a PCB, to the ridge gap antenna 10E using the intermediate steps comprising the transition between the SIW 20E and the antenna 10E to maximize the EM-field transmission.

As also discussed above, the transition between the SIW 20E and the circuit part, e.g. a PCB, comprising the transition from microstrip 12E to the SIW 20E directly attached to the first, here bottom, metal plate 1E is straightforward and the invention is not

limited to any particular transition between the circuit arrangement 11E and the SIW 20E.

The second part of the transition, to which the invention is specifically directed, comprises the transition between the SIW 20E and the slot antenna 10E.

In the embodiment shown in Fig.8A, showing the arrangement 100E in an open, not assembled, state, the antenna 10E comprises a so called gap waveguide slot antenna comprising a periodic or quasi-periodic structure 18E e.g. formed by a plurality of metallic pins 118 extending substantially perpendicularly to the second metal plate 2E forming e.g. a bed of pins, and arranged to face the circuit arrangement 11E comprising the SIW 20E provided on the first metal plate 1E. The first metal plate 1E also comprises an antenna slot 115. The pin structure 18E is similar to the pin structure described with reference to Figs.6 and 7, but implemented for an antenna, and will not be further described here. It should be clear that it can be varied as discussed with reference to Figs. 6 and 7.

The second metal plate 2E comprises a feeding ridge 4E with a λg/4 stub 5E connected to the free end of the ridge 4E. The λg/4 stub 5E, as also discussed above, serves the purpose of providing an electromagnetic coupling of the EM-field between the SIW 20E waveguide and the ridge 4E of the ridge gap waveguide slot antenna 10E, effectively creating a short-circuit, and hence providing a contactless transition. For illustrative purposes, the second metal plate is not shown to scale with the first metal plate.

The feeding ridge 4E comprises a T-section 116 adapted for exciting the slot 115 in the first metal plate 1E. The SIW 20E may optionally be provided with tuning means 17 comprising vias and a notch for the purposes of impedance tuning, which however are not necessary for the functioning of the inventive concept.

Fig.8B shows the transition arrangement 100E of Fig 8A in a state in which the first and second metal plates 1E,2E are to be assembled, i.e. here the second plate 2E is shown in an elevated assembling position above the first metal plate 1E, such as to provide a contactless transition and the T-section 116 is disposed above the slot 115. The microstrip input port 19E is schematically indicated.

Fig.9 shows a transition arrangement 100F according to the invention comprising **a** microstrip integrated circuit-to-horn antenna transition. The E-field from e.g. a microstrip line 12F of the circuit arrangement 11F, e.g. a PCB, is electromagnetically coupled to the horn antenna 10F using the intermediate transition between the SIW 20F and the antenna 10F to maximize the power transmission.

The transition 12F from the microstrip to the SIW 20F, which is directly attached to the first, here bottom, metal plate 1F of the horn antenna 10F, is straightforward and the invention is as mentioned above not limited to any particular transition between the circuit arrangement 11F and the SIW 20F, but is directed to the transition between the SIW 20F and the horn antenna 10F.

In the embodiment shown in Fig.9, showing the transition arrangement 100F in an open, e.g. unmounted, state, the antenna

10F comprises a step tapered horn comprising two oppositely located step-tapered horn sections 191,191, the first and second metal plates 1F,2F thus comprising, in an assembled, mounted, state, one another facing stepped surfaces forming the step-tapered horn sections 191,191. The circuit arrangement 11F comprising the SIW 20F is provided on an upper surface of the first metal plate 1F, here at an opposite end to the step-tapered horn 191. On the corresponding upper surface of the second metal plate 2F an impedance transformer, e.g. a Chebyshev transformer, 14F is provided which is extended by a λg/4 stub 5F arranged to be located at a slight distance from the SIW 20F as discussed with reference to the preceding embodiments, such that a contactless transition is provided between the SIW 20F horn and the horn antenna 10F, i.e. achieving that the fields get off the circuit arrangement, e.g. the chip, and into the antenna 10F in a contactless manner by inverting the impedance and creating a back-short circuit.

The SIW 20F may optionally be provided with tuning means 17 comprising additional vias and a notch for the purposes of impedance tuning, which however are not necessary for the functioning of the inventive concept.

It should be clear that alternatively transitions as described with reference to Fig.2C can be used in any of the arrangements shown in Figs.4-9.

It is a particular advantage that through the invention a resonance free, low-loss contactless antenna-circuit or chip transition arrangement or package can be provided.

A waveguide or a transmission line port may e.g. serve as input for an input signal, an input frequency, which hence is fed through such waveguide or transmission line.

It should be clear that the invention is not limited to the specifically illustrated embodiments, but that it can be varied in a number of ways within the scope of the appended claims.

Particularly it is applicable for in principle any circuit of an arbitrary size, active or passive, and it is not limited to any specific frequencies. Also, the invention is not limited to any specific circuit arrangements, but it is applicable to any circuit arrangement, e.g. RF circuits, MMICs, hybrid circuits, and is also intended to cover other (active or passive) circuits. It is also not limited to any particular number or type of waveguides, antennas, nor to any particular ports, or to the arrangement and locations of ports, there may be one, two, three or more ports serving as input and/or output ports. The invention also covers stubs of different shapes, rectangular, sector shaped, triangular etc. Further, the invention covers different types of planar transitions, e.g. also comprising coplanar transmission lines.

CLAIMS

1. A transition arrangement (100;100_1;100A;100B;100C; 100D;100E;100F) for providing, or comprising, at least one transition between a substrate integrated waveguide, SIW, (20;20A,20A;20B,20B;20C,20C;20D,20D;20E;;20F) e.g. of, or associated with, a circuit arrangement (11;11A;…;11F) comprising one or more circuits, and a waveguide and/or antenna structure or interface (10;10A,10A;10B;10C,10C;10D,10D;10E;10F), wherein the transition arrangement comprises a first conducting plate or block (1;1_1;1A;1B;1C;1D;1E;1F) and a second conducting plate or block (2;2_1;2A;2B;2C;2D;2E;2F) comprising a plate or split-block assembly comprising at least one waveguide and/or antenna port (25),

c h a r a c t e r i z e d i n

that the SIW, or each, SIW (20;20A,20A;20B,20B;20C,20C;20D,20D; 20E;20F) is arranged on said first conducting plate or block (1;1_1;1A;1B;1C;1D;1E;1F),

that a number of ridges and/or impedance matching or transforming structures (4;4_1;4A,4A;14B,14B;4C,4C;14D,14D;4E;14F) is/are connected to the second conducting plate or block (2;2_1;2A;2B;2C; 2D;2E;2F), such that for the, or each, transition between a said substrate integrated waveguide, SIW, (20;20A,20A;20B,20B; 20C,20C;20D,20D;20E;20F) and a said waveguide and/or antenna structure or interface (10;10A,10A;10B;10C,10C; 10D,10D;10E;10F), the, or each, ridge and/or impedance matching or transforming structure (4;4A;14B;4C;14D;4E;14F) is associated with, or extended with, an open circuit $\lambda_g/4$ stub (5;5_1;5A,5A;5B,5B;5C,5C;5D,5D; 5E;5F) for inverting impedance and providing a short-circuit for electromagnetically coupling the EM-field between the SIW(20;20A,20A;20B,20B;20C,20C;20D,20D;20E;20F) and the ridge or

impedance matching or transforming structure (4;4_1;4A,4A;14B,14B;4C,4C;14D,14D;4E;14F) in an assembled state of the first and second conducting plates or blocks (1,2;1A,2A;…;1F;2F),

that the impedance matching or transforming structure (4;4_1;4A,4A;14B,14B;4C,4C;14D,14D;4E;14F) and the open circuit $\lambda_g/4$ stub (5;5_1;5A,5A;5B,5B;5C,5C;5D,5D;5E;5F) are so arranged that, when the first and second conducting plates or blocks (1,2;1_1,2_1;1A,2A;…;1F;2F) are assembled, a side or surface of the open circuit $\lambda_g/4$ stub (5;5_1;5A,5A;5B,5B;5C,5C; 5D,5D;5E;5F) being located opposite to the side or surface of the stub (5;5_1;5A,5A;5B,5B;5C,5C;5D,5D;5E;5F) that is connected to the second plate (2;2_1;2A;2B;2C;2D;2E;2F), will be disposed at a slight distance, e.g. corresponding to an air gap, from a portion of a first ground plane (9;9_1;9A;….;9F) of a said SIW (20;20A,20A;20B,20B;20C,20C;20D,20D;20E;20F), without any galvanic contact between the SIW (20;20A,20A;20B,20B;20C,20C;20D,20D;20E;20F) and the ridge and/or impedance matching or transforming structure (4;4_1;4A,4A;14B,14B;4C,4C;14D,14D;4E;14F) and between the SIW (20;20A,20A;…;20F) and the open circuit $\lambda_g/4$ stub (5;5_1;5A,5A;5B,5B;5C,5C;5D,5D;5E;5F), such that a contactless, substantially planar, transition is formed between the SIW (20;20A,20A;…;20F) and the waveguide and/or the antenna structure (10;10A,10A;10B;10C,10C;10D,10D;10E;10F).

2. A transition arrangement (100;100_1;100A;100B;100C;100D;100E;100F) according to claim 1,

c h a r a c t e r i z e d i n

that the, or each, SIW (20;20A,20A;…;20F) and/or the circuit arrangement (11;11A;…;11F) comprising or associated with the SIW

(20;20A,20A;…;20F), is/are adapted to be releasably connected or grounded to said first conducting plate or block (1;1_1;1A;…1F).

3. A transition arrangement (100;100_1;100A;100B;100C;100D; 100E;100F) according to claim 1 or 2,
c h a r a c t e r i z e d i n
that the circuit arrangement (11;11A;…;11F) comprises an RF circuit, an active circuit arrangement, e.g. one or more active MMICs, or a passive circuit arrangement.

4. A transition arrangement (100;100_1;100A;100B;100C; 100D;100E; 100F) according to any one of the preceding claims,
c h a r a c t e r i z e d i n
that it is adapted for high RF-frequency signals.

5. A transition arrangement (100;100A;100B;100C;100D;100E;100F) according to any one of the preceding claims,
c h a r a c t e r i z e d i n
that the first and second conducting plates or blocks (1,2;1_1,2_1;1A,2A;….;1F,2F) are adapted to be mountable/demountable e.g. releasably interconnectable, e.g. by means of interconnecting means, e.g. screws or similar, or possible to assemble/disassemble contactlessly, alignment means optionally being provided for assisting in aligning the first and second conducting plates or blocks when mounted or assembled.

6. A transition arrangement (100;100_1;100A;100B;100C;100D;100E; 100F) according to any one of the preceding claims,
c h a r a c t e r i z e d i n
that the, or each, SIW (20;20A,20A;…;20F) comprises a dielectric substrate (6;6A,6A;….;6F) which on opposing sides is provided with

a first ground plane (9;9_1;9A,9A;….;9E;9F) and a second ground plane (9';9_1';9A',9A';….;9E';9F') respectively, said first and second ground planes being electrically connected by means of vias (7) crossing the dielectric substrate (6;6A,6A;….6F).

7. A transition arrangement (100;100_1;100A;100B;100C;100D;100E;100F) according to claim 6,
c h a r a c t e r i z e d i n
the second conducting ground plane (9'; 9_1';9A',9A';….;9F) provided on one side of the dielectric substrate (6;6A,6A;….;6F) of the SIW is connected to the first conducting plate (1;1_1;1A,1A;….;1E;1F), or to the circuit arrangement (11;11A;11B;…11F), that the first SIW ground plane (9;9_1;9A,9A;….;9F) is arranged to serve as a common ground plane for the SIW (20;20A,20A;…;20F) and the $\lambda_g/4$ stub (5;5_1;5A,5A;5B,5B;5C,5C;5D,5D;5E;5F), and in that second ground plane (9';9_1';9A',9A';….;9E';9F') is arranged to serve as a common ground plane for the SIW (20;20A,20A;…;20F) and the waveguide and/or antenna structure (10;10A,10A;…;10F).

8. A transition arrangement according to any one of the preceding claims,
c h a r a c t e r i z e d i n
that the SIW is disposed on a carrier substrate or a low permittivity application board connected, e.g. bond wired, to a chip comprising the circuit arrangement.

9. A transition arrangement (100;100_1;100A;100B;100C;100D;100E;100F) according to any one of claims 1-7,
c h a r a c t e r i z e d i n

that the SIW (20;20A,20A;…;20F) is disposed on a chip or a naked die comprising the circuit arrangement e.g. comprising one or more of any one of an amplifier, a mixer, a frequency multiplier, etc. in any combination.

10. A transition arrangement (100;100_1;100A;100B;100C;100D) according to any one of the preceding claims,
c h a r a c t e r i z e d i n
that the at least one transition comprises a transition between a SIW (20;20A,20A;20B,20B;20C,20C;20D,20D) and a waveguide (10;10A,10A;10B,10B;10C,10C;10D,10D).

11. A transition arrangement (100;100_1;100A;100C) according to claim 10,
c h a r a c t e r i z e d i n
that the waveguide structure comprises at least one ridge waveguide (10;10A,10A;10B,10B;10C,10C;10D,10D), and in that the ridge or impedance matching or transforming structure comprises a ridge (4;4_1;4A,4A;4B,4B;4C,4C;4D,4D).

12. A transition arrangement (100A;100C) according to claim 11,
c h a r a c t e r i z e d i n
that it comprises a microstrip IC to ridge waveguide back-to-back transition comprising two SIW (20A,20A;20C,20C)-to-waveguide structure transitions, each comprising a ridge (4A,4A;4C,4C) connected to a said open circuit $\lambda_g/4$ stub (5A,5A;5C,5C).

13. A transition arrangement (100B;100D) according to claim 10,
c h a r a c t e r i z e d i n
that comprises at least one rectangular and/or groove gap waveguide (10B,10B;10D,10D), and in that the or each ridge and/or impedance

matching or transforming structure comprises a ridge (4B,4B;4D,4D) connected to each a said open circuit $\lambda_g/4$ stub (5B,5B;5D,5D).

14. A transition arrangement (100B;100D) according to claim 13, characterized in that it comprises a microstrip IC to waveguide back to back transition comprising two SIW (20B,20B;20D,20D)-to-waveguide structure transitions, each with an impedance matching or transforming structure (14B,14B;14D,14D) comprising e.g. a Chebyshev transformer connected to a respective ridge (4B,4B;4D,4D).

15. A transition arrangement (100E;100F) according to any one of claims 1-9, characterized in that the at least one transition comprises a transition between a SIW (20E;20F) and an antenna structure (10E;10F).

16. A transition arrangement (100E) according to claim 15, characterized in that the antenna structure comprises a slot antenna, a slot (115) being provided in the first conducting plate or block (1E), the impedance matching or transforming structure provided on the second conducting plate or block (2E) comprising a ridge (4E) with a T-section (116) for feeding the slot (115).

17. A transition arrangement (100F) according to claim 15, characterized in that the antenna structure (10F) comprises a horn antenna wherein the electromagnetic field coupled from the circuit arrangement

(11F) via the SIW (20F) is adapted to feed the horn antenna comprising step tapered horn sections (119,119).

18. A transition arrangement (100C;100D;100E) according to any one of the preceding claims,
c h a r a c t e r i z e d i n
that the second conducting plate or block (2C;2D;2E) comprises a periodic or a quasi-periodic structure (18C;18D;18E) arranged such that, in an assembled state of the transition arrangement, said periodic or a quasi-periodic structure faces the SIW (20C,20C;20D,20D;2E), the periodic or the quasi- periodic structure (18C;18D;18E) comprising a pin structure with a plurality of pins (118) or similar arranged to form a bed of pins or similar, the pin structure being located at a slight distance, e.g. corresponding to an air gap which is smaller than λ/4, from the first conducting plate (1C;1D;1E).

19. A transition arrangement (100C;100D;100E) according to claim 18,
c h a r a c t e r i z e d i n
that the pins (118), corrugations or similar of the periodic or quasi-periodic structure (18C;18D;18E) have dimensions adapted for a specific, selected, frequency band.

20. A transition arrangement (100E;100F) according to any one of the preceding claims,
c h a r a c t e r i z e d i n
that the first conducting plate or block (1;1A;…;1F) is adapted to receive or host the, or each SIW, or the circuit arrangement (11;11A;….;11F) comprising the, or each, SIW (20;20A,20A;…;20F), and in that said at least one SIW or circuit arrangement is/are

detachably mountable onto or in the first conducting plate or block (1;1A;…;1F).

21. A transition arrangement (100;100A;100B;100C; 100D;100E; 100F) according to any one of the preceding claims,
c h a r a c t e r i z e d i n
that the open circuit $\lambda_g/4$ stub (5;5A,5A;5B,5B;5C,5C;5D,5D; 5E;5F) has a smaller height than the ridge or a section of the impedance matching or transforming structure (4;4A,4A;14B,14B;4C,4C; 14D,14D;4E;14F), with which it is associated such that a step is formed, that, when the first and second conducting plates or blocks (1,2;1A,2A;…;1F;2F) are assembled, the, or each, step will be located facing an edge of the, or a, respective SIW (20;20A,20A;20B,20B;20C,20C;20D,20D;20E;20F), and in that an outer edge of the ridge and/or impedance matching or transforming structure (4;4A,4A;14B,14B;…;4E;14F) protruding beyond the open circuit $\lambda_g/4$ stub (5;5A,5A;….;5F) will be located at a slight distance, e.g. corresponding to an air gap, from a respective SIW (20;20A,20A; 20B,20B;20C,20C;20D,20D;20E;20F) outer edge perpendicular to said first conducting plate or block (1;1A;…;1F), and from the first conducting plate or block (1;1A;…;1F).

22. A transition arrangement (100_1) according to any one of claims 1-20,
c h a r a c t e r i z e d i n
that the SIW (20) arranged in a groove (101) provided in the first conducting plate or block (1_1) such that a slight distance comprising an air gap is provided between an edge (102) of the groove in the first conducting plate or block (1_1).

23. A method for providing a transition between a circuit arrangement and a waveguide and/or antenna structure comprising the steps of:

- providing a substrate integrated waveguide, SIW, (20;20A,20A;…;20F), e.g. of, or associated with, a circuit arrangement (11;11A;…;11F) comprising one or more circuits, and a waveguide and/or antenna structure or interface (10;10A;10B;10C;..;10F), wherein the transition arrangement comprises a first conducting plate or block (1;1_1;1A;…;1F) and a second conducting metal plate or block (2;2_1;2A;…;2F) comprising a split plate or block assembly comprising at least one waveguide and/or antenna port (25),

c h a r a c t e r i z e d i n

that it comprises the steps of

- connecting a ridge or an impedance matching or transforming structure (4;4_1;4A,4A;14B,14B;4C,4C;14D,14D;4E;14F) to the second conducting plate or block (2;2_1;2A;…;2F), and, for the, or each, transition between a substrate integrated waveguide, SIW, (20;20A,20A;…;20F) and a waveguide and/or antenna structure (10;10A;10B;10C;..;10F), associating or extending the ridge or impedance matching or transforming structure (4;4_1;4A,4A;…;14F) with an open circuit $\lambda_g/4$ stub (5;5_1;5A,5A;….;5F) for inverting the impedance and providing a short-circuit for electromagnetically coupling the EM-field between the SIW (20;20A,20A;…;20F) and the ridge or impedance matching or transforming structure (4;4_1;4A,4A;…;14F) when the first and second conducting plates or blocks (1,2;1_1,2_1;2,2A;…;1F,2F) are assembled,
- assembling the first and second conducting metal plates or blocks (1,2;1_1,2_1;2,2A;…;1F,2F) by arranging them so with respect to one another that a side or surface of the open

circuit $\lambda_g/4$ stub (5;5_1;5A,5A;….;5F) opposite to the side of the stub (5;5A,5A;….;5F) being connected to the second plate, will be disposed at a slight distance, e.g. corresponding to an air gap, from a portion of a first ground plane (9;9_1;9A;….;9F) of a said SIW (20;20A,20A;20B,20B;20C,20C;20D,20D;20E;;20F), without any galvanic contact between the SIW (20;20A,20A;20B,20B;20C,20C;20D,20D;20E;20F) and the ridge and/or impedance matching or transforming structure (4;4_1;4A,4A;14B,14B;4C,4C;14D,14D;4E;14F) and between the SIW (20;20A,20A;…;20F) and the open circuit $\lambda_g/4$ stub (5;5_1;5A,5A;….;5F), such that a contactless, substantially planar transition is formed between the SIW (20;20A,20A;…;20F) and the waveguide and/or the antenna structure (10;10A,10A;…;10F).

ABSTRACT

The present invention relates to a transition arrangement (100) comprising a transition between a substrate integrated waveguide, SIW, (20) of a circuit arrangement and a waveguide and/or antenna structure (10). It comprises a first conducting plate (1) and a second conducting plate (2).

The SIW (20) is arranged on said first conducting plate, and an impedance matching structure (4) is connected to the second conducting plate. For a transition between the SIW (20) and the waveguide structure, the impedance matching structure (4) is extended with an open circuit $\lambda_g/4$ stub (5) for inverting the impedance to effectively provide a short-circuit connection, thereby electromagnetically coupling the EM-field between the SIW and the impedance matching structure (4), which is so arranged that, when the first and second conducting plates are interconnected, or merely assembled in a contactless manner in the case of gap structures, the open circuit $\lambda_g/4$ stub (5) is disposed above the SIW without any galvanic contact between the SIW and the impedance matching structure (4) and between the SIW (20) and the $\lambda_g/4$ stub (5), providing a planar, contactless transition.

(Fig. 1)

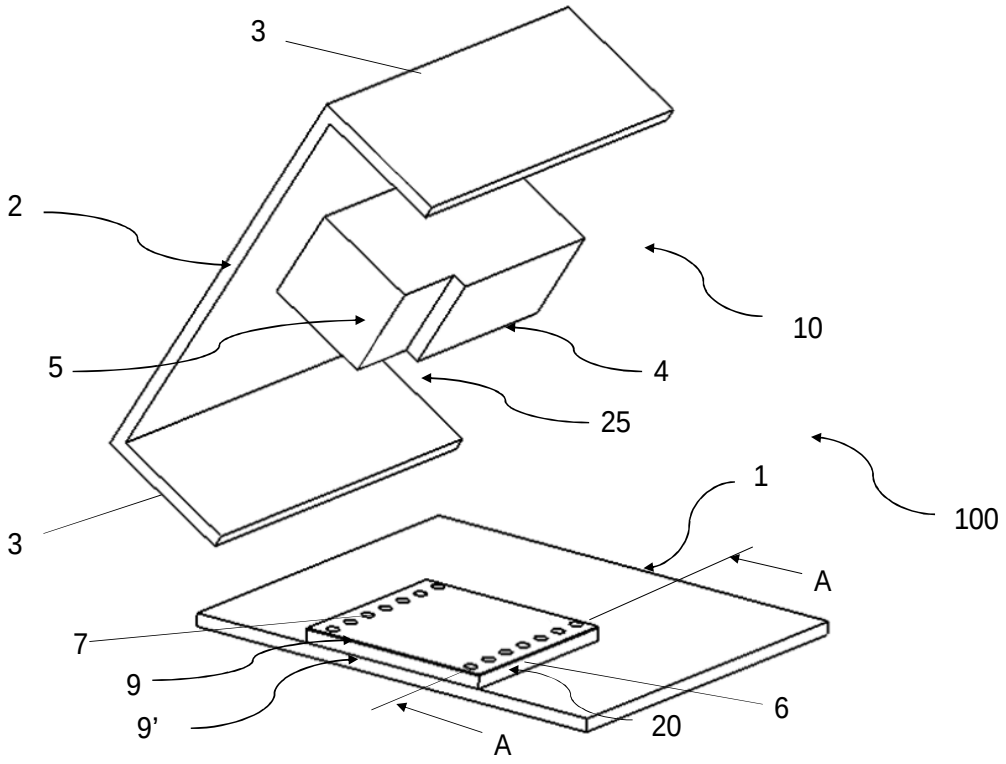

Fig.1

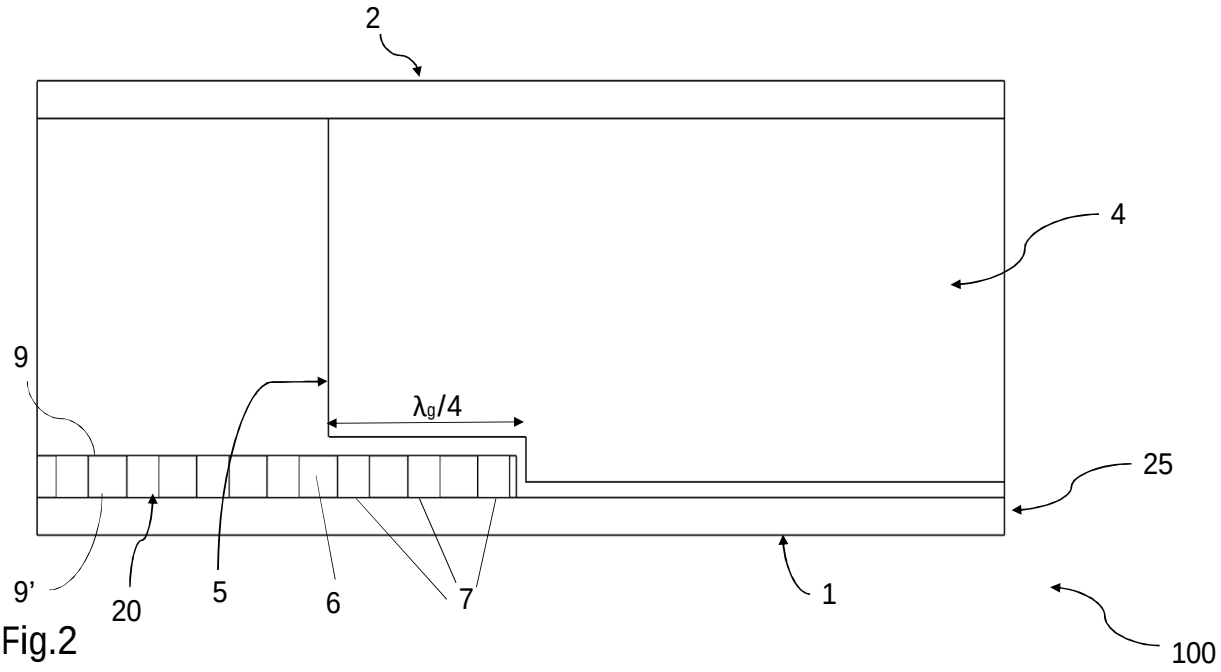

Fig.2

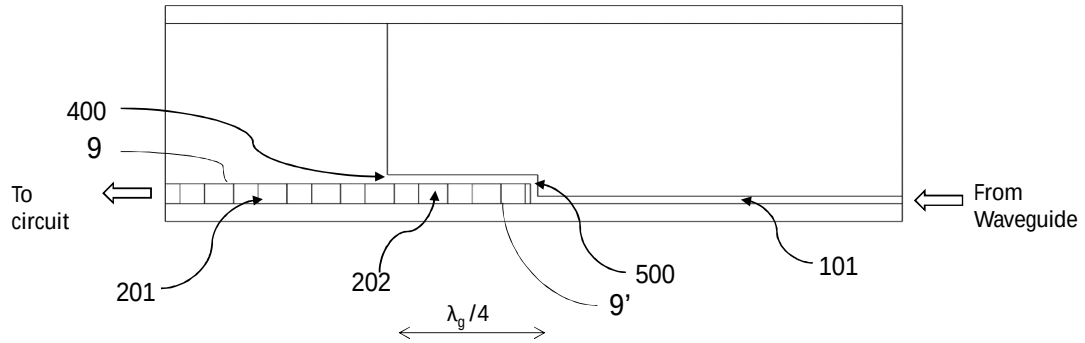
400
9
To
circuit
From
Waveguide
201
202
500
101
9'
$\lambda_g/4$

Fig.2A

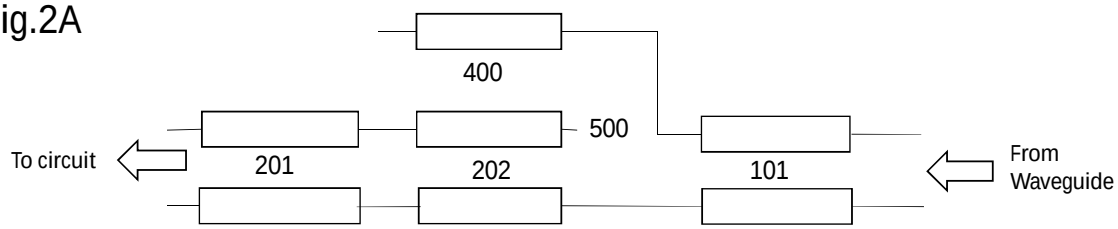
400
To circuit
201
202
500
101
From
Waveguide

Fig.2B

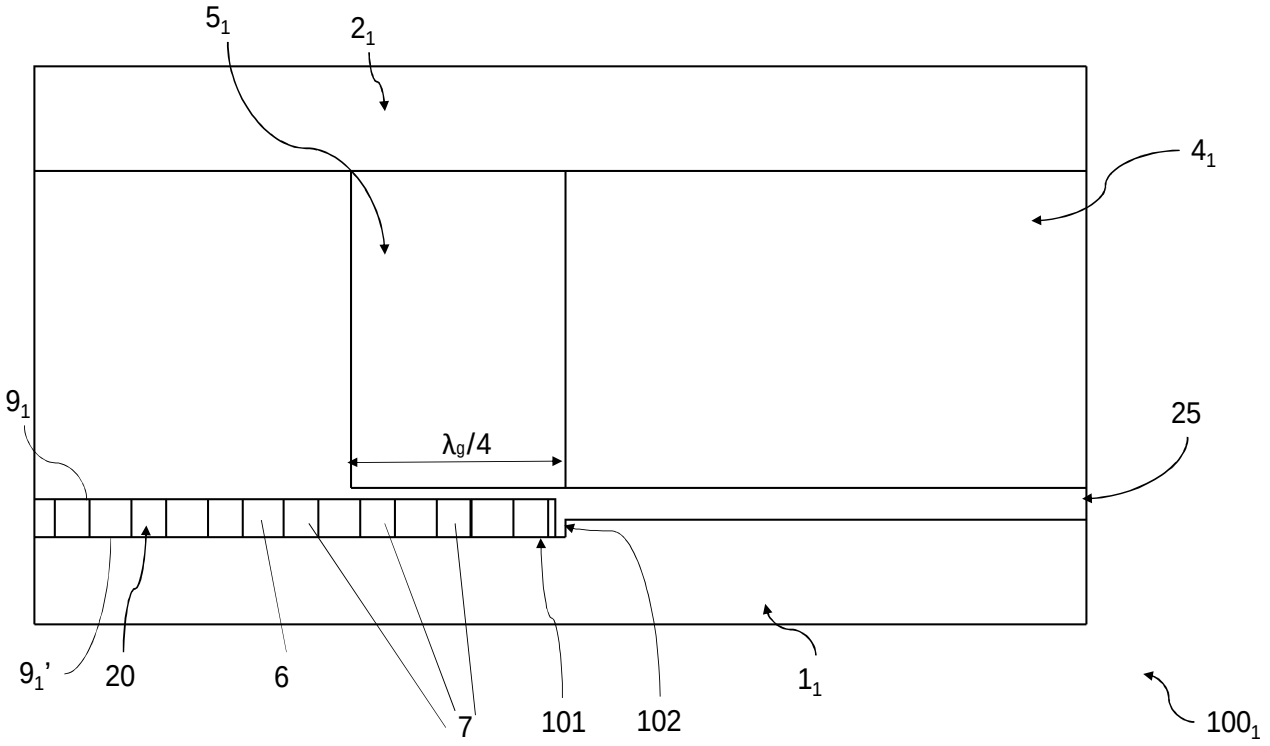

Fig.2C

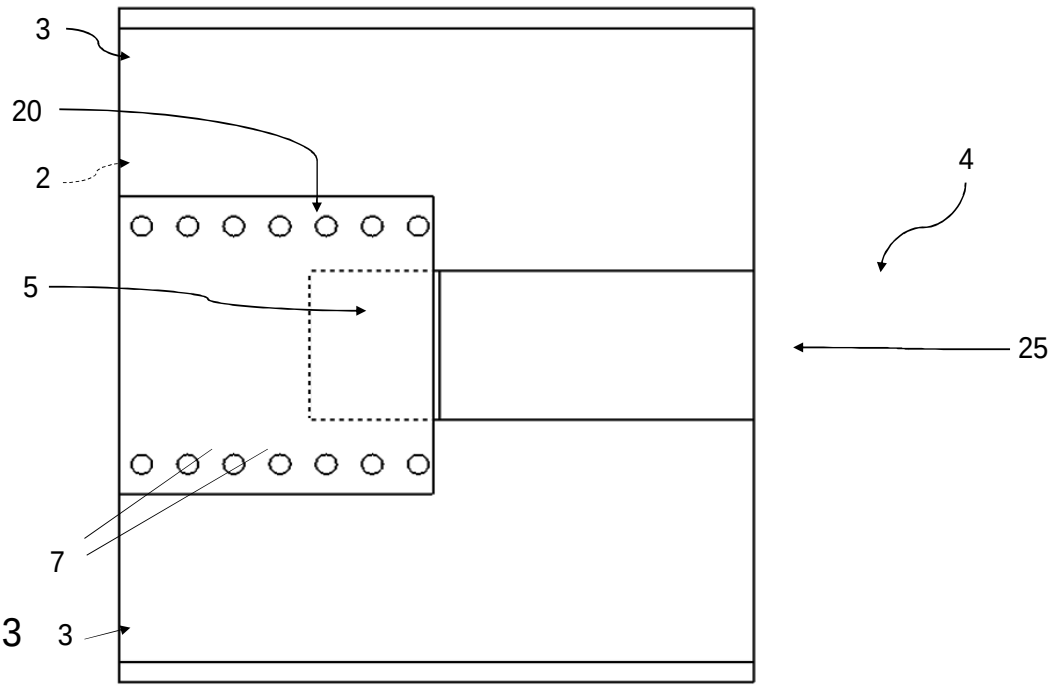

Fig. 3

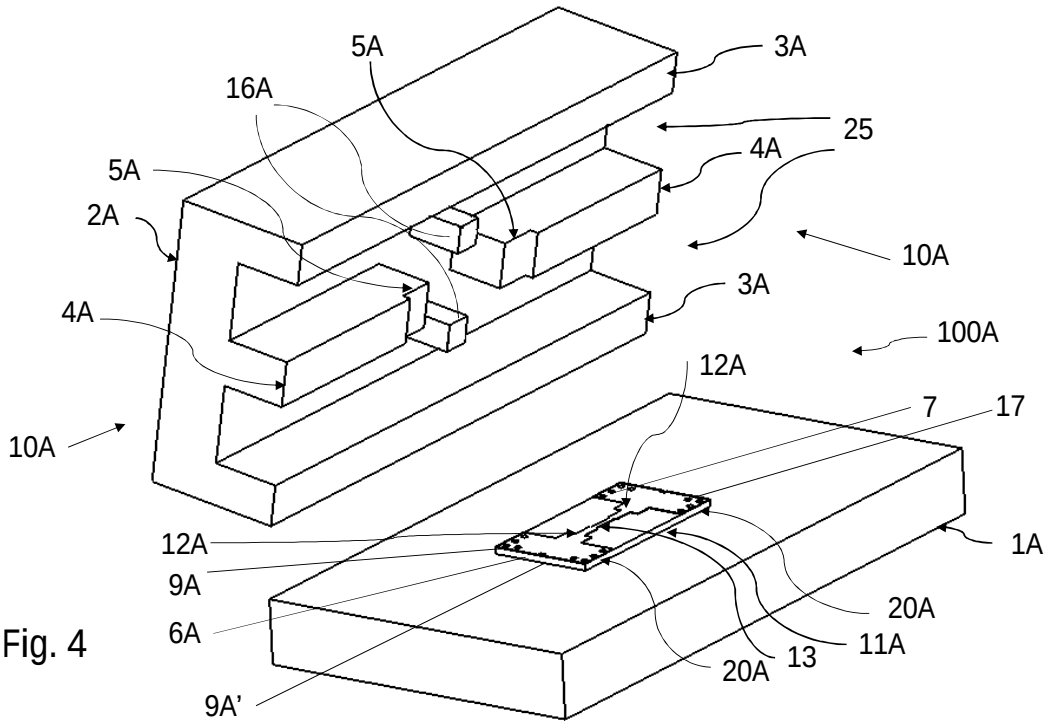
5A
3A
16A
25
5A
4A
2A
10A
3A
4A
100A
12A
7
17
10A
1A
12A
9A
20A
6A
11A
13
20A
9A'

Fig. 4

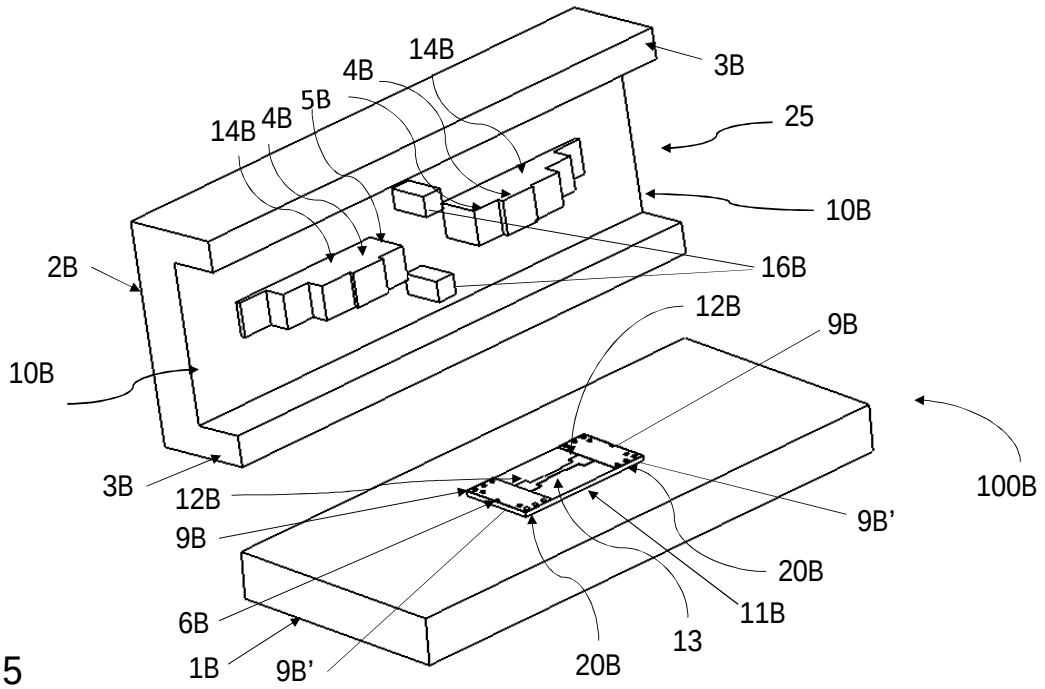
14B
4B
3B
5B
14B
4B
25
10B
2B
16B
12B
9B
10B
3B
12B
100B
9B
9B'
20B
11B
6B
13
1B
9B'
20B

Fig.5

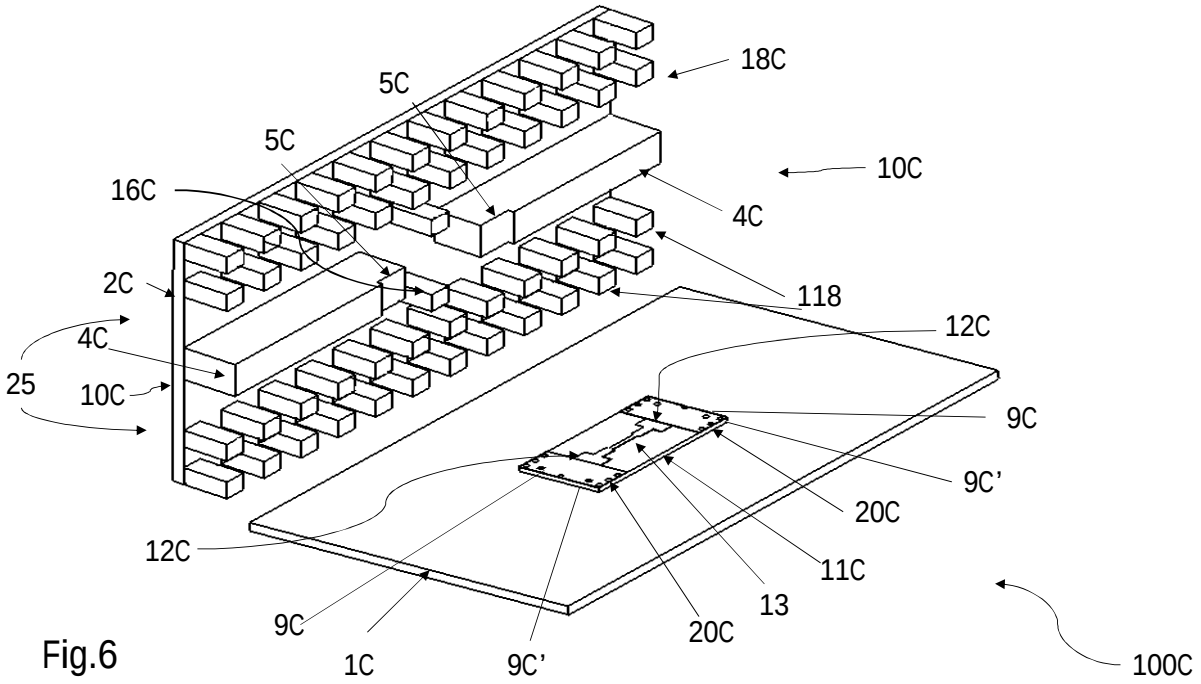
18C
5C
5C
10C
16C
4C
2C
118
12C
4C
25
10C
9C
9C'
20C
12C
11C
13
9C
20C
1C
9C'
100C

Fig.6

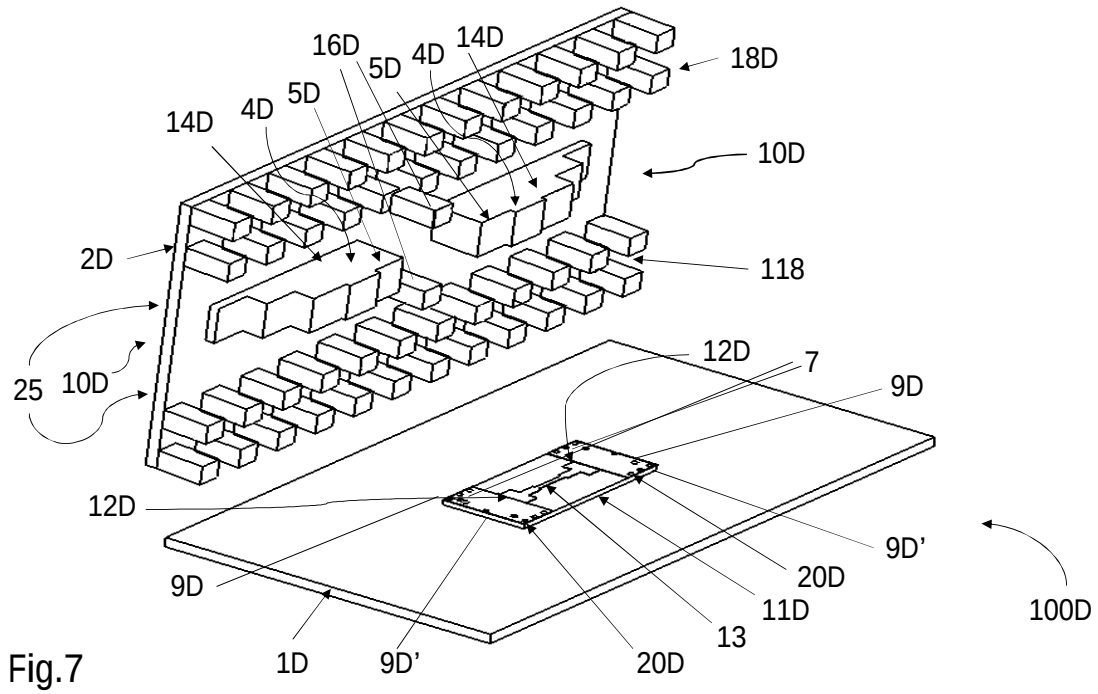
16D
5D
4D
14D
18D
14D
4D
5D
10D
2D
118
25
10D
12D
7
9D
12D
9D'
20D
11D
13
100D
9D
1D
9D'
20D

Fig.7

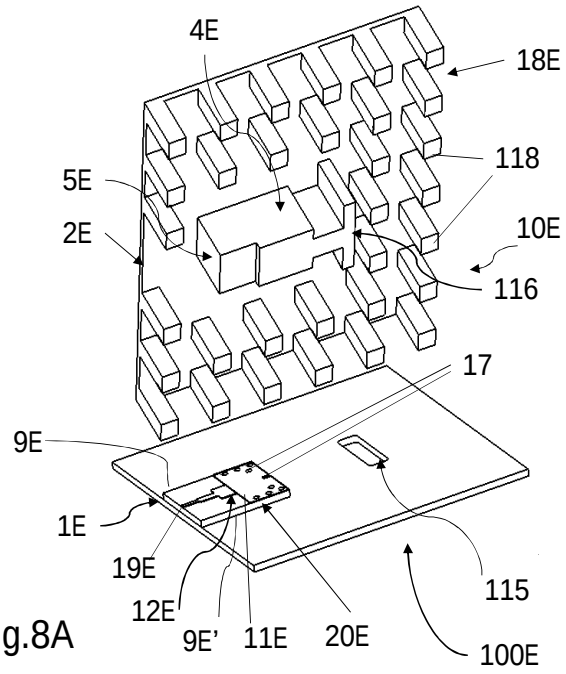
4E
18E
118
5E
2E
10E
116
17
9E
1E
19E
12E
9E'
11E
20E
115
100E

Fig.8A

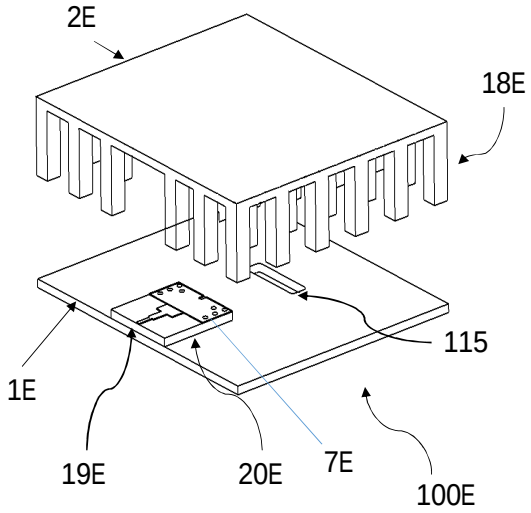
2E
18E
115
1E
19E
20E
7E
100E

Fig.8B

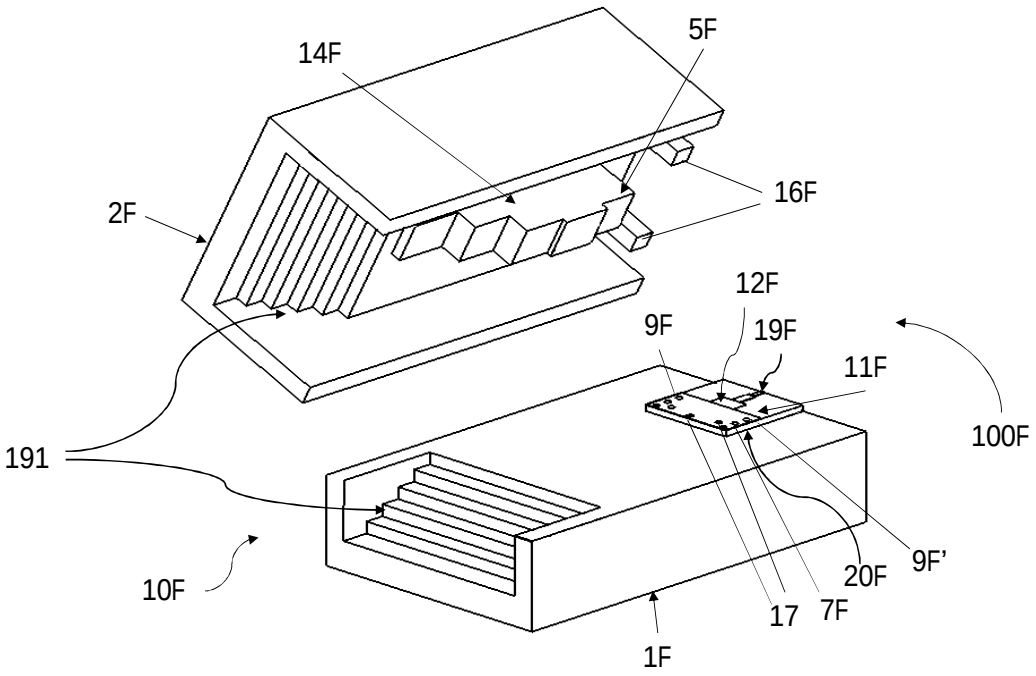

Fig.9

Bibliography

[1] Y. Miura, J. Hirokawa, M. Ando, Y. Shibuya, and G. Yoshida, "Double-layer full-corporate-feed hollow-waveguide slot array antenna in the 60-ghz band," *IEEE Trans. Antennas Propag.*, vol. 59, no. 8, pp. 2844 –2851, Aug. 2011.

[2] J. Hirokawa, Z. Miao, and M. Ando, "Millimeter waveguide fabrication to reduce transmission loss by diffusion bonding, light-curing resin or dielectric partially-filling," in *Microwave Conference, 2008. APMC 2008. Asia-Pacific*, pp. 1–4.

[3] Y. Zhang, J. Ruiz-Cruz, K. Zaki, and A. Piloto, "A waveguide to microstrip in-line transition with very simple modular assembly," *IEEE Microw. Wireless Compon. Lett.*, vol. 20, no. 9, pp. 480–482, Sep. 2010.

[4] A. Rebollo, B. Larumbe-Gonzalo, R. Gonzalo, and I. Ederra, "Three metamaterial-based gap waveguides between parallel metal plates for mm/submm waves," in *The $8^{r}th$ European Conference on Antennas and Propagation (EuCAP 2014)*, pp. 2591–2593.

[5] K. Y. Han and C. keng Pao, "A v-band waveguide to microstrip inline transition," in *2012 IEEE MTT-S International, Microwave Symposium Digest (MTT)*, pp. 1–3.

[6] P.-S. Kildal, "Three metamaterial-based gap waveguides between parallel metal plates for mm/submm waves," in *Proceedings of the 3^{rd} European Conference on Antennas and Propagation (EuCAP 2009)*, pp. 28–32.

[7] P.-S. Kildal, E. Alfonso, A. Valero-Nogueira, and E. Rajo-Iglesias, "Local metamaterial-based waveguides in gaps between parallel metal plates," *IEEE Antennas Wireless Propag. Lett.*, vol. 8, pp. 84–87, 2009.

[8] B. Molaei and A. Khaleghi, "A novel wideband microstrip line to ridge gap waveguide transition using defected ground slot," *IEEE Microw. Wireless Compon. Lett.*, vol. 25, no. 2, pp. 91–93, Feb. 2015.

[9] A. Zaman, T. Vukusic, M. Alexanderson, and P.-S. Kildal, "Design of a simple transition from microstrip to ridge gap waveguide suited for mmic and antenna integration," *IEEE Antennas Wireless Propag. Lett.*, vol. 12, pp. 1558–1561, Dec. 2013.

[10] A. A. Brazlez, A. Zaman, and P.-S. Kildal, "Investigation of a microstrip-to-ridge gap waveguide transition by electromagnetic coupling," in *AP-S International Symposium, IEEE Antennas and Propagation Society*, Jul. 2012, pp. 1–2.

[11] C. G. Arias, M. B. Escudero, A. V. Nogueira, and A. V. Jimenez, "Test-fixture for suspended-strip gap-waveguide technology on ka-band," *IEEE Microw. Wireless Compon. Lett.*, vol. 23, no. 6, pp. 321–323, 2013.

[12] E. G. Geterud, P. Bergmark, and J. Yang, "Lightweight waveguide and antenna components using plating on plastics," in *Proceedings of the* 7^{th} *European Conference on Antennas and Propagation (EuCAP 2013)*, pp. 1812–1815.

[13] D. Liu, B. Gaucher, U. Pfeiffer, and J. Grzyb, *Advanced Millimeter-wave Technologies: Antennas, Packaging and Circuits.* Chichester, U.K.: Wiley & Sons, 2009.

[14] J. Digby, C. McIntosh, G. Parkhurst, B. Towlson, S. Hadjiloucas, J. Bowen, J. Chamberlain, R. D. Pollard, R. E. Miles, D. Steenson, L. Karatzas, N. Cronin, and S. Davies, "Fabrication and characterization of micromachined rectangular waveguide components for use at millimeter-wave and terahertz frequencies," *IEEE Trans. Microw. Theory Tech.*, vol. 48, no. 8, pp. 1293–1302, Aug. 2000.

[15] P.-S. Kildal, "Definition of artificially soft and hard surfaces for electromagnetic waves," *Electronic Letters*, vol. 24, no. 3, pp. 168–170, Feb. 1988.

[16] M. G. Silveirinha, C. Fernandes, and J. Costa, "Electromagnetic characterization of textured surfaces formed by metallic pins," *IEEE Trans. Antennas Propag.*, vol. 56, no. 2, pp. 405–415, Feb. 2008.

[17] S. Sievenpiper, Z. lijun, R. Broas, N. Alexopolous, and E. Yablonovitch, "High-impedance electromagnetic surface with a forbidden frequency band," *IEEE Trans. Microw. Theory Tech.*, vol. 47, no. 11, pp. 2059–2074, Nov. 1999.

[18] E. A. Alos, A. Zaman, and P.-S. Kildal, "Ka-band gap waveguide coupled-resonator filter for radio link diplexer application," vol. 3, no. 5, pp. 870 –879, May 2013.

[19] A. Razavi, P.-S. Kildal, X. Liangliang, E. Alfonso, and H. Chen, "2x2-slot element for 60 ghz planar array antenna realized on two doubled-sided pcbs using siw cavity and ebg-type soft surface fed by microstrip-ridge gap waveguide," *IEEE Trans. Antennas Propag.*, vol. 62, no. 9, pp. 4564–4573, 2014.

[20] M. A. Sharkawy and A. Kishk, "Wideband beam-scanning circularly polarized inclined slots using ridge gap waveguide," *IEEE Antennas Wireless Propag. Lett.*, vol. 13, pp. 1187–1190, 2014.

[21] E. Rajo-Iglesias, A. Zaman, and P.-S. Kildal, "Parallel plate cavity mode suppression in microstrip circuit packages using a lid of nails," *IEEE Microw. Wireless Compon. Lett.*, vol. 20, no. 1, pp. 31–33, Jan. 2010.

[22] A. Kishk, A. U. Zaman, and P.-S. Kildal, "Numerical prepackaging with pmc lid efficient and simple design procedure for microstrip circuits including the packaging," *ACES Applied Computational Society journal*, vol. 27, no. 5, pp. 389–395, May 2012.

[23] E. Rajo-Iglesias, P.-S. Kildal, A. Zaman, and A. Kishk, "Bed of springs for packaging of microstrip circuits in the microwave frequency range," vol. 2, no. 10, pp. 1623–1628, Oct. 2012.

[24] S. Rahiminejad, A. Zaman, E.Pucci, H. Raza, V. Vassilev, S. Haasl, P. Lundgren, P.-S. Kildal, and P. Enoksson, "Micromachined ridge gap waveguide and resonator for millimeter-wave applications," in *Sensors and Actuators A: Physical*, vol. 186, 2012, pp. 264–269.

[25] N. Grumman, "http://www.northropgrumman.com/businessventures/microelectronics/product 2015.

[26] A. Polemi, S. Maci, and P.-S. Kildal, "Dispersion characteristics of a metamaterial-based parallel-plate ridge gap waveguide realized by bed of nails," *IEEE Trans. Antennas Propag.*, vol. 59, pp. 904–913, Mar. 2011.

[27] E. Rajo-Iglesias and P.-S. Kildal, "Numerical studies of bandwidth of parallel plate cut-off realized by bed of nails, corrugations and mushroom-type ebg for use in gap waveguides," *IET Microwaves, Antennas and Propagation*, vol. 5, no. 3, pp. 282–289, Mar. 2011.

[28] P.-S. Kildal, A. Zaman, E. Rajo-Iglesias, E. Alfonso, and A. Valero-Nogueira, "Design and experimental verification of ridge gap waveguide in bed of nails for parallel-plate mode suppression," *IET Microwaves, Antennas and Propagation*, vol. 5, no. 3, pp. 262–270, 2011.

[29] A. Zaman and P.-S. Kildal, "Wide-band slot antenna arrays with single-layer corporate-feed network in ridge gap waveguide technology," *IEEE Trans. Antennas Propag.*, vol. 62, no. 6, pp. 2992–3001, 2014.

[30] CST, "https://www.cst.com/," 2013.

[31] Y. Cassivi, L. Perregrini, P. Arcioni, M. Bressan, K.Wu., and G. Conciauro, "Dispersion characteristics of substrate integrated rectangular waveguide," *IEEE Microw. Wireless Compon. Lett.*, vol. 12, no. 9, pp. 333–335, Sep. 2002.

[32] D. Deslandes and K. Wu, "Integrated microstrip and rectangular waveguide in planar form," *IEEE Microw. Wireless Compon. Lett.*, vol. 11, no. 2, pp. 68–70, Feb. 2001.

[33] R. Jansen and N. Koster, "New aspects concerning the definition of microstrip characteristic impedance as a function of frequency," in *Microwave Symposium Digest, 1982 IEEE MTT-S International. Dallas, TX, USA*, pp. 305–307.

[34] E. Pucci and P.-S. Kildal, "Contactless non-leaking waveguide flange realized by bed of nails for millimeter wave applications," in *Proceedings of the* 6^{th} *European Conference on Antennas and Propagation (EuCAP 2012)*, pp. 3533–3536.

[35] S. Rahiminejad, E.Pucci, S. Haasl, and P. Enoksson, "Micromachined contactless pin-flange adapter for robust high-frequency measurements."

[36] D. M. Pozar, *Microwave Engineering*, 4th ed. Wiley & Sons, 2012.

[37] N. Osman and C. Free, "The behaviour and characterisation of circuit materials at high millimetre-wave frequencies," in *Automated RF Microwave Measurement Society (ARMMS) (Apr 2010).*